Combustion Characteristics

of South African Grown Fuelwoods

Mark Davis, B.Sc(Hons)

Submitted to the University of Cape Town in partial fulfilment of the requirements for the degree of Master of Applied Science.

Cape Town
September 1990

Declaration

I declare that this dissertation is my own original work. It is being submitted in partial fulfilment for the degree of Master of Applied Science at the University of Cape Town. It has not been submitted before for any degree or examination at any university.

Signed by candidate

M Davis

30 day of October 1990

Abstract

The principle objective of this investigation was to establish a methodology to compare and rank fuelwoods. This methodology would allow a wide range of tree species to be compared and ranked according to their combustion properties. Such a comparison would assist in the selection of species for woodlot development. This investigation attempted to examine the combustion kinetics of small samples in an attempt to achieve the stated aim.

Initially a literature review was performed. This covered anecdotal information on fuelwood preferences, an overview of wood composition, structure and combustion, and an in depth review of existing work on small sample combustion.

Different theoretical models were used to describe the processes in small sample combustion. A straight forward pseudo-rate constant model was used for both devolatilisation and char combustion. In addition, new versions of the shrinking core model and the progressive conversion model were developed.

A series of experiments were performed on twenty different wood species: eleven hardwoods and nine softwoods. Both heartwood and sapwood samples were used and experiments were performed at five different temperatures in the range from 450°C to 650°C. A number of parameters were derived for each species from the experimental data. Some were descriptive parameters such as ignition time, devolatilisation time, char burnout time and percentage char formed. Others were kinetics parameters derived from the application of the different theoretical models.

It was found that only the pseudo-rate constant models could be successfully applied to the experimental data.

Significant differences could be determined between species on the basis of the parameters derived, although not between heartwood and sapwood samples of a single species. There were general density and temperature trends as well as differences in behaviour between hardwoods and softwoods. In an attempt to relate these results to the usefulness of wood as a fuel, a ranking analysis on the individual parameters was performed. This showed that there existed a reasonably consistent ranking of the hardwoods which was independent of the wood density.

The main difficulty in using the experimental results to establish a fuelwood ranking methodology lies in the fact that the empirical work investigated micro scale events in wood combustion and was valid for small samples only. The main recommendation is that further work investigating macro properties of larger samples needs to be performed.

Acknowledgements

I would like to thank Dr Anton Eberhard for guidance and assistance for the duration of the project and for the supervision of the dissertation.

Also to Dr Jim Petrie for his advise and assistance with the theoretical aspects of the project.

I am also grateful to staff and students of CRAET for valuable discussion and advice as well as to workshop staff of the Energy Research Institute for their time in preparing samples and assistance in commissioning the experimental rig.

Finally to the Energy Research Institute and the Foundation for Research Development for financial assistance during the course of 1989/90.

Table of Contents

List of Tables

List of Illustrations

Nomenclature

Uppercase symbols

$\mathcal{A}$	pre-exponential factor [s^{-1}]
A	area [cm^2]
A_i	specific internal surface area [cm^2/g]
A_e	specific external surface area [cm^2/g]
Air Vel	air velocity [m/s]
C, C_o, C_s, C_f	molar concentration of oxygen: in bulk, at the surface, at the reaction front [mol/cm^3]
C_g	specific heat [J/g/K]
$[C_t]$	concentration of carbon sites [$sites/cm^2$]
C.V.	calorific value [kJ/kg]
D_A	molecular diffusivity [cm^2/s]
D_e	effective diffusivity [cm^2/s]
D_{trans}, D_{long}	thermal diffusivity: transverse, longitudinal [cm^2/s]
E, E_t, E_a	activation energy: true, apparent [kJ/mol]
J	mass flux of gas [$g/cm^2/s$]
$\mathcal{K}$, $\mathcal{K}_g$	thermal conductivity [J/cm/K/s]
K_m, K_e	overall rate constant: mass basis [$mol/s/mol/[C]^n$], external surface area basis [$mol/s/cm^2/[C]^n$]
K_D	molar diffusion rate constant = h_D / $\mathcal{M}_g$ [cm/s]
K_g	specific permeability [cm^2]
L	length [cm]
M	normalised mass = $(m - m_f)/(m_o - m_f)$
$\mathcal{M}_c$, $\mathcal{M}_g$, $\mathcal{M}_s$	molar mass of carbon, gaseous and solid reactant [g/mol]
MC_{wet}, MC_{dry}	moisture content: wet basis, dry basis [%]
N_r, N_m	progressive conversion model parameters
P, P_{ave}	pressure, average pressure [Pa]
$\mathcal{R}$	universal gas constant (= 8.31441 J/kg/mol)
R	initial radius [cm]
R_m, R_e	overall particle reactivity: mass basis [mol/s/mol], external surface area basis [$mol/s/cm^2$]
Re	Reynolds number
R_s, R_i, R_v	intrinsic reactivity: site basis, internal surface area basis, volume basis.
Sc	Schmidt number
Sh	Sherwood number
T	temperature [K, °C]
Tamb	ambient air temperature [°C, K]
Tair	combustion chamber inflowing air temperature [°C, K]
Tchamb	average combustion chamber air temperature [°C, K]
Theat	heater air temperature [°C, K]
Tflue	combustion chamber flue gas temperature [°C, K]
V	volume [cm^3]

Lowercase symbols

$a_1..a_4$	multiple regression constants
c	constant
d	diameter [cm]
dP	pressure drop [Pa]
dPair	square root of the pressure drop over an orifice plate [Pa]
h_D	mass tranfer co-efficient [cm/s]
k, k_s, k_i, k_v	intrinsic rate constant: site basis, internal surface area basis, volume basis
k_g	gas permeability [$cm^3_{[gas]}$.cm/dyne/s]
m	mass [g]
m	true reaction order
m_c	mols carbon per site [mol/site]
n	apparent reaction order
p	exponential constant
q	pyrolysis heat of reaction [J/mol]
r	radius [cm]
t	time [s]
v	velocity
$y, x_1..x_4$	multiple regression variables

Greek symbols

β	progressive conversion model parameter
ϕ	porosity
Γ	ratio of stoichiometric co-efficients = mols O_2 / mols C
η	effectiveness factor
ϱ	density [kg/m^3, g/cm^3]
ϱ_{spec}	specific gravity of wood
υ	viscosity [dyne.s/cm^2]
Ψ	= $(1/m_o)$ dm/dt [s^{-1}]
ζ	= r/R

Subscripts

a	apparent
ave	average
c	carbon
e	external surface area basis
f	reaction front, final
g	gaseous reactant
i	internal surface area basis
long	longitudinal
m	mass basis
o	initial, bulk
s	site basis, surface of sample, solid reactant
t	true
trans	transverse
v	volume basis
wet, dry	wet or dry basis

Chapter 1

Introduction

This project aimed to develop a technique for assessing the suitability of a wood species as a fuel. Although there is a certain amount of information on fuelwood preferences and considerable data on the silvicultural properties of trees, there is no proper measure of the usefulness of a wood species as a fuel.

This chapter will first give some background information relating to fuelwood scarcities and the resulting effects. The question of species choice for woodlot development will be considered and the principle objectives of this investigation outlined.

1.1 Fuelwood Scarcities

Fuelwood forms the primary energy source for about two billion people around the world (Financial Times, 1986: p7). Although detailed statistics are rare and often inaccurate, estimates have been made of fuelwood consumption and deficits for most developing countries (FAO, 1981).

In recent years there has been a growing awareness of the extent and the implications of fuelwood scarcities in developing countries. In 1975 Erik Eckholm drew attention to the dependence of the Indian, Central and Southern African sub-continents on wood as a domestic energy source (Eckholm, 1975). Since then, a number of publications have pointed to the

economic and social burdens as well as to the environmental consequences of reduced fuelwood stocks (Eckholm et al, 1984; Timberlake, 1985; Goldenberg et al, 1987).

In South Africa biomass (mainly in the form of fuelwood) presently accounts for about 7% of primary energy. This is consumed mainly in the less-developed rural and homeland areas (Williams & Eberhard, 1988: p227). Since the majority of South Africa's population do not have access to electricity, there is a heavy dependence on wood to supply domestic energy needs. Wood accounts for 60% and 27% of rural and peri-urban useful energy consumption respectively (Eberhard, 1989: p5).

A recent study by Aron, Eberhard & Gandar (1989) has attempted to quantify the fuelwood situation in South Africa. They estimate the total wood deficit in all homeland areas to be in the region of 3.4 million tonnes. To meet this deficit would require around 425 000 ha of additional plantation (p12).

A number of publications have reported on the increased social and economic costs resulting from fuelwood scarcities. In a study of six rural areas in South Africa, it was found that women spent on average four hours per fuelwood collection trip, carrying headloads of about 30 kg (Eberhard, 1986[a]: p33). In addition to this, there are considerable health risks associated with fuelwood scarcities where reduced energy consumption in cooking and heating affects the diet and welfare of the family (Best, 1979: p25).

Economically, the effect of fuelwood scarcities is to increase the portion of the family budget spent on energy. The transport cost of wood can significantly affect household expenditure on fuel (Eberhard, 1986[b]: p4). Bembridge (1986: p14) reports that households from three villages in the Transkei spent on average 10% of their income on energy. In urban areas, households without electricity spend up to three times as much as those with electricity (Wilson & Ramphele, 1989: p47).

Suggested strategies to alleviate the fuelwood crisis have concentrated on both demand and supply management. Demand management policies involve both economic measures (World Bank, 1983: p15) and the design and dissemination of fuel efficient stoves. For a variety of reasons most stoves

programmes, with a few notable exceptions, have failed. Further, there is little evidence to show that these attempts are reducing the overall rate of fuelwood consumption (Baldwin, 1988: p278).

Supply strategies have concentrated either on the provision of alternative fuels or the plantation of more woodland. Electrification is probably the preferred option for urban and peri-urban areas for a number of reasons (Eberhard, 1986[b]: p9-10), although the cost of full electrification in rural areas could probably not be justified.

The common approach to afforestation in Southern Africa has been state woodlot development, although this is not the only possible approach. Commercial farm forestry is practised widely in India where farmers plant trees and sell a variety of forestry products (Eckholm et al, 1984: p60). Another approach is communal forestry where trees are grown on public land. These schemes allow landless and poor households access to the benefits of tree plantations (Williams, 1986: p81). However, Gandar (1988: p249) reports that the total area of woodlots in South Africa is only around 20 000 ha.

The effects of fuelwood scarcities are being felt in many areas of Southern Africa. One of the most immediate and pressing needs is the extension of existing tree plantations to increase the supply of fuelwood. A crucial question in woodlot development is the choice of tree species. It is in the area of species selection that this project hopes to make a contribution.

1.2 Species Selection for Fuelwood Plantations

The factors which affect the choice of tree are speed of growth, resistance to decay and termites, ease of harvesting and transport as well as combustion properties (Best, 1979: p29). The silvicultural properties of trees are closely related to the climate of the region in question. Considerable work has been done internationally in assessing the growth properties of tree species in different areas (Burley, 1978; Jones, 1978; NAS, 1980). Locally, Richard Poynton (1976, 1984) has published silvicultural properties of an extensive list

of indigenous and alien trees grown in Southern Africa. In the Southern African region, most woodlots have been planted with Eucalyptus species.

However, as regards the combustion characteristics of different species, very little information exists. A study by Eberhard (1987) experimentally determined the calorific values for a wide range of wood species. However, this study showed that calorific value is approximately constant for all species and is not a useful parameter for distinguishing between species. A certain amount of anecdotal information on fuelwood preferences exists although this is by no means extensive and is not sufficient to provide a ranking of the different species.

1.3 Primary Objectives

The primary aim of this project was to investigate the combustion of wood with a view to identifying a technique by which different species could be compared on the basis of their worth as a fuel.

Since different woods often have very different densities, comparisons should be made on the basis of mass rather than volume. The important questions to consider can be listed as follows:

* what is the overall process of combustion?
* which models can adequately describe wood combustion?
* in what way does the composition, density and structure of wood affect its combustion?
* what parameters are useful in distinguishing between species?
* how do these parameters relate to the fuel potential of wood?

This investigation was conducted through a number of stages. Firstly a review of the overall process of combustion was conducted. This was followed by a more detailed look into the different models which have been used to describe wood combustion. From this study, potentially useful combustion parameters were identified. Experimental procedures and calculation techniques were then developed in order to obtain these parameters. A series of experiments

were conducted and the results analyzed. These experimental results were then examined in order to both isolate differences between species and to identify an appropriate method of comparing species.

1.4 Report Outline

Chapter two will give an overview of the essential processes involved in wood combustion. This will then be elaborated in chapters three and four which will review the models and experimentally derived results which have been used to describe wood combustion. Chapter three will focus on pyrolysis and devolatilisation whilst chapter four will consider char combustion. The theory and calculation techniques used in this investigation will then be described in chapter five. The experimental apparatus and procedures used will be outlined in chapter six and this will be followed by a presentation and discussion of the results in chapters seven and eight. Lastly, chapter nine will outline the conclusions from this study and make recommendations.

Chapter 2

Properties of Wood

This chapter will firstly review the structure, composition and properties of wood. This will be followed by a brief overview of the different processes involved in wood combustion. Lastly the criteria for fuelwood selection will be discussed.

2.1 The Structure and Composition of Wood

Wood may be divided into two general categories: softwood and hardwood. Softwood comes from gymnosperms, trees with needles or scale-like leaves. They are mostly evergreen and are also referred to as conifers. Examples of gymnosperms are cedar, pine and cypress. Hardwood comes from dicotyledonous angiosperms. These trees have broad leaves and are deciduous. Common angiosperms are oak, eucalyptus and maple.

The composition of wood will be discussed in terms of its physical structure, chemical composition and moisture content.

2.1.1 The physical structure

Wood is the name given to the main tissue comprising the stems, roots and branches of the so-called "woody plants". A cross-section of the trunk reveals a central pith surrounded by concentric growth rings. Surrounding these is the bark. A growth ring is the wood produced by the tree in a single season. Those cells produced in early spring comprise the earlywood, whilst those produced later in summer make up the latewood. Earlywood is softer and more porous than latewood.

The growth rings themselves are also divided into two types: sapwood and heartwood. Sapwood is comprised of the outermost layers and is generally about 1.5 - 5 cm thick. Heartwood is made up of the inner, older layers and provides the mechanical support. The sapwood is the youngest wood and is generally softer and more moist than heartwood (Desch, 1968: p16).

Wood tissue is comprised of fibres or cells. These cells are divided into two categories: prosenchyma and parenchyma. Prosenchyma includes vessels, tracheids and libreform fibres. These provide mechanical strength and facilitate transport of water and air. The diameter of these cells varies from 0.02 to 0.5 mm. The parenchyma cells contain living protoplasm. They reserve food such as starch, fats and resins. These cells range in length from 0.5 to 1.5 mm and in diameter from 0.07 to 0.1 mm (p16, p341, Murty-Kanury & Blackshear, 1970[a]: p16).

The internal structures of softwood and hardwood differ considerably. The conducting and supporting tissue in softwood is composed of tracheid fibres. These fibres are long and hollow, tapered towards the ends and sealed. They usually range in length from 2.5 to 7.0 mm. The fibres are arranged longitudinally and are fairly uniformly distributed across a small cross-section. The flow region inside these fibres typically ranges from 20 to 30 microns in diameter (Simmons, 1983: p4).

Parenchyma cells in softwood provide for storage of fats and sugars. They are either arranged in radial lines (known as rays) or lie with the tracheids. They have thin walls and are pitted. Softwood also contains resin canals which store significant amounts of resin.

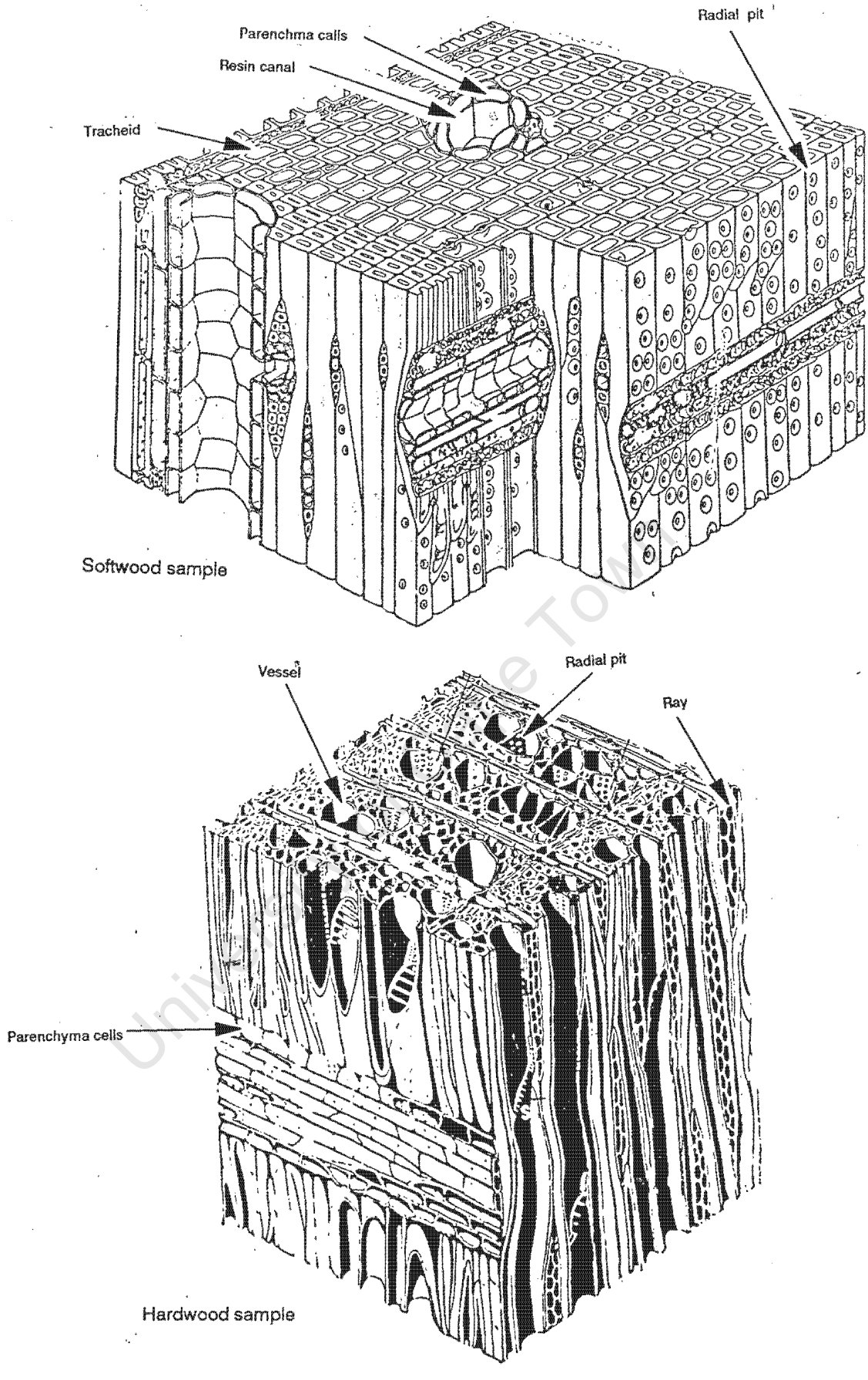

(Source: Siau, 1971)

Figure 2.1: Internal Structure of Wood

Compared to softwood, hardwood is more complex in structure. The conducting vessels form long canals with each component cell having no end walls. These vessels may appear singly or in groups. Earlywood vessels tend to be larger than latewood vessels. The pore size and vessel distribution vary considerably among the hardwood species. Diffuse-porous hardwood has relatively small pores dispersed uniformly through a cross-section. Pore diameters are generally in the range 20-30 microns. Ring-porous hardwood has vessels with very large pores (up to 300 microns in diameter) in early springwood. As the season's growth progresses, the pore size becomes considerably smaller (Simmons, 1983: p4).

Like softwood, hardwood also contains support cells and living parenchyma cells. Hardwood fibres are similar in structure to softwood tracheids and provide mechanical support. The storage parenchyma cells in hardwood are arranged both longitudinally and in ray bundles (more developed than in softwoods). Resin canals are rare in hardwoods.

In both softwood and hardwood there exist pits connecting vessels and tracheids transversely. In softwood this pitting is fairly limited. This means that transverse permeability is considerably less than longitudinal permeability. Pitting is generally more extensive in hardwood.

2.1.2 The chemical composition

Dry wood is made up of cellulose, hemicellulose, lignin, extractives and ash forming materials (Simmons, 1983: p6). The relative quantities of these substances may vary among the different species. Table 2.1 gives the chemical composition, ultimate analysis and proximate analysis for softwoods and hardwoods.

Cellulose is the principle constituent, almost 50% by weight of most dry wood (Roberts, 1970: p263). Findley (1975: p56) reports that analysis of thirteen softwood species and ten hardwood species gave the percentage mass of cellulose as 46% and 49% respectively. The structure of cellulose is the same in all types of wood except for the degree of polymerization. The empirical

formula is $(C_6H_{10}O_5)^n$ with a molecular weight of about 106 (Dadkhah-Nikoo & Bushnell, 1987: p129). The presence of hydroxyl groups on the sides of the chain gives cellulose a high affinity for water adsorption through hydrogen bonding (Simmons, 1983: p5). This water-cellulose interaction has an important effect on the moisture content and drying of wood.

Hemicelluloses differ from cellulose in that they consist of pentoses as well as hexoses (Findley, 1975: p52). The hemicelluloses are amorphous and have a lower degree of polymerization than cellulose. The types of hemicelluloses differ considerably between species. Hardwood contains many pentosans while softwood is richer in hexosans. Simmons (1983: p5) suggests that this difference could cause some variation in combustion properties between species.

Lignin serves as a cement between fibres, a stiffening agent within fibres and as a barrier to enzymatic degradation of the cell wall. It has a complex structure and is more abundant and polymeric in softwood than in hardwoods. Lignin comprises 23 to 33% of the wood in softwood and only 16 to 25% in hardwood (Simmons, 1983: p6). During combustion lignin produces 45% char whereas cellulose produces only 15% (Roberts, 1970: p264).

Analysis	Component	Softwood (percent of weight)	Hardwood (percent of weight)
Chemical Composition	Cellulose	43	43
	Hemicellulose	28	35
	Lignin	29	22
Ultimate Analysis (dry basis)	Hydrogen (H)	6.1	6.2
	Carbon (C)	53.0	51.0
	Oxygen (O)	38.8	39.9
	Sulphur (S)	–	–
	Nitrogen (N)	0.1	0.2
	Ash	1.7	2.5
Proximate Analysis	Volatiles	40.6	52.4
	Fixed Carbon	12.4	12.9
	Ash	1.0	2.7
	Moisture	46.0	32.0

(source: Tillman, 1981: p179)

Table 2.1 Composition of Hardwood and Softwood

Extractives are extraneous plant compounds which may include oils, hydrocarbons, terpenes, fatty acids, tannins etc. Softwood generally contains more organic extractives in the form of resin than hardwood. The presence of these volatile components may affect the combustion characteristics of the wood. Dadkhah-Nikoo & Bushnell (1987) suggest that extraneous compounds such as resins, although low in volume, can play an important role in determining properties such as durability, colour, odour, inflammability and calorific value. A higher resin content raises the calorific value (Eberhard & Poynton, 1986: p28.5).

Ash is the noncombustible matter left when the wood is completely burned. The ash content of wood is typically less than 1% although this can increase to 2-5% in the bark due to collection of dirt and sand (Simmons, 1983: p6).

There is a remarkably small variation in the elemental composition of wood. Carbon generally comprises 49-50% of the substance, hydrogen 6%, oxygen 43-44% and nitrogen, sulphur and ash 0.5-1% together (Eberhard, 1987: p16).

2.1.3 The moisture content

The moisture content of wood can be described in two ways: on a wet basis and on a dry basis. The moisture content on a wet basis is given by:

$$MC_{wet} = \frac{\text{mass of water}}{\text{mass of wet wood}} \times 100\ \%$$

and on a dry basis is given by:

$$MC_{dry} = \frac{\text{mass of water}}{\text{mass of dry wood}} \times 100\ \%$$

Moisture can exist in wood in three forms: water vapour in air spaces of the cell cavities, capillary water in the cell lumens and hygroscopic or bound water in the cell walls. The water vapour in the cell cavities is at the same potential energy state as if it were outside the wood structure. There exists a

small bonding between the capillary water and the cells due to capillary action, although this is small. The bound water consists of water molecules adsorbed onto cellulose molecules by hydrogen bonding. When all available sites are occupied with water molecules, the wood is said to be at fibre saturation point. For most wood this is about 30% of the dry weight (Simmons, 1983: p7).

The adsorbed water molecules are held with varying energies. Adsorbed water is held with the highest energy when the wood is nearly completely dry and decreases to zero at fibre saturation point. The equilibrium moisture content of wood is the bound water content when the sample is in equilibrium with its environment. It is a function of relative humidity and temperature and varies for different climatic regions (Todd, 1981: p1). Figures of the equilibrium moisture content of wood have been published for a number of different sites in South Africa (van Vuuren et al, 1978: p11). Van Vuuren et al report that air dried wood (dried for 6 to 12 months) in Cape Town has a moisture content of around 15% on a dry basis. Changes in humidity may cause variation in this value, but only within a range of three or four percentage points.

The moisture contained in wood has an important impact on the available energy in the combustion process. Natural wood has a moisture content (on a dry basis) of about 35% (Dadkhah-Nikoo & Bushnell, 1987: p130). When wood burns, this water has to be separated from the cell walls (if it is bound water), heated up to the combustion temperature and vapourized.

Another influence of moisture is to place a ceiling on the temperature of the core of the fuel particle until all the water is vaporized (Roberts, 1970: p180). Water vapour in the gaseous products flowing out of the sample also has the effect of lowering the flame temperature.

2.2 Physical and Thermal Properties of Wood

The combustion of wood will be influenced by certain physical and thermal properties of the wood and char structures. This discussion will cover the density, porosity, permeability, conductivity, shrinkage and calorific value of wood.

2.2.1 Density and porosity

A sample of wood consists of the solid material of the cell wall and the cell cavities which contain air, water and small quantities of resin and other substances. The specific gravity of the cell wall material has been found to be 1.46 (Siau, 1971: p4) and is constant for all wood species. However, owing to differences in anatomical structure, different species will contain different quantities of wood substance per unit volume, and so densities will vary among the species.

In addition to this, the density within one species may vary considerably. Wood laid on during the early years of a tree's life will be lighter than that laid on later (van Vuuren et al, 1978: p3). This results in a radial density gradient with lighter wood in the centre of the tree. This radial density gradient tends to decrease with the height from the base.

Tables giving the green density and density at 10% moisture content of a wide range of trees grown in South Africa have been published (van Vuuren et al, 1978; Otto et al, 1977).

The porosity (ratio of the volume of pores to the volume occupied by the cell walls) of wood is in the range 0.4 to 0.75. The specific gravity of real wood is influenced by the porosity and the moisture content (Murty Kanury, 1970[a]: p342):

$$\varrho_{spec} = \frac{1.5\,(1-\phi)}{1 + 0.0135\,MC_{dry}\,(1-\phi)}$$

2.2.2 Permeability

Permeability in wood is very much a function of the wood structure. The size and number of vessels, tracheids and pits has considerable impact on both longitudinal and transverse permeability.

From Darcy's law the permeability of a gas may be defined by (Siau, 1971: p41):

$$k_g = \frac{V L P}{t A dP P_{ave}}$$

where k_g = permeability of gas ($cm^{3}_{[gas]}.cm.dyne^{-1}.s^{-1}$),
V = volume of gas (cm^3) which flows through a tube of area A (cm^2), length L (cm) in time t (s),
P = pressure at which volume V is measured ($dyne.cm^{-2}$)
dP = the pressure difference between upstream and downstream ends of the specimen ($dyne.cm^{-2}$),
P_{ave} = average pressure in the specimen ($dyne.cm^{-2}$).

Specific permeability, K_g (cm^2) is given by the product of permeability, k_g and viscosity of the fluid concerned, υ ($dyne.sec.cm^{-2}$):

$$K_g = k_g \upsilon$$

The range in wood permeability is in the region of 10^8:1. Table 2.2 shows the permeabilities of a few woods.

Permeabilities in the transverse direction are considerably lower than those in the longitudinal direction. This is more noticeable in hardwoods where the effect of vessels is to increase the longitudinal permeability.

Generally sapwood has a greater permeability than heartwood. Also hardwood has a greater longitudinal permeability than softwood, although their transverse permeabilities are approximately the same.

Permeability ($cm^3_{[air]}.cm.dyne^{-1}.s^{-1}$)	Species
Longitudinal	
10^{-2}	Red Oak
10^{-3}	Bass Wood
10^{-4}	Maple, Pine (sapwood)
10^{-5}	Spruces (sapwood), Cedars (sapwood)
10^{-6}	White Oak (heartwood)
10^{-7}	Beech (heartwood), Cedars (heartwood)
Transverse	
10^{-8}	
10^{-9}	(species order as for long. perm.)
10^{-10}	

(Source: Siau, 1971: p55)

Table 2.2: Permeabilities for Selected Species

2.2.3 Conductivity and heat capacity

The transfer of heat through a substance depends on the specific thermal conductivity, specific heat capacity and thermal diffusivity of the material. The conductivity of dry wood is low as the presence of air spaces in cells acts as insulation. The cellular structure also explains why heat is conducted two to three times as rapidly along the grain as compared to across the grain (Desch, 1968: p189). For the same reason dense woods conduct heat faster than light woods. The thermal conductivity of wood in the transverse direction is in the range 4 - 20 x 10^{-4} $J.cm^{-1}.K^{-1}.s^{-1}$ and in a longitudinal direction, in the range 10 - 50 x 10^{-4} $J.cm^{-1}.K^{-1}.s^{-1}$ (p346, Murty Kanury & Blackshear, 1970[a]).

The moisture content has an effect on the thermal conductivity of wood since the presence of moisture increases the rate of heat transfer from the surface to the interior.

The specific heat capacity of wood is about 50% higher than that of air, i.e. about 1.5 $kJ.kg^{-1}.K^{-1}$. This high specific heat tends to decrease the rate at which heat is transferred (Siau, 1971: p70).

2.2.4 Thermal diffusivity

Figures for the thermal diffusivity of selected species are reported by Murty Kanury & Blackshear (1970[a]: p346). Diffusivity along the grain was found to be two to three times higher than across the grain. For sixteen species the average diffusivity across the grain was 3.7×10^{-4} $cm^2.s^{-1}$ with a range from 0.84×10^{-4} to 7.2×10^{-4} $cm^2.s^{-1}$. There is less information available for diffusivity along the grain but for the six species covered by Murty Kanury's report the average diffusivity was 7.8×10^{-4} $cm^2.s^{-1}$. Table 2.3 reports the diffusivities for species where both transverse and longitudinal diffusivity are known. Murty Kanury reported that diffusivity did not vary with temperature or moisture content.

Wood	Density ($g.cm^{-3}$)	D_{trans} ($cm^2.s^{-1}$)	D_{long} ($cm^2.s^{-1}$)
Oak	0.82	5.0×10^{-4}	8.6×10^{-4}
Teak	0.64	4.2×10^{-4}	9.1×10^{-4}
Ash	0.74	4.1×10^{-4}	7.4×10^{-4}
Mahogony	0.70	3.8×10^{-4}	7.4×10^{-4}
Fir	0.54	3.3×10^{-4}	8.1×10^{-4}
Pine, white	0.45	2.6×10^{-4}	6.2×10^{-4}

(Source: Murty Kanury & Blackshear, 1970[a]: p346)

Table 2.3: Thermal Diffusivity of Selected Species

2.2.5 Shrinkage

Green wood undergoes significant shrinkage as it dries to equilibrium moisture content. Wood is an anisotropic material and generally shrinks about twice as much tangentially as it does radially, and very little longitudinally. Tables of longitudinal, tangential and radial shrinkage during drying have been published for a wide range of species (van Vuuren et al, 1978).

One of the effects of heating on wood is to cause further shrinkage which can result in mechanical failure. As the temperature increases, bound water is lost causing the whole structure to contract. During combustion, the stresses induced by shrinkage and high pressures may cause the wood to split and crack. This has important consequences in the combustion process as it allows

2.2.7 Calorific value

The calorific value of wood is the quantity of energy that can be released during combustion. There are two measurements of calorific value: the high (or gross) and the low (or nett) value. The former is where all the water formed during combustion is condensed to liquid form. The low calorific value is less than this by the latent heat of vaporization of the water.

Extensive tests have been performed on a wide range of South African grown species to determine their calorific values (Eberhard, 1987). The results are summarized in table 2.4.

Wood Type	No. Samples	Range ($MJ.kg^{-1}$)	Mean ($MJ.kg^{-1}$)
All woods	230	18.34 - 22.49	19.80
Heartwood	115	18.34 - 22.49	19.88
Sapwood	115	18.83 - 21.09	19.73
Hardwood	86	18.77 - 20.97	19.70
Softwood	13	20.07 - 21.25	20.43

(Source: Eberhard, 1987: p2)

Table 2.4: Gross Calorific Value of S A Grown Trees

It is clear that the calorific value of wood on a mass basis varies very little. This may be due to the fact that the chemical composition of wood varies very little. The gross calorific value may be described in terms of the constituent elements (Eberhard, 1987: p16):

$$C.V.(gross) = 1624\,H + 518.5\,C + 1.05\,O^2 - 17860\ KJ/kg$$

where H, C, O are the percentages of hydrogen, carbon and oxygen respectively. (This equation assumes that there is no moisture or sulphur present and that the nitrogen content is 1%).

Using a composition of C = 50%, H = 6% and O = 43% gives a calorific value of 19.75 $MJ.kg^{-1}$, very close to the experimentally determined results.

On a volumetric basis, different woods will have wide ranging calorific values due to differences in density.

2.3 Behaviour of Wood During Combustion

This section is intended to give a brief overview of the different processes and stages in wood combustion. Chapters three and four give more detail and review the literature concerning modeling and kinetics of devolatilisation and char combustion.

Wood combustion occurs through the following stages (Murty Kanury, 1972[b]: p76):

i) driving of moisture from the sample,
ii) devolatilization of non-pyrolysis products,
iii) pyrolysis of constituents,
iv) transfer of pyrolysis products to the boundary layer and combustion of the vapours,
v) combustion of the char.

For the sake of simplicity, these steps will be described as if they occurred independently and sequentially. In the real case of a burning fire, different stages will be occurring simultaneously in different parts of the wood.

2.3.1 Drying of the sample

When an elemental volume of wood is introduced into a hot gas stream, heat is convected and radiated to the sample surface. Some of this heat is reflected and re-radiated back to the surrounding space, the rest is conducted into the sample. At this stage, the heat transfer into the sample is governed by pure conduction (Murty Kanury, 1972[a]: p135). The conductivity of wood is however anisotropic and the rate of heat transfer is affected by the orientation of the wood fibres. The conduction of heat into the particle is maintained by the temperature gradient that is set up between the sample surface and the centre.

Once the boiling point of water is reached, drying begins to take place rapidly. Capillary water vaporizes in the regions where the temperature is high enough. Bound water is also separated from the cellulose and is vaporized. As temperatures inside the sample increase, all the water will vaporize and move out.

2.3.2 Devolatilization of non-pyrolysis products

The extractives present in the wood are vaporized as the temperature inside the wood increases. The different substances have different boiling points and so will be removed at different temperatures. The vapours flow out of the sample and may combust in the boundary layer surrounding the sample. The volume of this constituent of the wood is small by comparison and these volatiles are rapidly removed (Simmons, 1983: p12).

2.3.3 Pyrolysis of wood constituents

Devolatilisation of pyrolysis products refers to the production and release of volatiles from the organic constituents of wood. It involves a complex series of reactions which decompose the hydrocarbons present. The factors which affect the pyrolysis process are temperature, chemical composition, physical structure as well as catalytic and autocatalytic effects (Roberts, 1971[a]: p893).

The large number of reactions involved in pyrolysis can be grouped into primary and secondary pyrolysis. The primary reactions are dependent only on temperature whereas the secondary reactions occur as a result of catalytic or autocatalytic effects. Thus they are influenced by other factors such as residence time, gas-solid interactions etc. (Pyle & Zaror, 1984: p148).

Pyrolysis of wood occurs over a broad temperature range. Cellulose decomposes in a temperature range of 330°C - 380°C. The characteristic product is levoglucosan with yields of above 50%. Hemicelluloses react between 230°C and 330°C and follow a similar pyrolysis path to that of cellulose (Simmons, 1983: p14). However, they tend to yield more gases and less tar. Also no levoglucosan is produced. Lignin undergoes pyrolysis over a

greater temperature range, 250°C - 500°C. Product yields tend to be high in char (around 55%) (Simmons, 1983: p15). Hemicellulose is the most reactive and lignin the least reactive of the wood constituents (Roberts, 1970: p264).

There is considerable disagreement over the heat of reaction of pyrolysis. Published estimates vary from an endothermic value of 370 J/g to an exothermic value of -1700 J/g (Roberts, 1971[b]: p79). The reasons for this spread in reported figures lie in the differing contributions of the components of wood and the sensitivity of wood pyrolysis to the conditions of combustion.

2.3.4 Transfer and combustion of volatiles

Once formed, the pyrolysis products diffuse either into the sample or towards the surface. As they move towards the cooler inner regions, they may condense. As the interior temperatures increase, the substances will revaporize. This will manifest itself as an endothermic process in the wood. Those vapours which migrate towards the surface will set up a convection opposite to the heat conduction already present (Pyle & Zaror, 1984: p148). Since the wood structure affects the porosity and permeability of wood, the magnitude of this effect will vary from species to species. The convection effect increases as the size of the particle increases (Murty Kanury & Blackshear, 1970[b]: p7).

The pyrolysis products and other gases eventually migrate to the boundary layer surrounding the sample, where they serve as fuel for flaming combustion. This fuel is composed of short-chained hydrocarbons, vaporized tars, CO_2, CO, H_2 and water vapour (Simmons, 1983: p15). When temperatures are sufficiently high and the correct air/fuel mix is attained, the volatiles will ignite. This combustion now serves as the major heat source to the particle.

2.3.5 Combustion of char

The residue of the pyrolysis process is char and ash. The char (composed primarily of carbon) can react with a number of gases: O_2, H_2, H_2O and CO_2. Although the O_2 reaction is dominant, the carbon/water vapour interaction can be important (Simmons, 1983: p17).

There are five steps involved in the char reaction process:

i) transfer of heat and mass across the boundary layer around the particle,
ii) transfer of mass and heat through the porous structure,
iii) reactions within the structure,
iv) transfer of gaseous products out of the structure and
v) transfer of these products across the boundary layer.

The rate limiting step depends on the air stream conditions, the properties of the char and the intrinsic chemical kinetics.

Heat transfer across the boundary layer is accomplished by a combination of radiation, conduction and convection. Where the particle is suspended in a hot air stream, convective transfer is dominant. Reactant mass transfer may be modeled by a simple form of Fick's law (Laurendeau, 1978: p247).

Within the particle, transfer of mass and heat depends very much on the conditions of combustion and the structure of the particle. There are two types of approaches to modeling this process: either through pore diffusion models or macroscopic models, where Fick's law is used with an effective diffusivity.

The influence of internal mass transport on overall reactivity depends very much on combustion conditions. Where the chemical reaction within the particle is slow there will be a constant reactant concentration across the boundary layer and throughout the particle. In this case the intrinsic chemical kinetics control the process. Where the chemical reaction is faster, or where diffusion through the particle is slow, internal mass transport becomes significant and can become the limiting step. Lastly, where chemical kinetics and internal diffusion are fast, boundary layer diffusion becomes the controlling step.

2.4 Selection of a Good Fuelwood

2.4.1 Fuelwood preferences

A number of studies have investigated the fuelwood preferences expressed by people in different parts of the country. Eberhard (1986[a]) collected anecdotal information from six villages located in Ciskei, Transkei, eastern Transvaal and the north-west Transvaal. Gandar (1983) conducted fuelwood investigations in Kwazulu and Cunningham (1984) reported on wood consumption in northern Kwazulu/Natal. Other areas researched include regions in Botswana (Kgathi, 1984), Swaziland (Gwitta-Magumba, 1983) and Gazankulu (Liegme, 1983). Archer (1988) has collected detailed information on fuelwood preferences and wood collection from a number of areas in Namaqualand.

Most reports suggest that there is a high degree of selectivity when wood is collected. Liegme (1983) reports that three of the forty-two species collected in Gazankulu made up 77% of the total weight collected. Archer (1988) reports that Rhus undulata is by far the most popular fuelwood in Namaqualand and where it is available constitutes the greatest mass of collected wood bundles. Generally the preferred species for fuelwood are hardwoods with a relatively high density.

A comprehensive summary of anecdotal information concerning fuelwood preferences around southern Africa (up until 1987) is presented by Eberhard[2] (1987: Appendix A).

2 This does not include the work by Archer (1988).

2.4.2 Species Selection

Poynton (1984: p18) lists the important qualities to be looked for in a tree grown for fuelwood as being:

i) well suited to the local climate, unless grown under irrigation;
ii) capable of adapting to the edaphic conditions of the site;
iii) cheap and easy to establish;
iv) of vigorous growth;
v) amenable to management in woodlots;
vi) able to regenerate naturally;
vii) possessed of good burning properties.

Poynton further describes the attributes looked for in a firewood as being (1984: p20)

> "a capacity for prolonged, steady burning without emitting sparks, excessive smoke or noxious vapours and for making long-persistent, glowing coals which at length disintegrate to leave nothing but fine ash. A moderate density and ease of cleaving are additional recommendations. Light, resinous woods which are quickly consumed in a fire and fail to produce long-lived coals do not in this sense constitute particularly good firewoods although they may be useful for kindling."

It is not only the positive combustion properties of wood that determine its popularity as a fuel. Some species have considerable drawbacks that detract from its usefulness. The presence of thorns on the sample is a hindrance to collection and management of the wood. Gleditsia triacanthos (Honey Locust) for example has persistent spines on its stem (Eberhard & Poynton, 1986: p28.9). Similarly, some species have a powdery bark that can act as an irritant to the collector. The hardness of the wood affects the ease with which it can be chopped or broken into suitably sized pieces. Robinia pseudoacacia (Black Locust) for example has extremely hard heartwood (Eberhard & Poynton, 1986: p28.9).

Wood species that are susceptible to insect activity such as borer beetle are unpopular as they cannot be stored. Similarly, species that are light and porous and so collect sand and dirt if stored are unpopular and so usually avoided unless used immediately..

Another factor that affects the choice of a species is the quantity of smoke that is produced. Eucalyptus species grown in woodlots around Leliefontein in Namaqualand are unpopular because of the smell of the smoke which is considered to affect the taste of the food (Archer, 1988). Other species that are unpopular due to the smoke production are Spirostachys africana and Euphorbia tirucalli (Gandar, 1983).

In addition certain species are avoided as fuels since there exist certain beliefs surrounding their use. In Kwazulu Euclea species are believed to cause family strife while Vangueria infausta and Diospyros lycioides are held to attract lightening (Gandar, 1983).

2.4.3 The different uses of fuelwood

Wood is collected for use in a variety of different situations. Whether the wood is to be used as kindling, for cooking or for providing lasting warmth affects the type of tree that will be collected. In some cases a tree may be valued for reasons other than its fuel potential, for example the production of fruit, nuts or fodder for animals, the provision shade and the production of poles for fences and construction. This discussion will cover the desirable properties of wood for use in the combustion context.

Kindling

Archer (1988) reports that people in Namaqualand clearly differentiated between wood for kindling and wood for the main fire. The properties of good kindling are that it should be light, porous, ignite easily and burn with an intense flame.

The presence of resins and other extractives improves the flammability of the wood and is a desirable quality in kindling. The ability of a wood species to

ignite even when damp makes it useful for this purpose. Sarocaulon spp. (Boesmankers or Bushman's candle) are collected in Namaqualand specifically for kindling as it ignites easily, even when wet (Archer, 1988: p6).

Kindling is usually collected in the form of small twigs and chips. Thus a species that produces many small sticks will be popular.

Wood for cooking and heat

The most valued property of wood for these purposes is the ability to produce coals that burn slowly and steadily. Wood species that produce char which crumbles and burns quickly are not useful for domestic fires.

The rate of devolatilisation may affect the splitting and crackiing of the char. This is because the production of volatile gases results in a pressure build up inside the sample. This pressure can then cause the wood to splinter and crack.

Density is probably the most important property. A denser wood will release more energy on a volumetric basis as well as producing larger and denser coals. Most species indicated in the literature as being preferred for fuel are reasonably dense.

Since the presence of moisture in wood reduces the useful energy content and inhibits its ignition, the drying properties of a species are important. A wood that dries easily and quickly will make a better fuel than one that stays damp for a long time.

Two important factors that determine the heat generation of the fire are ventilation of the hearth/stove and heat retention around the fire. For an open fire made without a stove, these factors are especially important. Thus the choice of a species that will form sizeable coals which retain the heat is more critical for open fires.

The form of the wood produced by a tree is also significant. The tree must produce sticks that are easily handled yet large enough to produce good coals.

Crooked and branchy pieces of wood are difficult to carry and stack. Where a fire is built for warmth and space heating, large heavy pieces of wood are favoured as they will burn for a long time. The root base of a tree is popular for this.

2.5 A Scientific Description of Fuelwood

This discussion has highlighted some of the useful fuel properties of wood. These are listed and summarized below.

i) Flammability:
A good kindling must be highly flammable and ignite easily even when damp. This property will be affected by the internal structure and chemical composition as well as the size and form of the wood.

ii) Char formation:
A good firewood will produce large quantities of coals that do not crumble. This property is probably related to the density of the wood as well as its tendency to split and crack.

iii) Char burning:
The coals formed by the wood should burn slowly and steadily and produce a long lasting heat. These characteristics probably depend both on the reactivity of the actual char and on the size and density of the chars formed.

iv) Drying:
Since the presence of moisture negatively affects the combustion of wood, a valued property must be the speed of drying. Although this will be dependent on the sample size, it will also be affected by the permeability of the wood.

v) Quantity of heat released and char formed:
Although all wood species have a similar calorific value and the production of char is more or less consistent on a mass basis, the different densities of wood will mean that similar size particles will produce ranging quantities of heat released and char formed.

In addition to these properties, other factors will influence the usefulness of a wood species. Examples of these other properties are the production of dead wood, the form of the wood, the presence of thorns and the level of smoke production.

The processes in devolatilisation and char combustion involve a combination of mass and heat transfer effects as well as the intrinsic kinetics of the reactions. Chapters three and four will review these processes in more detail and report on the existing literature concerning modeling attempts and experimentally determined results.

3.1 Pyrolysis Kinetics

3.1.1 Pyrolysis mechanisms

Pyrolysis is a term which covers a large and complex series of reactions. The path which these reactions take is not fixed and can vary considerably under different conditions.

The three main constituents of wood (cellulose, hemicellulose and lignin) have quite different reaction kinetics. Hemicellulose is the most reactive and lignin the least. Each compound decomposes in a different temperature range. Also the actual course of the pyrolysis reactions is extremely sensitive to catalytic and autocatalytic effects. Vovelle et al (1982) examine the pyrolysis of wood in two stages: the first relates to hemicellulose and the second to cellulose pyrolysis. The two stages yield activation energies of 84 kJ/mol and 230-250 kJ/mol respectively. However, they conclude that pyrolysis of different constituents does overlap, implying that an overall activation energy can be obtained, which will be less than that for cellulose.

Traces of other materials may promote an alternative reaction path with half the activation energy (Roberts, 1970: p270). Lignin in particular is extremely sensitive to the presence of inorganic salts.

Despite this, it is common to combine the different constituents together as a single reactant (Alves & Figueiredo, 1988: p124). Another simplifying step is to group the reactions into primary and secondary pyrolysis. Primary pyrolysis constitutes the initial gasification reactions which transform the solid reactants into gaseous volatiles. Murty Kanury and Blackshear (1970[a]: p350) suggest that these initial reactions are followed by a very fast exothermic rearrangement of the gaseous products. These reactions are also part of the initial primary pyrolysis. The secondary reactions that can then occur depend very much on the conditions of combustion. They will be influenced by such factors as residence time, temperature and gas-solid interactions. The physical structure of wood restricts the movement of heat and product gases, although this restraint is more significant for temperatures

below 320°C. Because of this, the structure of the wood will affect secondary pyrolysis.

The primary and secondary reactions can be represented by figure 3.1.

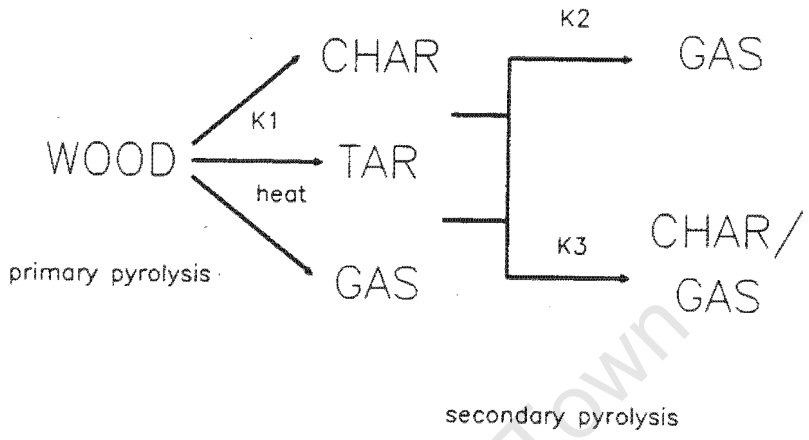

Figure 3.1: Primary and Secondary Pyrolysis

Whether path two or three above occurs depends on the permeability of the wood (Eberhard, 1987: p20). Reaction two is favoured where the wood sample has a lower permeability and results in less char being formed.

3.1.2 Thermal decomposition kinetics

The rate of mass loss during pyrolysis is dependent on both the temperature of the sample and the amount of solid reactant remaining. This is expressed by equation 3.1:

$$-dm/dt = \mathcal{A}(m-m_f)^n \exp(-E/\mathcal{R}T) \quad \ldots\ldots\ldots\ldots 3.1$$

If the reaction occurs isothermally, then the rate constant k can be used, where

$$k = \mathcal{A} \exp(-E/\mathcal{R}T) \quad \ldots\ldots\ldots\ldots\ldots\ldots 3.2$$

Assuming first order, i.e. n = 1, and using the substitution:

$$M = (m-m_f)/(m_o-m_f) \quad \ldots\ldots\ldots\ldots\ldots\ldots 3.3$$

then equation 3.1 becomes

$$dM/dt = -k M \quad \ldots\ldots\ldots\ldots\ldots\ldots\ldots\ldots 3.4$$

Applying equations 3.4 and 3.2 to pyrolysis as a whole implies that all the different reactions and the decomposition of the different constituents are considered together. Thus the reaction rates and activation energies are described as "pseudo" rate constants and "apparent" activation energies.

Alternatively, the decomposition of the different constituents can be treated independently. In this case equations 3.4 and 3.2 are applied to the reactions of each constituent. In this way rate constants and activation energies apply to each constituent only.

The formulation of the above equations has two assumptions implicit. Firstly that pyrolysis follows first order kinetics and secondly that dependence on temperature follows the Arrhenius form (equation 3.2). Not all researchers agree on the use of these two assumptions. Roberts (1970) reports that several investigations found a zero order reaction law for the first stage of pyrolysis, followed by a first order law. However, in these cases the zero order relationship applied only to the first 2% - 6% of the total mass loss.

Brown (1982) criticises the wide usage of the Arrhenius equation to relate reaction rate to temperature. He suggests that a compensation effect (a linear relationship between E and ln[A]) is apparent and so affects the analysis of the data). This effect makes the Arrhenius equation appear suitable when in fact another relation should be used. In two papers Agrawal (1985[a], 1985[b]) considers the application of the Arrhenius equation to a number of data sets. He concludes that there is no compensation effect and that although the Arrhenius equation has little physical significance, it is still a useful relationship to model cellulose and wood pyrolysis kinetics (Agrawal, 1985[b]: p51).

3.1.3 Heat of reaction

There exists considerable dispute over the value of the heat of reaction in pyrolysis. Roberts (1971[b]) notes that values ranging from 370 J/g (endothermic) to -1700 J/g (exothermic) have been reported in the literature. The range in the reported values may have its origin in the combustion conditions under which the measurements were made as well as the influence of secondary reactions.

Roberts (1971[b]) examines the various factors possibly affecting the heat of reaction in a pyrolysing wood sample. Firstly it should be noted that the presence of oxygen in the surrounding air stream does not have an influence. This is because the movement of gases out of the wood structure prevents the oxygen from entering the sample. The factors which can influence the heat of reaction are listed below.

i) Catalytic and autocatalytic effects can affect the rate and course of pyrolysis reactions.
ii) The ratio of lignin to cellulose can have an effect. Lignin undergoes pyrolysis more slowly than cellulose at temperatures greater than 340°C and its pyrolysis is not sensitive to autocatalytic effects.
iii) The structure of wood prevents the product gases from being removed quickly. Until temperatures are high enough to cause fissuring, this promotes autocatalysis.
iv) If the rate of heating is low or the solid is only heated to low temperatures, then the kinetics of pyrolysis will be highly sensitive to the combustion conditions.

Tinney (1965) assumed that two consecutive reactions took place, each having different kinetic constants. Values of -84 to -126 J/g (g = gram of product gases) were obtained for the first stage and -840 to -2100 J/g for the second stage were obtained. Roberts (1971[b]) suggests that the first range of values applies to the pyrolysis of cellulose and the second range applies to lignin.

Lee et al (1976) conducted a series of experiments using a constant surface heat flux applied both parallel and perpendicular to the grain. It was found that there are three zones of pyrolysis. Firstly there is an endothermic pre-pyrolysis stage, associated with early pyrolysis of lignin and hemicellulose.

This first stage is in the temperature range less than 250°C. This is followed by an exothermic second stage in the range 250°C to 340°C. Here the wood is undergoing active pyrolysis with the possibility of secondary reactions occurring. In this temperature range, lignin and hemicellulose decompose and the onset of cellulose pyrolysis occurs. The third zone is again endothermic and is in the temperature range 340°C to 520°C. Lee et al speculate that the endothermicity of this phase is due to the continued endothermic decomposition of cellulose, and the appearance of numerous fissures allows gases to escape thereby restricting the extent of secondary reactions.

Lee et al measured the heats of reactions of these three phases separately for different surface heat fluxes. An overall heat of reaction was then obtained by weighting each heat of reaction by the mass loss rate of the corresponding phase. It was found that this overall heat of reaction was strongly dependent on heating rates. This is summarized in the table below.

Surface Heating Rate $J.cm^{-2}.s^{-1}$		Heat of Combustion J/g			
3.18	(∥)	528	to	611	(endothermic)
8.37	(∥)	-104	to	-384	(exothermic)
8.37	(⊥)	-1716	to	-1089	(exothermic)

(source: Lee et al, 1976)

∥ = heating applied parallel to the grain.

⊥ = heating applied perpendicular to the grain.

Table 3.1: Heats of Combustion for Pyrolysis

Lee et al suggest that the exothermicity of higher heating rates is due to the promotion of secondary reactions by the higher temperatures in the solid.

Roberts (1971[b]) concludes that for situations where the combustion temperature is above 320°C, the heat of reaction is approximately constant at -160 to -240 J per gram of products formed. This heat of reaction is due only to primary pyrolysis. Secondary reactions are not important as the product gases are not trapped in the wood structure at these temperatures. However, for lower temperatures secondary reactions come into play as the product gases remain in the wood structure for a significant time period. This means that

heats of reaction may rise to an exothermic value of 1600 J/g and are strongly dependent on the conditions of combustion.

3.1.4 Experimentally determined kinetics data

For larger samples, the block of wood can be divided into four regions. Firstly there is the innermost region with the lowest temperature. Here the wood structure is intact and autocatalysis is occurring. Secondly there is a region where the wood has splintered, allowing gases to escape. Here autocatalysis is reduced and the most reactive constituents are undergoing pyrolysis. Thirdly, a region where pyrolysis of cellulose and hemicellulose is complete and only lignin is reacting. Lastly there is a region where all the wood has been pyrolysed to char, but where there may be secondary reactions of the product gases occurring. The values of the overall kinetic parameters will be influenced by the dominance of any one of these regions.

A s^{-1}	E (kJ/mol)	Comments	Source
4.0×10^{17}	234	**Group 1**	Brown(1982)
-	278	Temp range: 297-1100°C	Nunn et al (1985)
-	230 - 250	Cellulose constituent	Vovelle et al (1982)
7.0×10^{16}	226	Temp: 325-350°C	Agrawal (1985[a])
6.5×10^{16}	226	High temp: 1st order	Murty Kanury (1970[b])
7.0×10^{8}	126	**Group 2**	Brown (1982)
6.8×10^{9}	139		Lewellen et al (1977)
5.3×10^{8}	138		Bamford et al (1946)
5.3×10^{7}	125		Kung (1972)
1.0×10^{8}	125		Belleville et al (1984)
1.5×10^{3}	63	**Group 3**	Brown (1982)
3.0×10^{5}	96	Temp: 280-325°C	Agrawal (1985[a])
3.2×10^{5}	96	Low temp, 0th order	Murty Kanury (1970[b])
-	84		Vovelle et al (1982)
1.4×10^{7}	79		Murty Kanury (1972[b])
$2\text{-}3 \times 10^{3}$	66 - 69		Pyle & Zaror (1984)
-	48 - 89	Order: 1.9 -3.2	Duvvuri et al(1975)
730	65	Temp range: 357-525	Becker et al (1984)

Table 3.2: Kinetics Data for Pyrolysis

Brown (1982) suggests that there are three sets of results. The data presented in table 3.2 is grouped into these sets.

The kinetics of pyrolysis is only one part of the process of devolatilisation. In the cases where other steps are dominant, kinetics are irrelevant and reactions essentially proceed instantaneously. There are a number of other secondary physio-chemical effects which can affect the overall devolatilisation process. These are outlined in the next section.

3.2 The Secondary Effects in Wood Combustion

When considering the diffusion and penetration of heat into the burning sample, a number of secondary effects come into play. Early studies (Bamford et al, 1946; Murty Kanury, 1972[a]) only consider conduction through a uniform structure as the heat transfer mechanism. However, the influence of convection effects, variation of thermal properties and the possibility of mechanical failure affect the heat transfer process. Another consideration is the effect of the particle size on the different stages of devolatilisation and on the rate controlling step.

Different models go to different lengths in incorporating these secondary physio-chemical effects. The choice (or determination) of the relevant heat transfer properties of the wood and char also differs from study to study, as do the choice of pertinent chemical kinetics parameters and the complexity of the governing equations. Further, not all studies include the influence of convective heat transfer.

3.2.1 Particle size

For pyrolysis to be purely kinetically controlled, with heat transfer effects playing an insignificant role, the particle dimensions must be less than 0.2 mm (Simmons and Gentry, 1986: p117). Above this size, heat transfer effects are combined with chemical kinetics to control the pyrolysis process. Paticle size affects the thermal gradients inside the sample. These can particularly be

significant during devolatilisation. Becker et al (1984) investigated the combustion of thin (1.6 mm thick slabs) and thick (8 - 50 mm diameter branches) samples to establish the nature of controlling mechanisms. For the thin slabs at low temperatures, the process was controlled by first order chemical kinetics. At higher temperatures, a more complex three stage regime was recognised, each stage having a different rate constant. For thick samples at low temperatures, pyrolysis and heat transfer were found not to be very strongly coupled. The temperature distribution was calculated as though no reaction was occurring and the reaction rate calculated on the basis of this temperature distribution. The mass loss predicted in this way was found to match the experimental results adequately.

The total reaction time is also strongly dependent on the size of the sample (Ragland et al, 1988). The fact that a thicker slab generates more char is probably due to the fact that pyrolysis proceeds slower, tar collects and then undergoes reactions to yield products with a high char component (Belleville & Capart, 1984). Blackshear and Murty Kanury (1970) propose a relationship relating mass loss to particle size of the form:

$$\frac{\text{mass}}{\text{initial mass}} \quad \alpha \quad \frac{\text{time}}{(\text{diameter})^{1.6}}$$

Steward et al (1980/81) also report a similar result, but find that the power relationship varies between 1.3 and 1.5 depending on the type of wood used.

In a model form where heat is transferred into the sample as a thermal wave, Blackshear and Murty Kanury (1970) report that the thermal wave propagation is related to time/(diameter)^2. It is suggested that this difference is a consequence of the interaction of heat conduction with reaction rate kinetics.

3.2.2 Convection effects

Initially when the wood is being heated and has not yet begun to undergo thermal decomposition, the heat transfer inside the sample is described by pure heat conduction (Murty Kanury, 1972[a]: p135). Although most models assume cross-grain conduction, wood does have anisotropic thermal properties and conduction will be faster along the grain.

When a layer of pyrolysing solid has been formed, other effects come into play. The volatile products may move inwards, in which case their condensation and later revaporization will affect the temperature inside the sample (Kansa et al, 1977: p312). Alternatively, the vapours may diffuse towards the surface, in doing so setting up a convection opposite in direction to that of the heat conduction (Murty Kanury, 1971: p193).

In order to assess the relative importance of convection effects, it is helpful to obtain an expression governing the ratio of convection to conduction. This is given by Murty Kanury and Blackshear (1970[b]) as:

$$\frac{\text{energy flux by convection}}{\text{heat transfer by conduction}} = \frac{C_g(\varrho v)L}{\mathcal{K}_s}$$

where C_g = specific heat of gas [$J.g^{-1}.K^{-1}$]
ϱ = density [$g.cm^{-3}$]
v = velocity [$m.s^{-1}$]
L = characteristic length [cm]
$\mathcal{K}_s$ = conductivity of porous solid [$J.cm^{-1}.K^{-1}.s^{-1}$]

For convection effects to be negligible, this ratio should be considerably less than unity. If however this is not the case, a neglect of convection would result in an overestimation of the rate of heat transfer into the solid.

Murty Kanury and Blackshear (1970[b]) estimated values of $C_g(\varrho v)L/K_s$ from the literature as well as conducting a series of experiments. In all cases, the values obtained were greater than 0.1, and reached as high as 11. This indicates that convection effects should be included in modelling attempts. It is also interesting to note that as the size of the sample increased (the

characteristic length ranged from 0.4 to 5 cm), the relative importance of convection increased.

To incorporate the effects of forced convection, it is necessary to include a convection term in the gas energy equation as well as including a gas momentum equation (Darcy's law). These considerations introduce the velocity and pressure of the gas as additional variables. These variables can be related by a continuity equation and an equation of state for the gas (Kansa et al, 1977).

3.2.3 Thermal properties

Another important effect is the variation of the thermal properties of the sample as charring occurs. It is likely that the overwhelming influence on these properties is density. A possible way of describing this dependence is by weighting the properties of air and char by their volume fraction (p347, Murty Kanury, 1970[a]).

If oxygen has diffused into the structure, combustion of the pyrolysis products may occur. However if the boundary layer is flaming, then oxygen cannot penetrate the sample. The flame itself is a major heat source for the wood sample. An effect of moisture being released from the sample is to lower the flame temperature and so reduce the flame-solid heat transfer.

3.2.4 Mechanical failure

As the combustion process continues and moisture is removed, the sample may undergo shrinking. This effect together with the high temperatures and pressures of trapped gases put the sample under considerable stresses.

These stresses may cause the wood and char to fail mechanically. This affects heat transfer and mass transfer into and out of the sample. For a fissured region, heat transfer no longer takes place across a plane surface. Instead radiation and convection can penetrate into the solid via the cracks. It is also likely that gaseous products will move into the fissures and be removed from the sample (Roberts, 1971[a]: p844).

3.3 Mathematical Models

3.3.1 Overview of devolatilisation models

The essential stages in devolatilisation were outlined in section 2.3. The processes involved in these stages are: transfer of heat across the boundary layer and into the sample; diffusion of water vapour and vapourised extractives out of the sample; pyrolysis reactions and diffusion of pyrolysis products out of the sample.

Models of these processes firstly describe the heat flow across the boundary layer and into the wood. Next the heat penetration into the wood and the temperature profile within the sample are considered. The description used for this determines where in the sample the pyrolysis reactions are located. Thirdly the kinetics of the reactions are described, usually using first order equations.

The form of the model used depends on whether any of the three processes listed above are assumed to be rate limiting. Pyle and Zaror (1984) examine the form the model must take under different rate limiting conditions.

In the case where external heat transfer is the rate limiting step, the temperature through the sample will be uniform. Under these conditions the reaction zone can extend throughout the sample, provided the temperature is high enough. This situation will arise when diffusion through the sample is fast.

Where there is a slow rate of internal heat transfer, accompanied by relatively fast kinetics, the pyrolysis reactions will be restricted to a narrow reaction front. This front then propagates into the sample leaving a shell of char. Inside the sample there will be steep temperature gradients. Murty Kanury (1972[a]) assumes these conditions to construct "a simple thermal model" of devolatilisation.

Where both the heat transfer to and within the sample are fast, the kinetics of pyrolysis will constitute the rate limiting step. In this case the solid temperature will be the same as the external environment and the process will occur isothermally. Under these conditions pyrolysis reactions extend throughout the sample.

Lastly there is the general case where none of the three processes are assumed to be rate limiting. Under these circumstances the wood must be described by a changing temperature profile combined with a moving region of pyrolysis. In this case both temperature and the location of pyrolysis are functions of space and time. The first model of this general form was presented by Bamford et al in 1946.

Pyle and Zaror (1984) describe the basic descriptive equations that are required to model the processes of combustion. These include an equation describing the energy balance in a differential control volume and a mass loss equation describing the rate of thermal decomposition. It is also possible to include continuity equations and a gas phase momentum equation. The secondary physio-chemical effects which have been discussed above can be incorporated into this mathematical description. It is possible to introduce simplifications to these equations based on an assumption of what will form the rate limiting step.

Appropriate boundary and initial conditions are required, usually describing the heat flow into the sample at the boundary and the initial temperature state of the sample.

What follows is a review of the different models presented by in the literature.

3.3.2 Preheating and drying

The first stage in the combustion of wood is the heating and drying of the sample. The internal heat transfer during this stage is mainly through the mechanism of conduction although there will be some convective movement of moisture. The presence of moisture in wood can have a considerable effect on this pre-pyrolysis phase. When the temperature at a

point reaches the boiling point of water, it will remain at that temperature until all the water has evaporated. Energy must be supplied to provide the necessary latent heat. For example, air dried and natural wood would require around 338 and 790 J per gram of dry wood respectively. Many analyses assume that the wood has been dried beforehand.

This conduction controlled pre-pyrolysis phase ends when the decomposition reactions begin to occur. Most authors assume that this is when the solid reaches a critical temperature. Bamford et al (1946) however merely use the Arrhenius temperature dependence to limit the effect of pyrolysis during this early period.

Murty Kanury (1972[a]) divides the combustion process into three phases: a pre-heat phase, an "infinite body pyrolysis" phase and a "finite body pyrolysis" phase. The pre-heat phase starts when a heat flux is supplied to the surface of the wood and ends when the surface begins to pyrolyse, i.e. when the surface reaches a critical temperature. He argues that during this phase the steepest temperature gradients are found in a thermal layer near the surface. Thus the wood temperature outside this thermal layer can be considered to be at the initial temperature and the temperature profile inside the layer is linear. Drying occurs during this phase.

Simmons and Ragland (1986) obtained mass loss curves for wood samples with moisture contents varying from 0% to 200%. The presence of moisture reduces the burning rate throughout the whole combustion process. They conclude that drying and pyrolysis must be occurring simultaneously.

A common approach to account for water vaporisation is through the incorporation of a heat sink in an energy balance equation. Dadkhah-Nikoo and Bushnell (1987) include latent heat as an energy loss in a first law of thermodynamics equation. Similarly Shafizadeh and DeGroot (1977) incorporate an enthalpy change due to vaporisation. Ragland et al (1988) take this type of approach a step further by including a variable moisture content as water vapour will recondense in the cooler inner regions.

The most general way of accounting for moisture content is presented by Simmons (1983). Appropriate adjustments are made to the governing

equations to include the effect of drying. A rate of moisture evaporation term is added to the solid phase continuity equation. This accounts for the loss of mass in the solid structure as the moisture evaporates. A corresponding term is added to the gas continuity equation to account for the addition of water vapour to the gas flow. Thirdly, a heat sink is incorporated in the energy equation to account for the energy converted into latent heat of vaporization. The rate of moisture removal is described in terms of this heat sink. It is also necessary to keep track of the local moisture content to detect when all the moisture has been evaporated.

3.3.3 General models

The most general models attempt to describe the state of the wood sample at any time in the combustion process. They avoid assuming that any one of the separate processes involved is rate limiting.

The first of this type of model was formulated by Bamford et al (1946). In their analysis they used a heat conduction equation of the form:

$$\mathcal{K}\frac{\delta^2 T}{\delta^2 x} - q\frac{\delta \varrho}{\delta t} = c\,\varrho_w\frac{\delta T}{\delta t}$$

where $\mathcal{K}$ = thermal conductivity of wood [$J.cm^{-1}.K.s^{-1}$]
T = temperature [K]
ϱ = density of volatile products [$g.cm^{-3}$]
ϱ_w = density of unburnt wood [$g.cm^{-3}$]
q = pyrolysis heat of reaction (360 J used) [J]
c = specific heat of wood [$J.g^{-1}.K^{-1}$]

The term $q\,\delta\varrho/\delta t$ accounts for the heat released during pyrolysis. It is assumed that the rate of decomposition has a first order dependence:

$$\delta\varrho/\delta t = -\mathcal{A}\,\varrho\,\exp(-E/\mathcal{R}T)$$

The assumptions implicit in this formulation of the problem are (1) that the heat transfer is dominated by a conduction mechanism, (2) that the overall decomposition mechanism has an Arrhenius dependence with a heat of

reaction independent of temperature or oxygen supply and (3) that the thermal properties of wood, partially charred wood and char are the same. Since only an one dimensional model is used, the anisotropy of wood diffusivity is neglected and only cross grain flow is considered.

The initial conditions used by Bamford et al are that the initial temperature and volatile constituent mass is known and constant throughout the sample. The boundary condition at the flame-solid interface is that the heat flux into the wood is a result of forced convection and radiation to the surface and radiation from the surface. The dependence of this heat flux is limited to surface temperature determining outward radiation. The effect of varying volatile combustion rates in the flaming boundary layer is not considered.

The exclusion of heat transfer by convection of pyrolysis products can misrepresent the true rate of heat transfer. The model used by Petrella (1980) uses a heat balance equation which incorporates flame-solid interactions, external heat flux, heat losses and heat of reaction but excludes internal convective heat transfer. Kung (1972) however uses a model that incorporates (1) transient conduction, (2) internal heat convection of volatiles, (3) Arrhenius decomposition into volatiles and char, (4) endothermicity of the reactions and (5) variable density, specific heat and thermal conductivity. He concludes that the rate of reaction is strongly dependent on the outward convection of volatiles and the char conductivity.

The model presented by Kansa et al (1977) also includes the effects of internal forced convection. This is done by the incorporation of Darcy's law in a gas momentum equation.

The basic steps in Kansa's model are: (1) radiant and convective heat transfer to the solid surface, (2) radiation from the solid surface, (3) heat conduction into the solid, (4) pyrolysis of the wood into char and gas and (5) the convection of the product gases through the char.

The assumptions used by Kansa are firstly that the wood sample is dried beforehand. Secondly, the pyrolysis reactions are assumed to follow a first order Arrhenius dependence and are exothermic in nature (only primary pyrolysis is considered). The properties of the sample (eg porosity,

conductivity etc) are assumed to be a linear combination of the properties for virgin wood and char. A one-dimensional model was used which could be adjusted for parallel or cross grain flow by choosing appropriate values for the heat and mass transfer properties.

Six governing equations were used in Kansa's description: a gas continuity equation, a momentum equation for the gas (Darcy's law with the inertial terms neglected), energy conservation equations for the gas and solid, an Arrhenius type equation describing the pyrolysis reaction rate and the equation of state for gases. The effects of shrinkage were ignored and the solid and gas were assumed to be in local thermal equilibrium.

The model developed by Simmons (1983) is perhaps the most extensive work in terms of the range of factors which are incorporated. The basic simplifying assumptions are firstly that only small particles are considered. This allows pyrolysis and char combustion to be considered as sequential rather than overlapping events. Secondly, mass and heat flow within the sample are assumed to flow along and not across the grain. Unlike other models, the particle cross sectional area is allowed to shrink, although this shrinkage is a function of time only and not space. The last major assumption is that the vapour and solid phases are in thermal equilibrium within the sample. This assumption is justified by the fine pore structure within the wood.

There are four governing equations in Simmon's model: a gas phase continuity equation, a momentum equation, a solid phase continuity equation and an energy equation. The effects of enthalpy change (gas and solid), convection of gases, conduction of heat, pressure changes and pyrolysis heat of reaction are accounted for in the energy equation. The pyrolysis reaction rate is assumed to have an Arrhenius dependence. As previously mentioned, adjustments were made to these governing equations to account for the presence of moisture in the sample.

The necessary boundary and initial conditions that Simmons uses describe all the variables at the initial time and the temperature conditions at both boundaries as well as one boundary condition for density, pressure and velocity.

Although a model of this form is the most general, it involves a set of five coupled first order differential equations. If certain limiting assumptions are made, then the analysis is made considerably simpler. The next section considers models which assume internal heat transfer is the rate limiting step. These models generally represent heat transfer as a thermal wave.

3.3.4 Propagation of wave fronts

The underlying assumption of this type of model is that external heat transfer and reaction rate are considerable faster than internal mass and heat transfer.

This class of models usually divide the whole process into different stages in time. Different descriptions are used for different stages in the combustion process. Usually the start of pyrolysis in a region defines the onset of a new stage, thus the location of a pyrolysis zone within the sample is essential to the model. In the case where pyrolysis kinetics are fast, this zone is restricted to a narrow reaction front (Pyle and Zaror, 1984).

Phillips and Becker (1982) conducted a number of experiments over a wide range of temperatures and conclude that in the limit of high temperatures the reaction front propagates as a thin wave and the heat transfer is governed by convective heat transfer. This conclusion is confirmed by Capart et al (1988) who show that the chemical reaction is rapid compared with internal thermal diffusion for high temperatures (bulk gas temperature > 600°C) and small particles (diameter < 20 mm).

By dividing the process into three phases, Murty Kanury (1972[a]) establishes three different regimes of temperature distribution. The initial preheat phase uses the assumption of a linear temperature distribution in a restricted surface thermal layer. This establishes a known temperature distribution at the onset of surface pyrolysis.

The next phase describes the propagation of a thermal wave and a pyrolysis wave into the solid. Again linear temperature profiles are assumed. When the temperature at a point reaches a critical value, the wood is assumed to undergo complete, immediate and endothermic pyrolysis. An energy balance

equation is set up accounting for heat conduction into the solid, the endothermicity of pyrolysis, the rise in enthalpy of the wood and the char and the convection effect of outward flowing gases. The speed of propagation of the thermal and pyrolysis fronts can be determined, and thus the rate of mass loss predicted.

The third phase, termed "finite body pyrolysis" is similar to the previous stage with the exception that the thermal front has reached the centre of the sample. Again the rate of mass loss can be determined by solving for the relevant variables.

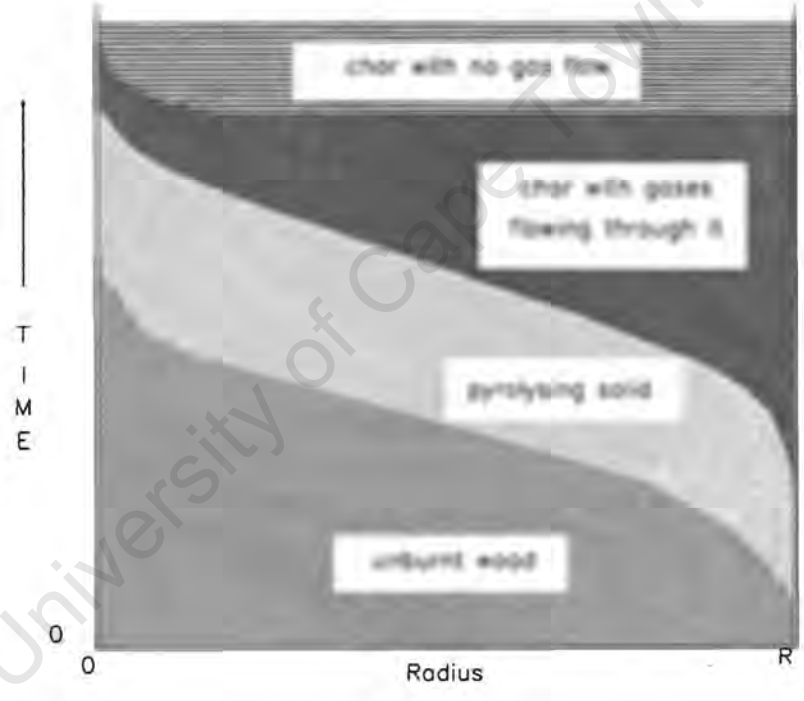

Figure 3.2: Pyrolysing Wave Front

The advantages in Murty Kanury's work are that the different combustion processes can be considered separately and that the wood and char can be assigned different thermal properties. There are however a number of assumptions that limit the scope of the study. The linear temperature profiles and the instantaneous and endothermic nature of pyrolysis are in conflict with other investigations.

Another wave front model is developed by Becker and Phillips (1982) who look at cases where the rate of mass loss is controlled by convective heat or mass transfer.

Wave front models can represent useful approximations to wood pyrolysis. However, their application is only appropriate where the assumption of slow internal heat transfer is valid.

3.3.5 Other approaches

A third class of models are designed to investigate specific aspects of combustion. These models and the experiments designed to validate them may use specialised combustion conditions.

An interesting approach is the one used by Dadkhah-Nikoo and Bushnell (1987). The governing equation used is based on the first law of thermodynamics. The combustion process is regarded as a "black box" with fuel and air as inputs and heat, exhaust and ash as outputs. The analysis then centres on obtaining estimates of efficiencies for comparison with different combustion fuels. A simple heat balance is written in the form:

$$\text{Energy Input} = \text{Energy Losses} + \text{Energy Output}$$

The energy input includes the enthalpy of the combustion air and the energy content of the wood. The energy losses include radiation losses, losses due to uncombusted char and incomplete oxidation of carbon (i.e. CO instead of CO_2 formed), heat loss due to heating of dirt and vaporization of moisture contained in the fuel and lastly the heat required to vaporize the water formed in combustion. The only energy output is the enthalpy of the flue gas.

Ward and Braslaw (1985) use only a first order weight loss equation. A series of experiments were conducted at constant temperatures and in a vacuum. This model is meant only for the special conditions of the experiments and is used to investigate the pyrolysis of different components of wood independently.

Simmons and Sanchez (1981) focus on the rate of evolution of product gases rather than the rate of solid mass loss in an attempt to more accurately model the pyrolysis kinetics themselves. Fine particles were used in experiments to avoid heat transfer problems. With these special conditions, most of the secondary effects are not important and a simple first order reaction rate expression is used.

The significance of these devolatilisation models to this investigation lies in the assessment of the relative importance of the different processes in devolatilisation. It is apparent that in most cases chemical kinetics are not the rate limiting step. Instead the overall rate of mass loss will be influenced by a number of secondary effects on internal heat and mass transfer as well as the intrinsic chemical kinetics.

Chapter 4

Kinetics and Models of Char Combustion

Wood combustion proceeds in two major stages: firstly devolatilisation or flaming combustion, and secondly char combustion. This chapter will discuss the kinetics and models of the second phase of wood combustion. Firstly an overview of the processes involved will be given. This will be followed by a description of the kinetics of solid gas interactions. The third part of this chapter will cover the different mathematical models used to describe char combustion. Lastly a summary of the published kinetics data for coal and wood char combustion will be given.

4.1 Overview of Char Combustion

After the organic constituents of wood have undergone pyrolysis, the remaining char reacts with different gases. This char is primarily composed of carbon, although there are quantities of hydrogen and oxygen present. Shafizadeh and Bradbury (1980) present an empirical formula for cellulose of $C_{6.7}H_{3.3}O_{1.0}$.

The char can react with a number of gases, namely H_2, H_2O and CO_2. However, the interaction with oxygen is dominant. Table 4.1 presents the heat of formation and relative rates for these reactions.

Reaction	Heat of Formation at 298K ($kJ.g^{-1}.mol^{-1}$)	Relative Rates at 800K & 0.1 atm
$C + O_2 \rightarrow CO_2$	- 394.0	100 000
$C + 2H_2 \rightarrow CH_4$	- 74.9	0.003
$C + H_2O \rightarrow CO + H_2$	131.0	3
$C + CO_2 \rightarrow 2CO$	172.0	1

(source: Laurendeau, 1978: p235)

Table 4.1: Reactions in Char Combustion

Glassman (1977) proposes the Boudouard reaction as the general initiator of char combustion:

$$C + CO_2 \rightarrow 2\ CO$$

This reaction is highly endothermic. The CO formed is released in volatile form and oxidation is completed in the flaming combustion zone.

Tillman (1981) describes two other possible reaction schemes. O_2 may be adsorbed directly onto the char, form a mobile species CO and desorb as CO and CO_2:

$$C^* + O_2 \rightarrow C(O)^* \rightarrow C(O)_m \rightarrow CO + CO_2$$

The asterisk implies an active site for the reaction and the subscript m indicates a mobile species. The other possible mechanism involves reaction of hydroxyl radicals with active sites as follows:

$$2\ OH + C \rightarrow CO + H_2O$$

$$OH + CO \rightarrow CO_2 + H$$

A sample of char must be considered as a porous solid containing the reactant carbon. Surrounding the sample is a boundary layer through which the other reactant, a gas (this reactant will largely be oxygen) must diffuse to reach the sample surface. Reactions can then occur at the surface between the carbon

and the gas. In addition to this, gas can penetrate the char structure and allow reactions to occur within the char sample itself.

There are a number of processes involved in this: gas diffusion through the boundary layer (reactants into and products out of the sample), gas diffusion within the char sample (again reactants and products) and reaction between the gas and the carbon in the char. These processes are interrelated and all can have an effect on the overall reaction kinetics.

In considering the kinetics of a burning char sample, a distinction must be made between overall and intrinsic kinetics. The latter describes only the actual reactions at active sites whilst the former will include the influence of other heat and mass transfer effects. The next section will outline the theory of overall and intrinsic reaction kinetics for solid-gas interactions.

4.2 Solid Gas Interactions

This section will firstly cover the definitions of overall and intrinsic reactivity together with a distinction between true and apparent kinetic parameters. This will be followed by a discussion of fundamental surface mechanisms of reaction and lastly a look at how the influence of intra-particle mass transport can be included in the equations.

4.2.1 Overall particle reactivity

The overall particle reactivity expresses the rate of solid mass loss as a result of all physical and chemical effects. It can be expressed on a molar basis or on an external surface area basis (Laurendeau, 1978: p245):

i) Molar basis: $[mol_{[reactant]}.s^{-1}.mol_{[sample]}^{-1}]$

$$R_m = K_{m,o}C_o^n = K_{m,s}C_s^n \quad \ldots\ldots\ldots\ldots\ldots 4.1$$

ii) External surface area: $[g_{[reactant]}.s^{-1}.cm^{-2}]$

$$R_e = K_{e,o}C_o^n = K_{e,s}C_s^n \quad \ldots\ldots\ldots\ldots\ldots 4.2$$

The two expressions are related by:

$$R_e = (V / A \mathcal{M}_s) \varrho R_m \quad \ldots\ldots\ldots\ldots\ldots\ldots 4.3$$

4.2.2 Intrinsic reactivity

The global intrinsic reactivity is the rate of mass loss due to intrinsic chemical kinetics only. It excludes additional physical or chemical effects which may be affecting the overall process. The intrinsic reactivity can be expressed in any of three ways: on a site basis, an internal area basis or a volume basis. Expressions for these are given below.

i) Site basis: (sites.cm^{-2}.s^{-1}):

$$R_s = k_s [C_t] C^m \quad \ldots\ldots\ldots\ldots\ldots\ldots 4.4$$

ii) Internal Area basis: (mol.cm^{-2}.s^{-1}):

$$R_i = k_i C^m \quad \ldots\ldots\ldots\ldots\ldots\ldots 4.5$$

iii) Volume basis: (mol.cm^{-3}.s^{-1}):

$$R_v = k_v C^m \quad \ldots\ldots\ldots\ldots\ldots\ldots 4.6$$

The three expressions are related by 4.7a and 4.7b:

$$R_i = \Gamma m_c R_s \quad \ldots\ldots\ldots\ldots\ldots\ldots 4.7a$$

$$R_v = \varrho A_i R_i \quad \ldots\ldots\ldots\ldots\ldots\ldots 4.7b$$

From 4.7 and b, relationships between k_i, k_v and k_s can be obtained.

4.2.3 True and apparent kinetic parameters

The overall pseudo rate constants, K_m and K_e can be expressed in terms of an apparent pre-exponential factor, $\mathcal{A}_a$ and an apparent activation energy, E_a using the Arrhenius expression:

$$K = \mathcal{A}_a \exp(-E_a/\mathcal{R}T) \quad \ldots\ldots\ldots\ldots\ldots\ldots \quad 4.8$$

Here K, $\mathcal{A}_a$ and E_a are an apparent rate constant, reaction order, pre-exponential factor and activation energy respectively.

Similarly, the intrinsic rate constants k_s, k_i, k_v can be expressed in terms of true parameters:

$$k = \mathcal{A}_t \exp(-E_t/\mathcal{R}T) \quad \ldots\ldots\ldots\ldots\ldots\ldots \quad 4.9$$

4.2.4 Fundamental surface mechanisms

Since the porous char solid is characterized by variations in local gas concentration, the local reaction rate is determined by the local gas concentration (if reaction order ≠ 0). The intrinsic rate constant, k_i is related to temperature by an Arrhenius expression as in equation 4.9.

Active site theory attempts to explain the mechanisms of surface reactions. This proposes that reactions occur at favoured sites on a gas/solid interface. These favoured or active sites occur where there exist carbon edges or dislocations, inorganic impurities, or oxygen/hydrogen functional groups. At such a site, there are three mechanisms which may occur: 1) reactant chemisorption (adsorption), 2) migration of intermediates and 3) product desorption. Adsorption of reactant and desorption of the resulting product can occur at a single site (single site mechanism). Alternatively migration can permit adsorption at one site, migration to a second site and desorption at this new site (dual site mechanism).

Langmuir-Hinshelwood kinetics provide an opportunity to express the kinetic parameters (activation energy, pre-exponential factor etc) in terms of more basic properties of the char/gas system. The mechanisms of active site theory are used together with the assumptions: 1) there is a uniform distribution of active sites, 2) the adsorption rate per site is independent of the amount

adsorbed, and 3) surface migration, if it exists, is so rapid that only adsorption or desorption can be rate limiting.

From active site theory, the intrinsic surface reactivity, R_i can be expressed as (see equation 4.7a):

$$R_i = m_c R_s([C_t],C_i,T)$$

For narrow ranges of C_i and T, complex Langmuir-Hinshelwood expressions for R_s may be approximated (Laurendeau, 1978: p242) by equation 4.4:

$$R_s = k_s [C_t] C_m$$

4.2.5 The influence of intra-particle mass transport

i) The effectiveness factor

The next step is to consider the relationship between intrinsic reactivity and overall particle reactivity. The intrinsic reactivity R_i can only be evaluated at a particular locality in the char sample. If R_i did not vary through the sample (i.e. if the gas concentration was uniform), then the overall reactivity R_m could be expressed by

$$R_m = \text{(total area available for reaction per gram)} \times R_{i,s}$$
$$= (A_i + A_e) R_{i,s}$$

Instead however, it is necessary to account for the decrease in reactant gas concentration closer to the centre of the char. This is usually done by incorporating an effectiveness factor, η:

$$R_m = (\eta A_i + A_e) R_{i,s} \quad \ldots\ldots\ldots\ldots\ldots\ldots 4.10$$

The effectiveness factor is a simple way of including the effect of a continuously changing reactant gas concentration inside the char sample. In situations where gas diffusion inside the solid is rapid, the gas concentration

will be approximately uniform and η " 1, otherwise η < 1. In most cases $\eta A_i >> A_e$ and equation. 4.10 may be approximated by:

$$R_m = \eta A_i R_{i,s} \quad \ldots\ldots\ldots\ldots\ldots\ldots 4.11$$

Incorporating equation. 4.10 into 4.11 obtains:

$$R_m = \eta A_i m_c [C_t] k_s C_s^m \quad \ldots\ldots\ldots\ldots 4.12$$

This shows that overall particle reactivity is dependent on the effect of changing reactant gas concentration inside the sample (η), specific internal surface area (A_i), active site concentration ($[C_t]$), intrinsic rate co-efficient (k_s) and surface reactant gas concentration (C_s).

In order to obtain reliable expressions for the effectiveness factor, η, it is necessary to consider the geometry of the sample as well as the mechanisms and conditions of mass transport through both the surrounding boundary layer and the char sample itself.

ii) Effective diffusivity

Another way of expressing the influence of intra-particle diffusion is through an effective diffusivity (D_e).

The mass flux is the sum of a convective and a diffusive component. Where isobaric conditions prevail, the convective contribution falls away. The mass flux of gas at any point in the solid can then be represented by Fick's Law equation:

$$J(r) = - \mathcal{M}_g D_e \, dC/dr \quad \ldots\ldots\ldots\ldots\ldots 4.13$$

The main difficulty with this diffusion model is the actual determination of the effective diffusivity. Usually a constant value is assumed, although realistically D_e will vary with both time and radius. Experimentally determined values can be related to the porosity in a number of ways (Laurendeau, 1978: p248). Two such expressions are presented in equations 4.14a and 4.14b:

$$D_e \alpha \phi^p, \quad p = 1,2,3 \ldots\ldots\ldots\ldots\ldots\ldots .4.14a$$

$$D^e \alpha \phi D_A \ldots\ldots\ldots\ldots\ldots\ldots\ldots\ldots .4.14b$$

Alternatively, expressions can obtained for the effective diffusivity through modeling the arrangement of pores inside the solid. An example of this approach can be found in Wheeler's classic pore model where the pore structure is assumed to be a homogeneous system of cylindrical pores. If this approach were to be used for wood, detailed knowledge of the pore structure would be required.

4.3 Char Combustion Models

A model of char combustion must take into account the three different processes: boundary layer diffusion, intra-particle diffusion and reaction kinetics. This discussion will cover rate limiting conditions, char burnout time, mass transfer through the boundary layer and lastly a description of the different models.

4.3.1 Rate limiting conditions

It is possible to describe three different scenarios of char combustion.

Case I is where the overall reactivity is controlled by the intrinsic reactivity. This will occur where the chemical reactions are slow with respect to mass transport. This may be due to conditions such as low temperatures, low pressures, low active site concentrations, small particle diameter or high porosity.

Case III is where the intrinsic reaction rate is so large that reactant gas concentration is virtually zero inside the sample. This implies that the process will be controlled by boundary layer diffusion solely. The conditions favouring this situation are opposite to those associated with case I, i.e. high temperatures, pressures and active site concentrations, large particle diameters and low porosities.

Case II is an "average" situation since it represents conditions where control is by chemical processes and internal pore diffusion. In this case it can be assumed that char surface and bulk gas concentrations are equal. This is obviously only an approximation to the practical case, although in many circumstances it is suitable.

The apparent activation energy under case I conditions equals the true activation energy and under case II conditions is a portion of the true value. Under case III conditions, the apparent activation energy will always be very small (Tillman, 1981: p244).

An approach can be used which obtains pseudo rate coefficients and activation energies without the use of any combustion model. Assuming an n^{th} order reaction, the rate of mass loss can be related to a pseudo rate co-efficient. If this rate co-efficient can be obtained for a number of reaction temperatures, an apparent activation energy can be derived (assuming an Arrhenius dependence on temperature). This approach lumps all the different effects together and is valid under type I conditions. The rate coefficients obtained are "pseudo" rate coefficients as they do not measure the actual kinetic rate of reaction. Similarly the activation energy is an apparent activation energy which will only approximate the true one. Petrie (1987) outlines a calculation technique for obtaining these parameters.

4.3.2 Char burnout time

The char burnout time will be dependent on the particle diameter. The form of this dependence can be useful in determining whether chemical kinetics or mass transfer is the rate limiting step. Beeston and Eisenhigh (1963) use the relation that for boundary layer mass transfer controlled situations, the char burnout time is proportional to the particle diameter squared. For small coal particles (less than 2 mm diameter) and a range of oxygen concentrations, the constant of proportionality was found to be 957 $s.cm^{-2}$.

In situations where the char burnout time is directly proportional to the particle diameter, the controlling mechanism must be the chemical kinetics.

where c = constant: 0.30 < c < 0.35,
(see appendix A for definitions and calculation procedures for Sh, D_A, Re and Sc).

Mulcahy and Smith (1969: p84) comment that turbulence in the flow has the effect of disturbing the stagnant layer around the particle and bring fresh reactant into the vicinity of the particle surface.

4.3.4 Two macroscopic models

For pore diffusion there are two different types of models: macroscopic and microscopic models. In macroscopic models there is an effective diffusivity which represents the flow resistance throughout the particle. The mass transport is then modelled using Fick's law. In microscopic models however, diffusion through a single pore is considered and the overall particle is regarded as a specific arrangement of pores. In this review, two types of macroscopic models will be considered, namely the shrinking core (or constant density) model and the progressive conversion (or constant volume) model. No microscopic models will be described.

i) The basic assumptions

The basic model assumptions used are:

i) spherical symmetry,
ii) all gas-solid reactions occur within the particle,
iii) the particle is isothermal,
iv) pseudo-steady state analysis,
v) gaseous reactants are dilute species in an inert component and
vi) intrinsic reactivity is modeled with a global, 1st order rate expression.

Assumption (i) allows a one dimensional analysis to be used. Assumptions (ii) and (vi) allow the usual rate equations to be used with reaction order 1[1]. Assumption (iii) eliminates the necessity to use an energy equation and thus simplifies the analysis considerably. Assumption (v) means that isobaric conditions can be assumed and thus convection within pores need not be considered (Laurendeau, 1978: p246).

These assumptions imply that the general gas-solid system simplifies to the three basic processes discussed in section 4.1.

ii) The shrinking core model

The shrinking core model assumes that the reactions occur at a well defined reaction front which recedes into the particle as combustion proceeds.

The physical description of the char sample is represented in figure 4.1. There exists a boundary layer surrounding the particle. The gaseous reactants must diffuse through this. There is then an ash layer which consists of the remaining solid after the char has undergone combustion. Again, the gaseous reactants must diffuse through this. The ash layer surrounds the unreacted char. At the interface between these two regions is the reaction front. This is a narrow band where the actual mass loss is occurring due to solid/gas reactions.

There are three descriptive equations in the shrinking core model: one describing mass transfer across the boundary layer, another describing the diffusion of reactant gas through the ash layer, and a third expressing the mass loss in terms of an effective rate constant at the reaction front. These three equations can be combined to give an overall effective rate constant at the surface of the sample (Laurendeau, 1978: p249).

Variations on this basic model have been considered. For example, it is not necessary to assume a first order reaction. Shen and Smith (1965) consider other extensions such as changing particle size and reversible surface reaction.

---

1 Although the stoichiometry of the reaction $C + O_2 \rightarrow CO_2$ supports a first order reaction, where oxygen supply is restricted, incomplete oxidation may occur: $C + 1/2\ O_2 \rightarrow CO$ which represents half order kinetics. Where both these reactions are occurring, the reaction order may be between 0.5 and 1.

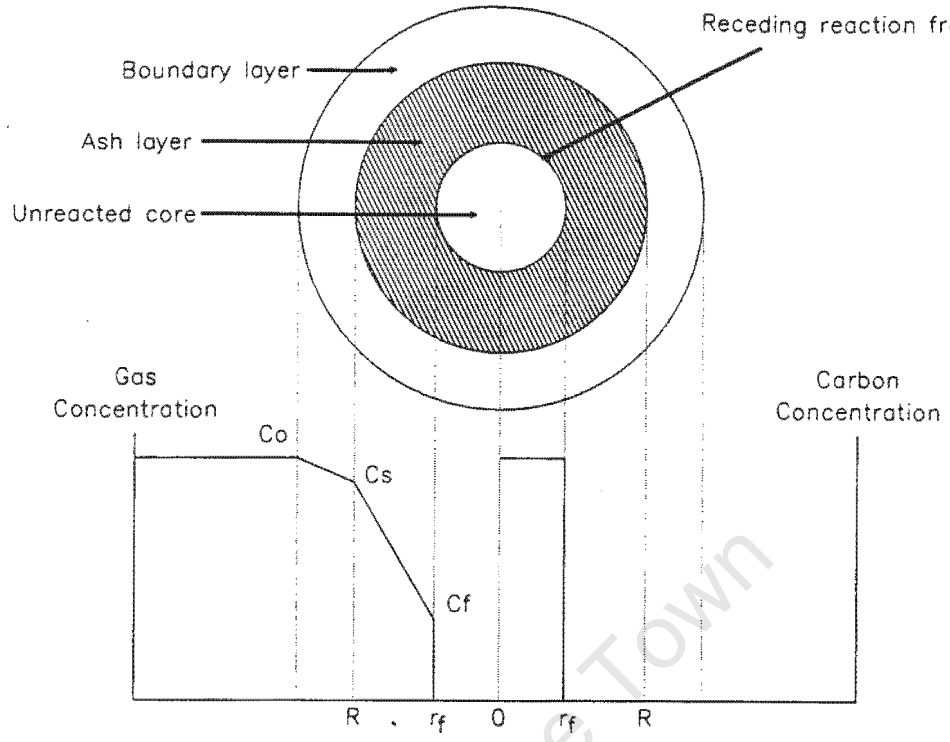

Figure 4.1: The Shrinking Core Model

Although the shrinking core model is probably the best simple description of solid-gas systems, its use is restricted to cases where the reaction band is limited to a narrow reaction front. In cases where the particle is characterised by a slow reaction rate, high porosity or small size, this will not be the case.

Cornelissen (1985) investigated the combustion of small wood samples in order to ascertain the appropriateness of this model to wood char combustion. The combustion process was interrupted at intervals and the state of the ash layer and unburnt core was examined. Although this experimental method disturbed the combustion process, it did indicate that a shrinking core model would be appropriate for the case of wood char combustion.

iii) Progressive conversion models

Progressive conversion models allow the physical description of the burning sample to include a zone rather than a front where the reactions are occurring (see figure 4.2).

There are two types of progressive conversion models. The first type assumes that there is no ash layer. The gas concentration through the sample is thus dependent on two factors: diffusion through the char and reaction with the char.

The gaseous concentration inside the spherical particle is given by the equation (assuming first order):

$$\frac{1}{r^2}\frac{\delta}{\delta r}\left[r^2 D_e \frac{\delta C}{\delta r} \right] - k_v C = 0 \quad \ldots\ldots\ldots\ldots 4.17$$

Ausman and Watson (1962: p325) derive the solution to this and obtain an expression for the gas concentration at any point in the sample. Using an appropriate reaction order and integrating across the sample, the overall mass loss can be obtained. This can be compared with experimental results and used to obtain the reaction rate constant. As before, this can be used in an Arrhenius relation to obtain the activation energy.

The second type of progressive conversion model assumes that after a certain time, an ash layer forms around the reacting solid. The sample is then split into two regions. The outer region is composed of ash and gas concentration is dependent solely on diffusion effects. The inner region is the zone where reactions are occurring and the gas concentration depends on diffusion and reaction rate.

Ausman and Watson (1962) also derive the solution to these two zones. It is possible to derive the time at which the situation changes from type one to type two model, i.e. when an ash layer forms.

This type two model is very similar to the shrinking core model in the case where effective diffusivity is considerably less after ash formation than before the ash was formed (Ishida and Wen, 1968: p316).

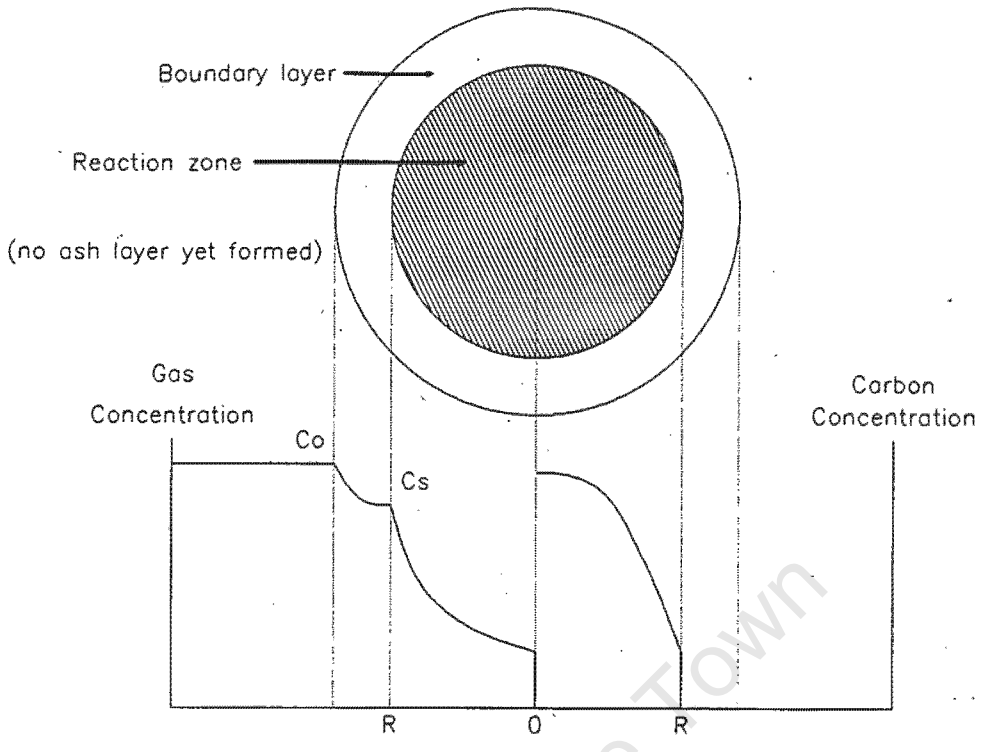

Figure 4.2: Progressive Conversion Model

The progressive conversion model is more general than the shrinking core model. This is because it allows char reactions to occur in a region of the sample rather than restricted to a narrow reaction front. The shrinking core model is however considerably simpler and will be appropriate under conditions where the reaction kinetics are not rate limiting.

4.4 Kinetic Data for Char Combustion

There have been a number of investigations designed to determine the reaction kinetics of coal char combustion. Coal combustion is similar to wood combustion in that there are two phases: a devolatilisation stage followed by char oxidation. However, the pore structure of coal and wood chars are completely different. This will affect the intra-particle diffusion differently for the two types of char. Also, in most applications coal char particle size is considerably smaller than that for wood chars. However, the intrinsic reaction

kinetics of coal combustion are of interest to wood studies. It is important however, to consider only those reported figures which have attempted to correct for mass transfer effects.

The true order of reaction is dependent on both temperature and oxygen concentration (Smith, 1982: p1053). For pure graphite samples, the reaction order at 625°C has been determined as 0.5 +- 0.15 (Mulcahy and Smith, 1969: p102). The activation energy for graphite has also been accurately determined as 251 +- 21 kJ/mol. However, for coal char samples, the variation in reported figures is quite broad. This may be attributed to both the heterogeneity of chars (which make the kinetics sensitive to intra-particle diffusion and temperature effects) and the sensitivity to catalysts.

Field (1969: p250) reports activation energies ranging from 125 kJ/mol (at 1000°C) to 42 kJ/mol (at 1500°C). The activation energy tends to decrease with increasing temperature. Burning was observed both on the surface and inside the particle. This implies that intra-particle diffusion effects could be affecting the results. The chemical rate constant at the surface (corrected for boundary layer transfer) was found to have a linear dependence on temperature:

$$K_{e,s} = -0.49 + 3.85 \times 10^{-4} T$$

Generally the activation energies for char samples (corrected for boundary layer mass transfer) tend to be lower than that for pure carbon. Table 4.2 below summarises some of the figures reported in the literature.

Reported by	Temperature [K]	Order	Activation Energy [kJ/mol]
Laurendeau (1978)	700 - 850	1	130
Dutta & Wen (1977)	700 - 850	1	130
Laurendeau (1978)	630 - 1800	0.5	138
Mulcahy & Smith (1969)	900 - 1650	1	150
Rubak et al (1984)	473 - 1373	1	137 - 172
Smith (1982)	775 - 1250	1	179
Field (1969)	1300 - 1800	1	125 - 42

Table 4.2: Activation Energies and Reaction Orders for Char Combustion

This chapter has reviewed the kinetic theory of solid gas interactions, models of char combustion and summarised some of the kinetic data presented in the literature for coal char combustion. Wood char combustion of small samples is amenable to the type of analysis presented here as it involves mass transfer across a boundary layer and into the sample where solid-gas reactions occur. The type of model most suitable will depend both on the nature of the wood structure and the conditions of the experiments. The next chapter will outline the theory and models used in this investigation.

Chapter 5

Theory and Calculation Techniques

This chapter will develop three different models that can be used to analyse wood combustion. The first is a straight forward pseudo-rate constant analysis. This can be used both for devolatilisation and for char combustion. The second model is the well known shrinking core model. This is better suited to char combustion than devolatilisation. The last model is the progressive conversion model. One form of this model will be described and two special cases of this form will be examined. Expressions will be obtained for the rate of mass loss and the effectiveness factor. This model can only be used for char combustion.

For each model, a description of an appropriate calculation technique will be given which will allow the model to be applied to experimental data. These techniques will demonstrate how the appropriate kinetic parameters can be derived.

Most of these models use the assumption that the particle is represented by a sphere. This reduces the equations to one dimension. In most cases however, the equations can be recalculated for a cylinder with sealed ends.

In the simple case where pyrolysis is viewed as one reactant undergoing a first order reaction, application of the above equation is straight forward. A plot of dM/dt against M will yield - k as the slope.

It is also possible to consider pyrolysis as the combination of a number of independent first order reactions. Each reaction corresponds to the decomposition of a different constituent. In this way, the above equations can be applied to each reaction and a rate constant obtained for each constituent, i.e.

$$dM_i/dt = -k_i M_i \quad \ldots\ldots\ldots\ldots\ldots\ldots\ldots\ldots 5.1$$

From the work by Vovelle et al (1983), it appears that separation into a non-cellulose constituent (which reacts first) and a cellulose constituent is the most appropriate two step schema. Let the cellulose constituent be denoted by the subscript 2 and the non-cellulose constituent by the subscript 1. Figure 5.1 is a typical reactivity vs time graph for the devolatilisation phase.

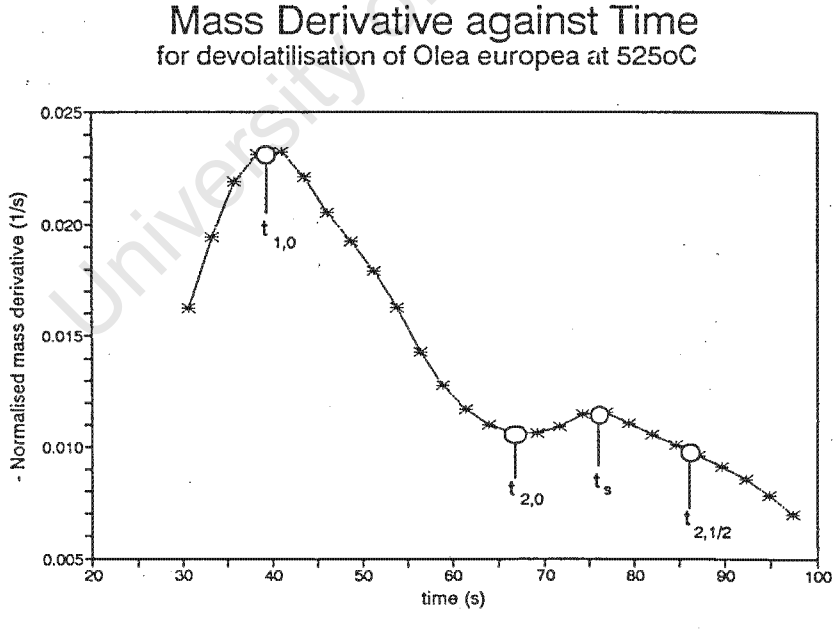

Figure 5.1: A Typical Reactivity Curve for Devolatilisation

5.2.2 For char combustion

Three separate process can be identified in char combustion: diffusion of reactant and product gases through the boundary layer, diffusion of these gases through the sample, and reaction between carbon atoms and the reactant gas. Using the pseudo-rate constant method for char combustion makes no distinctions between boundary layer diffusion, intra-particle effects or intrinsic kinetics. The individual resistances are lumped together into one overall pseudo rate constant, $K_{e,o}$.

i) Mass transfer over the boundary layer

Using a simple integrated form of Fick's law, the mass flux of gas through the boundary layer can be expressed as:

$$J_s = h_D (C_o - C_s) \quad \ldots\ldots\ldots\ldots\ldots\ldots 5.3$$

Since the mass flux of reactant gas must be related to the overall particle reaction rate, the reactivity can be written:

$$R_e = J_s / \mathcal{M}_g = h_D / \mathcal{M}_g (C_o - C_s) \quad \ldots\ldots\ldots 5.4$$

$$= K_D (C_o - C_s) \quad \ldots\ldots\ldots\ldots\ldots\ldots 5.5$$

Where K_D is the diffusional rate constant, defined by $K_D = h_D / \mathcal{M}_g$.

ii) The equations

The overall reactivity at the particle surface may be written as in equation 5.6 (assuming first order):

$$R_e = K_{e,s} C_s \quad \ldots\ldots\ldots\ldots\ldots\ldots 5.6$$

The mass transfer across the boundary layer may be written as in equation 5.3b:

$$R_e = K_D (C_o - C_s)$$

Combining 5.6 and 5.4b gives:

$$R_e = (1/K_D + 1/K_{e,s})^{-1} C_o \quad \ldots\ldots\ldots\ldots 5.7$$

Comparing this with equation 5.6 shows that:

$$K_{e,o} = (1/K_D + 1/K_{e,s}) \quad \ldots\ldots\ldots\ldots\ldots\ldots 5.8$$

In this case, $K_{e,o}$ is the pseudo-rate constant.

iii) Constant density during reaction

For char combustion, the assumption of constant density can be used. As combustion proceeds, the sample shrinks in volume leaving an ash layer of negligible mass.

For the case of a spherical sample, the mass, m and the original mass, m_o may be represented in terms of the radius, r and the density ϱ:

$$m = {}^4/_3 \pi r^3 \varrho$$

and

$$m_o = {}^4/_3 \pi R^3 \varrho, \quad R = \text{original radius.}$$

Then the external surface area of the unreacted core is given by:

$$A = 4 \pi r^2 = 4 \pi R^2 (m/m_o)^{2/3}$$

The reactivity R_e can be expressed in terms of the carbon mass loss by the equation:

$$R_e = (\Gamma / \mathcal{M}_c) (1 / A) \, dm/dt$$

Thus, the reactivity is given by:

$$R_e = - \frac{\Gamma / \mathcal{M}_c}{4\pi R^2 (m/m_o)^{2/3}} \frac{dm}{dt} = K_{e,o} C_o \quad \ldots\ldots\ldots\ldots 5.9$$

The slope of a plot of $d(m/m_o)/dt$ against (m/m_o) will provide an expression for the overall rate constant $K_{e,o}$ as:

$$K_{e,o} = - (\text{slope} * m_o * \Gamma) / (4\pi R^2 \mathcal{M}_c C_o) \quad \ldots\ldots 5.10$$

C_o refers to the molar concentration of oxygen in the bulk atmosphere in units of mol/cm^3. The value of this is listed in table 5.1. R (cm) refers to the radius of the sample assuming a spherical shape. For the cylinders used with a

diameter of 1.4 cm and a height of 1.4 cm, R was calculated so the volume of a sphere, radius R would equal the volume of the cylinders. The value thus calculated is listed in table 5.1.

It is possible to separate out the influence of boundary layer diffusion from the overall rate constant. If an estimate of K_D is known, and obtaining an empirical value for $K_{e,o}$, it is possible to use equation 5.8 to find $K_{e,s}$:

$$K_{e,s} = (1/K_{e,o} - 1/K_D)^{-1} \quad \ldots\ldots\ldots\ldots\ldots 5.11$$

The rate constant $K_{e,s}$ lumps together intrinsic kinetics and intra-particle effects, but excludes boundary layer diffusion.

The overall rate constant, $K_{e,s}$ will approximate the intrinsic rate constant. Where kinetics are the rate limiting step, this approximation will be a good one.

5.2.3 Activation energy

In order to obtain an apparent activation energy, the overall rate constant can be assumed to have an Arrhenius dependence on temperature. Again, the stronger the influence of intrinsic kinetics on the whole process, the closer the apparent activation energy will be to the true one.

The Arrhenius equation can be rewritten in the form

$$\ln(K) = \ln(\mathcal{A}) - E/\mathcal{R}T \quad \ldots\ldots\ldots\ldots\ldots 5.12$$

Thus a plot of ln(K) against 1/T should yield a straight line with intercept = ln($\mathcal{A}$) and slope = - E/$\mathcal{R}$.

5.3 Shrinking Core Model

5.3.1 Assumptions

The shrinking core model assumes that the particle is represented by a core of unreacted solid, surrounded by a layer of ash. The reactions occur on a narrow front located between the solid core and the ash layer. As the reaction proceeds, the unreacted core shrinks in volume but retains a constant density.

The equations here are calculated assuming that the particle is a sphere and that the combined volume of the ash layer and core remains constant.

The process is divided into three phases: boundary layer diffusion, diffusion through the ash layer and reactions at the front.

5.3.2 The equations

Boundary layer diffusion is represented by equation 5.4b:

$$R_e = K_D (C_o - C_s)$$

which may be rewritten in the form:

$$(\Gamma / \mathcal{M}_c\, 4\pi R^2)\, dm/dt = - K_D (C_o - C_s) \quad \ldots\ldots\ldots\ldots\ldots\ldots 5.13$$

The rate of gaseous mass transfer through the ash layer is described through the use of an effective diffusivity as in equation 4.13:

$$J(r) = - D_e\, dC/dr$$

The mass of reactant gas passing through a shell, radius r is related to the solid mass loss by the stoichiometric ratio Γ and the molecular weight of carbon $\mathcal{M}_c$:

$$(\Gamma / \mathcal{M}_c)\, dm/dt = (4\pi r^2 D_e / \mathcal{M}_g)\, dC/dr \quad \ldots\ldots\ldots\ldots 5.14$$

Integrating from the reaction front at $r = r_f$ to the external surface at $r = R$ yields:

$$\frac{\Gamma}{\mathcal{M}_c \; 4\pi R^2} \; \frac{dm}{dt} = - \frac{r_f D_e}{R(R - r_f)} (C_s - C_f) \quad \ldots\ldots\ldots\ldots 5.15$$

The kinetics at the reaction front can be represented by the equation:

$$R_e = K_{e,f} C_f$$

which can be written:

$$\frac{\Gamma}{\mathcal{M}_c \; 4\pi R^2} \; \frac{dm}{dt} = - \frac{r_f^2}{R^2} \; K_{e,f} C_f \quad \ldots\ldots\ldots\ldots 5.16$$

Combining 5.13, 5.15 and 5.16 yields (note that for simplicity r_f has been replaced by r):

$$\frac{-\Gamma}{\mathcal{M}_c \, 4\pi R^2} \; \frac{dm}{dt} = \left[\frac{R(1 - r/R)}{D_e \, r/R} + \frac{1}{K_D} + \frac{1}{r^2/R^2 \, K_{e,f}} \right]^{-1} C_o \quad \ldots\ldots\ldots 5.17$$

Thus the overall rate constant, $K_{e,o}$ may be written as:

$$K_{e,o} = \left[\frac{R(1 - r/R)}{D_e \, r/R} + \frac{1}{K_D} + \frac{1}{r^2/R^2 \, K_{e,f}} \right]^{-1} \quad \ldots\ldots\ldots 5.18$$

As can be seen from equation 5.18, the shrinking core model represents the overall rate constant, $K_{e,o}$ as a combination in parallel of three resistances from boundary layer diffusion, intra-particle diffusion and reaction kinetics.

This derivation can be reworked for a cylinder with sealed ends and an expression obtained for the overall rate constant:

$$K_{e,o} = \left[\frac{R \ln(R/r)}{D_e} + \frac{1}{K_D} + \frac{1}{r/R \, K_{e,f}} \right]^{-1} \quad \ldots\ldots\ldots 5.19$$

5.3.3 Application

Using the assumption that the sample is a shrinking core of constant density, the ratio r/R may be written:

$$\zeta \equiv r / R = (m / m_o)^{2/3}$$

Substituting ζ for r/R and Ψ for $d(m/m_o)/dt$ in equation 5.17 and rearranging yields:

$$(R/D_e)\{\zeta (1-\zeta) \Psi\} + (1/K_D) \{\zeta^2 \Psi\} + (1/K_{e,f}) \Psi = - (4 \pi R^2 C_o \mathcal{M}_c / m_o) \zeta^2 \quad . \quad 5.20a$$

Equation 5.20a is in the form

$$a_1 x_1 + a_2 x_2 + a_3 x_3 = a_4 y \quad . \quad . \quad . \quad . \quad . \quad . \quad . \quad . \quad . \quad . \quad . \quad . \quad . \quad 5.20b$$

where

$$a_1 = R / D_e \quad . \quad . \quad . \quad . \quad . \quad . \quad . \quad . \quad . \quad . \quad . \quad . \quad . \quad . \quad . \quad . \quad . \quad . \quad 5.21a$$

$$a_2 = 1 / K_D \quad . \quad . \quad . \quad . \quad . \quad . \quad . \quad . \quad . \quad . \quad . \quad . \quad . \quad . \quad . \quad . \quad . \quad . \quad 5.21b$$

$$a_3 = 1 / K_{e,f} \quad . \quad . \quad . \quad . \quad . \quad . \quad . \quad . \quad . \quad . \quad . \quad . \quad . \quad . \quad . \quad . \quad . \quad . \quad 5.21c$$

$$a_4 = - 4 \pi R^2 C_o / m_o \quad . \quad . \quad . \quad . \quad . \quad . \quad . \quad . \quad . \quad . \quad . \quad . \quad . \quad 5.21d$$

and

$$x_1 = \zeta (1 - \zeta) \Psi \quad . \quad . \quad . \quad . \quad . \quad . \quad . \quad . \quad . \quad . \quad . \quad . \quad . \quad . \quad . \quad . \quad . \quad 5.22a$$

$$x_2 = \zeta^2 \Psi \quad . \quad . \quad . \quad . \quad . \quad . \quad . \quad . \quad . \quad . \quad . \quad . \quad . \quad . \quad . \quad . \quad . \quad . \quad 5.22b$$

$$x_3 = \Psi \quad . \quad . \quad . \quad . \quad . \quad . \quad . \quad . \quad . \quad . \quad . \quad . \quad . \quad . \quad . \quad . \quad . \quad . \quad . \quad 5.22c$$

$$y = \zeta^2 \quad . \quad . \quad . \quad . \quad . \quad . \quad . \quad . \quad . \quad . \quad . \quad . \quad . \quad . \quad . \quad . \quad . \quad . \quad . \quad 5.22d$$

A multiple linear regression using 5.20b will yield values for $a_1 ... a_3$. These values can then be used in equations 5.21a..5.21c to find estimates for D_e, K_D and $K_{e,f}$.

5.4 Progressive Conversion Model

5.4.1 Assumptions

The progressive conversion model uses intrinsic rate constants to describe the kinetics inside the reacting particle. The model allows reactions to occur anywhere inside the particle, and calculates the rate of these reactions at any point in the particle on the basis of the local reactant gas concentration. There are two types of progressive conversion model. One assumes that the entire sample is reacting and the other allows the formation of an inert ash layer around the reacting core. Ideally, the first type of model should be used until all the solid reactant has been used up at the surface. After this, the second type of model should be used. In this analysis, only the first type of model is considered.

5.4.2 The equations

The gaseous concentration inside the particle is given by the equation (assuming first order):

$$\frac{1}{r^2}\frac{\delta}{\delta r}\left[r^2 D_e \frac{\delta C}{\delta r} \right] - k_v C = 0 \quad \ldots\ldots\ldots\ldots 5.23$$

Ausman and Watson (1962) use boundary conditions expressed in equations 5.24a and b and derive the solution expressed in equation 5.25.

At r = R: $D_e \delta C/\delta r = K_D (C_o - C_s)$ 5.24a

At r = 0: C is finite 5.24b

$$C = \frac{C_o R \sinh\{N_r r/R\}}{\beta r \quad \sinh\{N_r\}} \quad \ldots\ldots\ldots\ldots 5.25$$

where $N_r^2 = R^2 k_v / D_e$ 5.26a

$N_m = D_e / R K_D$ 5.26b

$$\beta = 1 - N_m(1 - N_r/\tanh(N_r)) \quad \ldots\ldots\ldots \quad 5.26c$$

Substituting r = R into equation 5.24a yields the relation between bulk and surface concentration as being:

$$C_o = \beta C_s \quad \ldots\ldots\ldots\ldots\ldots\ldots \quad 5.27$$

This result can also be obtained by substituting r = R into equation 5.25.

Note that in the case where boundary layer diffusion is not important, i.e. $h_D \rightarrow \infty$, then $N_m \rightarrow \infty$ and $\beta \rightarrow 1$, thus equation 5.27 reduces to $C_o = C_s$, as expected.

5.4.3 The rate of mass loss

The total rate of mass loss will be given by the integral over the whole volume:

$$(\Gamma / \mathcal{M}_c)\, dm/dt = -\int_v k_v C \, dV$$

Performing this integration gives the result:

$$-\frac{\Gamma\, dm}{\mathcal{M}_c\, dt} = 4\pi R\, C_o\, D_e \left[\frac{N_r}{\tanh(N_r)} - 1\right]\left[\frac{1}{1 + N_m(N_r/\tanh(N_r) - 1)}\right] \quad \ldots \quad 5.28a$$

$$= 4\pi R^2 K_D (1 - 1/\beta) C_o \quad \ldots\ldots\ldots \quad 5.28b$$

Equation 5.28 shows that the mass loss is linear with respect to time, but non-linearly dependent on boundary layer diffusion (h_D), intra-particle effects (D_e) and intrinsic kinetics (k_v).

Note that equation 5.28b can also be derived by substituting $C_o = \beta C_s$ (equation 5.27) into the expression for overall reactivity (see equation 5.13):

$$R_e = (-dm/dt) / (4\pi R^2 \Gamma / \mathcal{M}_c) = K_D (C_o - C_s)$$

5.4.4 Two simplified cases

With the condition

$$N_m(N_r/\tanh\{N_r\} - 1) >> 1$$

then equation 5.28a reduces to

$$(\Gamma / \mathcal{M}_c)\, dm/dt = -4\pi R^2 C_o K_D$$

i.e. $$R_e = h_D C_o$$

This represents control by boundary layer diffusion.

Conversely, if it is assumed that boundary layer diffusion is not important, i.e. $\beta = 1$ and

$$N_m(N_r/\tanh\{N_r\} - 1) << 1$$

then equation 5.28a reduces to:

$$-(\Gamma / \mathcal{M}_c)\, dm/dt = 4\pi R C_o D_e (N_r/\tanh\{N_r\} - 1)$$

Using a Taylor series approximation for $\tanh\{N_r\}$, this expression can be simplified to:

$$\frac{R^2}{6 D_e} = \frac{1}{k_v} + \frac{V C_o}{2\Gamma/\mathcal{M}_c\ dm/dt} \qquad \ldots\ldots 5.29$$

Equation 5.24 is a relation between the effective diffusivity, D_e and the intrinsic rate constant, k_v in the case where boundary layer diffusion is not important.

5.4.5 The effectiveness factor

From equations 4.11 ($R_m = \eta A_i R_{i,s}$) and 4.7b ($R_{v,s} = \varrho A_i R_{i,s}$) the relation between R_m and $k_{v,s}$ can be found:

$$R_m = (\eta / \varrho) R_{v,s} = (\eta / \varrho) k_v C_s$$

Also, $R_m = -(\Gamma / m_o)\, dm/dt = -(\Gamma/\varrho V)\, dm/dt$

Combining these two expressions for R_m gives:

$$-\Gamma \, dm/dt = \eta \, V \, k_v \, C_s$$

Substituting 5.28b for dm/dt and using $C_o = \beta \, C_s$ (equation 5.27) yields the expression for the effectiveness factor as being:

$$\eta = 3 \, \mathcal{M}_c \, K_D \, (\beta - 1) \, / \, (R \, k_v) \quad \ldots\ldots\ldots \quad 5.30a$$

$$= (3 \, \mathcal{M}_c \, / \, N_r^2) \, (\, N_r / \tanh(N_r) - 1) \quad \ldots\ldots \quad 5.30b$$

Equations 5.30a and b provide expressions for the effectiveness factor which can be evaluated when a value for the parameter N_r is known.

5.4.6 Application

This model can best be used to find estimates for D_e and η by using known values for h_D and k_v. In this analysis, the form of the model where boundary layer diffusion was unimportant, i.e. $h_D \rightarrow \infty$ and $\beta = 1$, was used. A value of k_v was found from the literature.

From equation 5.29, D_e can be calculated. This value can then be used in equation 5.26a to find an estimate for N_r. This value of N_r can then be used in equation 5.30b to find an estimate for η. Since η is a measure of the penetration of oxygen into the sample, it gives a comparative measure of the effect of physical structure on the combustion process.

5.5 The Constants Required

Table 5.1 lists the constants and their values that were necessary to implement these calculation techniques.

This chapter has outlined the kinetic theory that forms the basis of this investigation. A number of calculation techniques have been outlined that obtain values for kinetic parameters from mass loss data. The models that have been described here make a number of assumptions. It is possible that

not all of these will be appropriate for the case of small wood particle combustion. It is necessary to match experimental data against these models firstly to test their appropriateness, and secondly to obtain kinetic parameters for different wood species.

Chapter 6 will describe the experimental procedures and apparatus that were used to generate mass loss data.

Symbol	Description	Value
P	% cellulose in wood [a]	46 % in softwoods 49% in hardwoods
R	radius of spherical sample	0.636 cm
C_o	molar concemtration of O_2	2.559×10^{-3} / T mol/cm^3
$\mathcal{M}_c$	molar mass of carbon	12 g/mol
$\mathcal{M}_g$	molar mass of O_2	32 g/mol
$\mathcal{R}$	universal gas constant	8.31441 J.K^{-1}.mol^{-1}
Γ	stoichiometric ratio	1
k_v	intrinsic rate constant for carbon [b]	
	$= \mathcal{A} \exp(-E/\mathcal{R}T)$	$E = 1.30 \times 10^5$ J.mol^{-1}
		$\mathcal{A} = 1 \times 10^7$ g.cm^{-3}.s^{-1}.atm^{-1}
V	volume	2.1551 cm^3

T = temperature of gas [K]
[Sources: a = Findley, 1975; b = Dutta & Wen, 1977[1]]

Table 5.1: Constants Required for the Calculation Techniques

1 of the values reported in the literature, those by Dutta and Wen were obtained from experiments whose conditions most closely resembled the conditions of the experiments conducted in this study.

Chapter 6

Experimental Apparatus and Procedures

The principle aim of this investigation was to develop a suitable technique for an evaluation of the fuel potential of different wood species. To achieve this, it was necessary to consider the actual combustion mechanisms of a burning wood sample. The combustion characteristics of different wood species must be experimentally determined. These can then be examined to ascertain what the differences between individual wood species are.

The previous chapter outlined the theoretical basis of wood combustion and presented calculation techniques to obtain the different kinetic parameters. This chapter will describe the experiments that were conducted. Firstly, the experimental aims will be briefly stated. Next the experimental apparatus will be described. This will be followed a description of the experimental design and the preparation of the samples.

6.1 Experimental Aims

The aim of the experiments was to obtain data which could be used to characterise and compare the combustion of different wood species.

The data required was continuous mass readings from a combusting wood sample under controlled conditions. This would allow the calculation of relevant kinetic parameters for combustion reactions. It was necessary to

obtain these parameters for samples burning at a constant temperature. Experiments were also to be performed for a range of temperatures to provide information on the temperature dependence of the kinetic parameters.

6.2 Experimental Apparatus

The experimental apparatus must be designed in such a way as to provide a controlled environment in which combustion can occur. This implies suspending the sample in a steady air flow at a constant temperature. In addition, instrumentation must be used to obtain continuous mass readings of the combusting sample as well as a measure of the temperature at which the reactions are occurring.

Figure 6.1 shows a schematic representation of the experimental rig used.

The wood sample under investigation was suspended in the quartz combustion chamber by a lightweight metal chain attached to the weighing apparatus.

A constant volume of air was supplied by a small blower. A gate valve and a tap allowed control of the rate of air supply. The air is preheated by the exhaust gas before entering the heating chamber. There it is heated to the required temperature. The heat source is a Kanthal silicon carbide electric element powered by a thyrister drive unit. The air is then fed into the combustion chamber from below, and the exhaust gas is extracted from above the wood sample.

To calculate the air velocity in the combustion chamber, it was necessary to determine the bulk flow in the supply tube upstream of the heating chamber, and to account for expansion due to temperature increases. A 10.4 mm orifice plate was inserted in the supply tube and an ultra-low differential pressure transducer used to measure the temperature drop across the plate. A k-type thermocouple was positioned inside the supply tube to measure the ambient air temperature and so determine the density of the incoming air. The rate of mass flow in the pipe can be calculated using standard orifice plate

calculations. This figure must then be corrected for expansion due to temperature increases and converted to a velocity measure. Appendix D derives the formula for this. The final form of the equation used is presented below.

$$\text{Air Vel} = 0.03553 * \text{dPair} \sqrt{[\text{Tamb}/352.3]} * \text{Tchamb} / \text{Tamb}$$

where dPair = square root of pressure drop over the orifice plate ($\sqrt{Pa}$)
Tamb = ambient air temperature (K)
Tchamb = combustion chamber temperature (K)

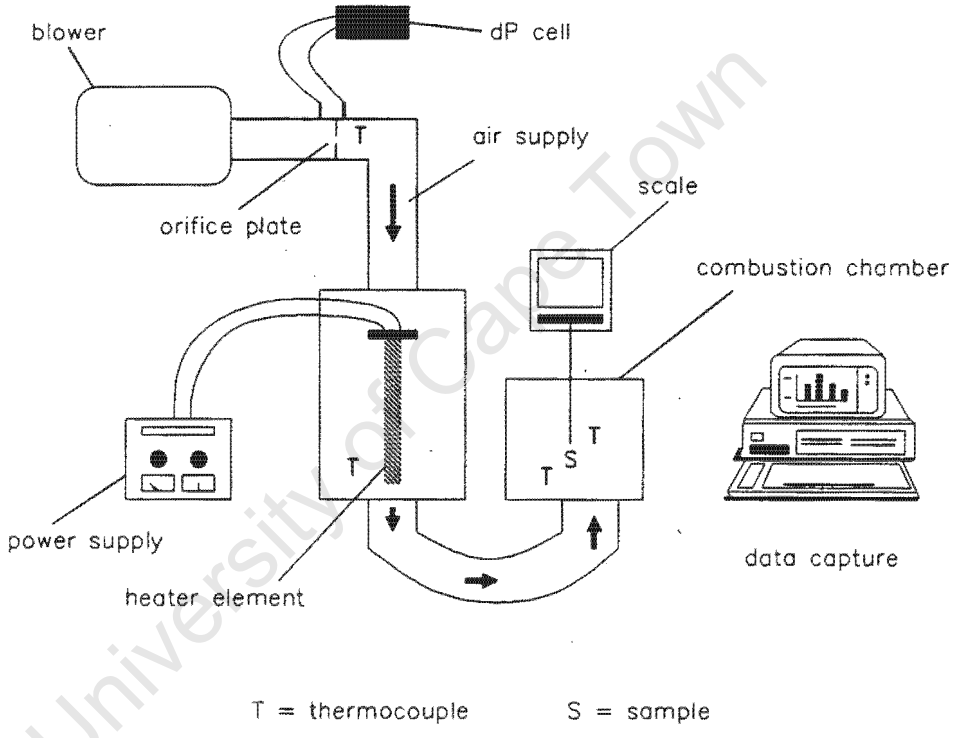

Figure 6.1: Schematic Representation of Experimental Rig

Two K-type thermocouples were placed inside the combustion chamber, one positioned just above the sample and one just below the sample. The average of these two readings was taken as the combustion chamber temperature. A fourth thermocouple, S-type, was placed inside the heater chamber to monitor the temperature there.

A Mettler AE 100 scale was used to measure the mass of the burning sample. The scale was positioned just above the combustion chamber and shielded from excessive heat. The sample was then suspended from the hook beneath

the weighing pan. The Mettler scale was fitted with a data interface unit which allowed on-line data capture through a serial port connection.

The air flow in the combustion chamber has a drag effect on the suspended sample. This was corrected for by the data capture software in the following way. At the time that the air is turned on, there occurs a sudden decrease in the mass. This mass change is taken as the drag force at this time. Similarly, when the air is turned off at the end of the experiment an increase in the mass reading can be observed. This is taken as the drag force at the end of the experiment. The second drag force will be less than the first as the sample has decreased in size and so presents a smaller surface area to the air flow. The drag force at any time between when the air is turned on and when it is turned off, is determined by a linear interpolation of the drag between these two points.

The other instruments (thermocouples and pressure transducer) gave voltage signals which were amplified to a 0 - 10V range. These signals were then fed into a PC-30 A/D conversion card. All instruments were carefully calibrated. The A/D card linearly converted a 0 - 10V signal to an integer in the range 0 - 4095. This reading was then scaled to the appropriate units in the software. Scalefactors were obtained from the calibration procedures. These are presented in table 6.1. The Mettler scale could be self calibrated and provided a real number to four decimal places in the gram. The specifications for the instruments used are presented in appendix C.

Data capture and processing software was written to obtain on-line data measurements. Appendix B shows a functional structure of this software.

Instrument	Scale Factor	Error
TC - ambient	0.02442	***
TC - heater	0.3905	0.0021
TC - hot air	0.2962	0.0006
TC - flue gas	0.2972	0.0018
DP cell[1]	0.0104	0.00007

TC = thermocouple

1 the pressure transducer also had an offset of 1.95 $\sqrt{Pa}$

Table 6.1 Calibration Scale Factors and Errors

6.3 Experimental Design

In the design of the experiments the following considerations had to be accounted for:

i) The experiments must provide data which can enable the calculation of the necessary combustion parameters.
ii) Experiments must be performed at a range of temperatures to establish the temperature dependence of these parameters.
iii) A suitable range of species must be selected for testing.
iv) The experiments must provide information on the variability of these parameters in order to ascertain whether differences between species are significantly larger than differences within a species.

The first two considerations meant that mass loss and temperature data was to be obtained from combusting samples for a range of temperatures. Experiments were performed for each type of wood at five different temperatures. An even spread of temperatures from 450°C to 700°C was obtained. The air velocity was held constant at 1.6 $m.s^{-1}$ for all experiments.

The third consideration meant that a range of both hardwood and softwood samples had to tested. In addition, tests were performed on both heartwood and softwood samples. Twenty species were selected for testing. These are listed in table 6.3. For each species five tests were performed at different temperatures for both heartwood and softwood samples.

The last consideration meant that in addition to the experiments described above, it was necessary to perform repeated tests for a selection of samples at a few different temperatures. Repeated tests were performed for six species (both heartwood and sapwood samples) at three different temperatures. At each temperature both a high density (a hardwood) and a low density (a softwood) species were combusted. Both heartwood and sapwood samples were tested. Table 6.2 shows the layout of these tests.

Species name	Temperature (°C)	No. Runs
Maytenus acuminata	425	3 H, 4 S
Cupressus torulosa	425	4 H, 4 S
Acacia sieberana	550	4 H, 4 S
Cupressus lusitanica	550	4 H, 4 S
Grevillea robusta	625	4 H, 4 S
Araucania angustifolia	625	4 H, 4 S

H = heartwood sample, S = sapwood sample

Table 6.2: Repeated Tests

6.4 Selection and Preparation of Samples

Table 6.3 lists the wood species used in the experiments.

Species name	Density (kg/m^3)	Hard/Soft	
Olea europea subs. africana	1029	H	*
Ptaeroxylon obliquum	970	H	*
Maytenus acuminata	930	H	
Eucalyptus maidenii	867	H	
Terminalia sericea	820	H	
Eucalyptus maculata	795	H	
Eucalyptus delgatensis	755	H	
Acacia sieberana	611	H	*
Grevillea robusta	564	H	
Podocarpus latifolius	527	S	*
Podocarpus falcatus	507	S	*
Cedrus libani	502	S	
Cupressus torulosa	478	S	
Cupressus lustanica	440	S	
Albies religiosa	440	S	
Gmelina arborea	439	H	
Araucania angustifolia	431	S	
Pinus patula	423	S	
Sequoia sempervirens	403	S	
Erythrina lysistemon	298	H	*

* = an indigenous species

Table 6.3: Species Selection and Densities

These species were selected to provide a range of densities and a spread between hardwoods and softwoods. Three Eucalypts of different densities were represented. Comparisons between these species determined whether the Eucalypts as a group can be expected to have different combustion characteristics. Three species (two softwoods: Cupressus lusitanica, Albies religiosa and one hardwood: Gmelina arborea) have very similar densities. Comparisons between these species will established whether species of similar densities will necessarily have similar combustion characteristics or not.

The common names of these species are given in appendix E. Species marked with an asterisk are indigenous to South Africa.

Samples were prepared from both heartwood and sapwood sections from each species. The wood from which the samples were cut had been air dried for over a year.

The samples were small cylinders of length 14 mm and diameter 14 mm. The axis of the cylinder lay with the grain. This size was small enough so that devolatilisation and char combustion were distinct phases, yet large enough to provide a sizeable mass. The samples were contained in a small nickel-chromium wire cage. This prevented ash from falling off the sample.

6.5 Experimental Procedure

The procedure for each experiment was as follows:

All electronic monitoring equipment was switched on and warmed up. The combustion chamber temperature was stabilised at the required level. The air flow was also stabilised at 1.6 $m.s^{-1}$. The software was initiated for data capture.

The air supply was switched off and the sample was loaded. The data capture routines were then commenced. After 10 seconds the air was switched on. Data capture continued until no further mass loss was observed. The air was

then turned off. Data capture continued for a further 30 seconds before being terminated.

Chapter 7

Results

This chapter is divided into five sections. The first section describes the initial data processing performed by the data capture and analysis software. The second section focuses on the descriptive parameters that were derived from the experimental data. Statistical tests were performed on these parameters for the series of repeated experiments. The results of these tests will be presented and discussed. The third and fourth sections focus on devolatilisation and char combustion models respectively. The success of these models in matching the data will be discussed and the results of statistical comparisons between species reported on. Again the data sets from the repeated experiments will largely be used. The last section will draw on the discussion presented in this chapter to decide which parameters can be used to distinguish between species. Chapter eight will then take this discussion further, extending the analysis to the complete set of twenty species.

7.1 Data Processing

Each experiment yielded a time series of values for the following parameters: mass, orifice plate pressure drop (DPair), ambient air temperature (Tamb), heater chamber temperature (Theat) and two temperature readings inside the combustion chamber (Tair and Tflue: these read the temperatures just below and just above the sample respectively). It is necessary to use these variables to identify the different stages of the experiment and to create transformed

variables for use in the analysis. These processing steps were performed by the data capture software. Appendix B describes the operation of this software.

7.1.1 Stages of an experiment

The experiment occurred in several discreet stages. The first data processing task was to identify when these stages started and stopped. For approximately the first fifteen seconds the data capture was run with the sample suspended but no air flow in the combustion chamber. The air was then switched on. This was marked by a sudden increase in DPair. After a short period the sample ignited and flaming combustion was observed to occur. When devolatilisation was complete, char combustion continued until no further mass loss was observed. At this time, the air was switched off.

The times at which the air was turned on and off could be identified by the sudden changes in the value of variable DPair. These times, together with the corresponding changes in mass, were used to calculate the drag effect during the experiment and so correct the mass data. The time at which the sample ignited is marked by the start of the sudden decrease in the mass curve and an increase in the variable Tflue. The end of devolatilisation and the beginning of char combustion is marked by the change in the slope of the rate of mass loss curve as the rate of mass loss levels out. The end of char burn is where there is no longer any decrease in the mass readings.

The software allows the user to identify these times by the display of selected graphs. For a description of this see appendix B.

7.1.2 Calculating the derivative

For the application of the different kinetic models, it is necessary to calculate the mass derivative with respect to time for both the devolatilisation and char combustion phases. The data processing software allows the user to do this in one of two ways. Firstly it is possible to fit a straight line to a fixed number of mass data points and use the slope as the derivative. This is repeated for each mass point using a data set centred around the point in question.

Alternatively, a similar procedure may be used with a quadratic fitted instead of a straight line. In addition it is possible to smooth the derivative by using a moving average routine. This is useful for char combustion where the derivative is of the order 10^{-3} g/s and hence sensitive to slight fluctuations in the mass data.

For the data presented here, the derivative was calculated using a quadratic fitted to nine data points at a time. In addition, for the char combustion phase a moving average smoothing routine over eleven points was used. Figure 7.1 presents the raw mass data and the calculated derivative for one sample.

The quality of the mass data is the most important consideration. In general, and as can be seen for the case presented in figure 7.1, the mass data is smooth and with very little fluctuation. The effect of the air being turned on and off can be clearly seen.

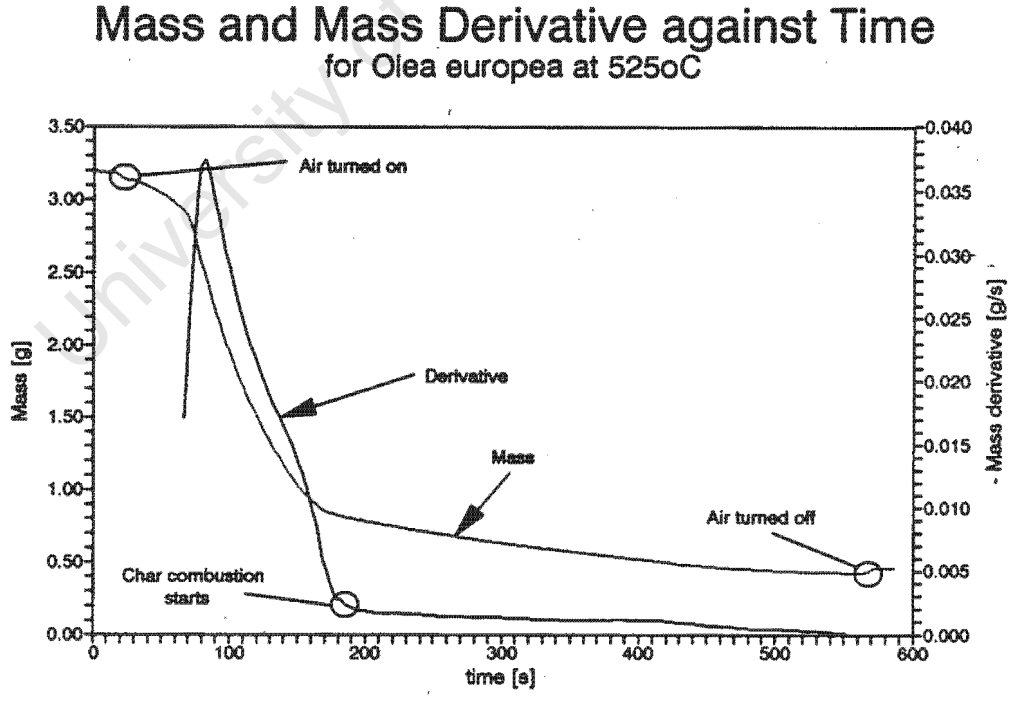

Figure 7.1: Mass and dm/dt vs time for Olea Europea

7.1.3 Transformed variables

For the implementation of the different models, it was necessary to calculate a number of transformed variables derived from the raw data. These variables were calculated and stored in an ASCII file which could be imported into a spreadsheet package for analysis.

For the devolatilisation phase, the variables required were firstly normalised mass derivative. This was calculated as the mass derivative divided by the mass of volatiles released. In addition the normalised mass was required. This was calculated by the expression:

$$M = (m - m_f) / (m_o - m_f)$$

where m_o and m_f refer to the mass readings at the start and at the end of devolatilisation.

For char combustion, different sets of data were required. Firstly, to calculate the average rate of mass loss required the untransformed variables mass and time. Secondly, to calculate the overall rate constant required normalised mass derivative, calculated as the derivative divided by the initial mass of char. Also this model required the normalised mass raised to the power of two-thirds. Lastly, the shrinking core model required the transformed variables defined by equations 5.22a to 5.22d.

In addition, the average combustion chamber temperatures during both the devolatilisation and char combustion phases were required. These were obtained by averaging Tair and Tflue for the duration of these two phases.

7.1.4 Calculation of descriptive parameters

"Descriptive parameters" refers to ignition time, normalised devolatilisation time, normalised char burnout time and amount of char formed. The definitions of each of these is given below.

Ignition time is calculated as the time lapse between when the air flow in the combustion chamber was switched on and the onset of flaming combustion. At high temperatures this was practically instantaneous.

Devolatilisation time is taken as the time from the onset of flaming combustion to the start of char combustion. This is then normalised by dividing by the total mass of volatiles released during this period. The units are s/g. In a similar way, the char burnout time is the time from onset of char combustion to its finish, normalised by the quantity of char burnt. Again the units are s/g.

The amount of char formed is measured as a percentage of the total mass reacted during the experiment.

7.2 The Descriptive Parameters

For the six species on which repeated tests were performed, comparisons of the descriptive parameters were made firstly between heartwood and sapwood samples, and secondly between pairs of species. The way in which these tests were constructed allowed for the following comparisons to be made:

i) between heartwood and sapwood samples of a dense and a light species at three different temperatures;
ii) between a dense and a light species at three different temperatures.

Comparisons were made using two tailed Wilcoxin non-parametric tests. This test was selected as an appropriate non-parametric technique since these comparisons involved only eight or sixteen values. The test is described in appendix F.

Comparing the ignition times of all six species showed that no significant distinctions could be made between heartwood and sapwood samples of one species at any of the temperatures. Similarly no distinctions between heartwood and sapwood samples could be made on the basis of char burnout times or percentage char formed. Using a significance level of 5%, only Cupressus torulosa (a softwood at a low temperature) and Acacia sieberana (a

hardwood at a medium temperature) showed significant differences between the devolatilisation times of their heartwood and sapwood samples.

Because of this result, the values of these descriptive parameters for sapwood and heartwood samples were averaged to give a combined value representative of the species.

Comparisons were then made of these descriptive parameters between the pairs of species at the three temperatures. This showed that at the low and medium temperatures, there were significant differences between the values of all parameters. However, at the highest temperature, no significant differences could be established.

The results of these comparisons are summarised in table 7.1

Comparing heartwood against sapwood

Species	Temp	Ignit t	Devol t	Char t	% Char
Maytenus acuminata	Low	N	N	N	N
Cupressus torulosa	Low	N	Y	N	N
Acacia sieberana	Medium	N	Y	N	N
Cupressus lusitanica	Medium	N	N	N	N
Grevillea robusta	High	N	N	N	N
Araucania angustifolia	High	N	N	N	N

Comparing a hardwood against a softwood

Species	Temp	Ignit t	Devol t	Char t	% Char
Maytenus acuminata vs Cupressus torulosa	Low	Y	Y	Y	Y
Acacia sieberana vs Cupressus lusitanica	Medium	Y	Y	Y	Y
Grevillea robusta vs Araucania angustifolia	High	N	N	N	N

Y = a significant difference could be distinguished
N = no significant difference could be distinguished

Table 7.1: Results of Wilcoxin Tests

7.3 Devolatilisation Data and Model Fits

7.3.1 The data

The mass loss curves for devolatilisation showed an initial preheat phase (prior to ignition) followed by a stage of rapid mass loss which was terminated by a sharp tail off in the rate of mass loss. At low temperatures the preheat phase could be of significant duration, especially for the denser species. In these cases a significant quantity of volatiles was released during this period. The main stage of rapid pyrolysis continued until approximately 80% of the mass had reacted. At this time the rate of mass loss stabilised as the slower process of char combustion began.

During the period of rapid mass loss, the particle was enveloped in flame. The reading of the thermocouple situated just above the sample increased sharply, typically by about 75°C, whilst the thermocouple below the sample gave constant readings. The average temperature reading over this period is influenced by the high flame temperature. At the same time, the flame is providing a major heat source for the particle. During this phase of combustion there are complex heat transfer processes occurring across the boundary layer and within the sample. Because of this the average combustion chamber temperature can not be taken as an accurate measure of the sample internal temperature.

7.3.2 Devolatilisation model fits

Applying the overall rate constant model to the devolatilisation data involved a linear regression between the normalised rate of mass loss and the normalised mass. For the six species on which repeated tests were performed, the correlation coefficients were typically of the order of 0.95. This indicated that the model fitted the experimental data well. Figure 7.2 shows a plot of this regression for Olea europea heartwood specimen at 525°C and shows the best fit line to the points. The data clearly shows a linear relationship. Towards the end of devolatilisation (where normalised mass $\rightarrow$ 0) the data points deviate from the linear relationship. This is due to some overlapping between devolatilisation and char combustion.

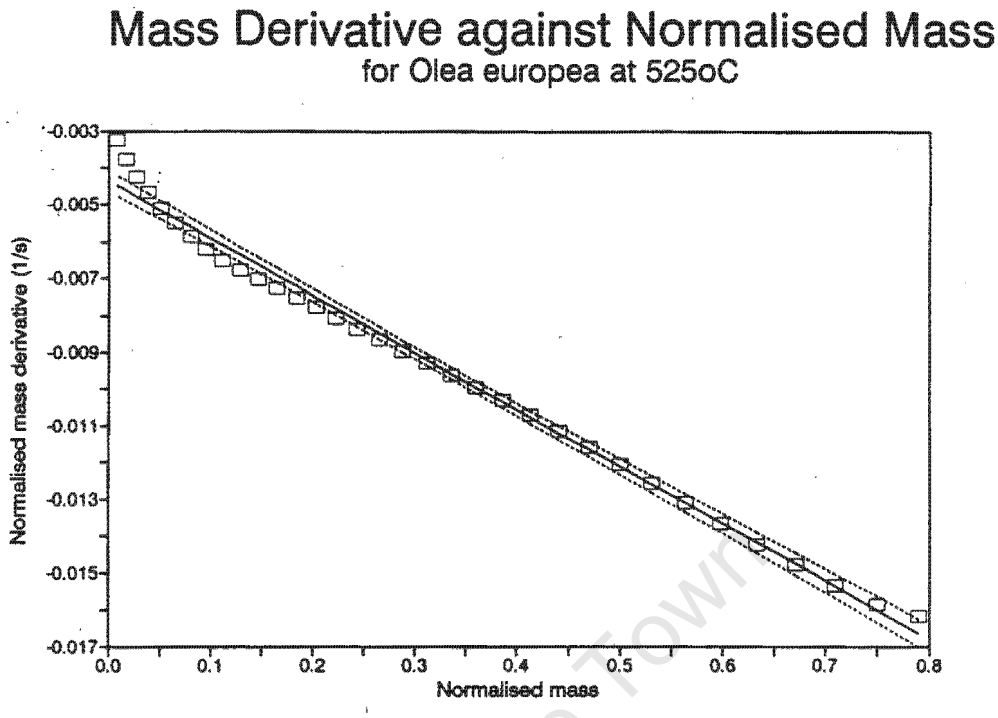

Figure 7.2: Regression Plot for Devolatilisation Model

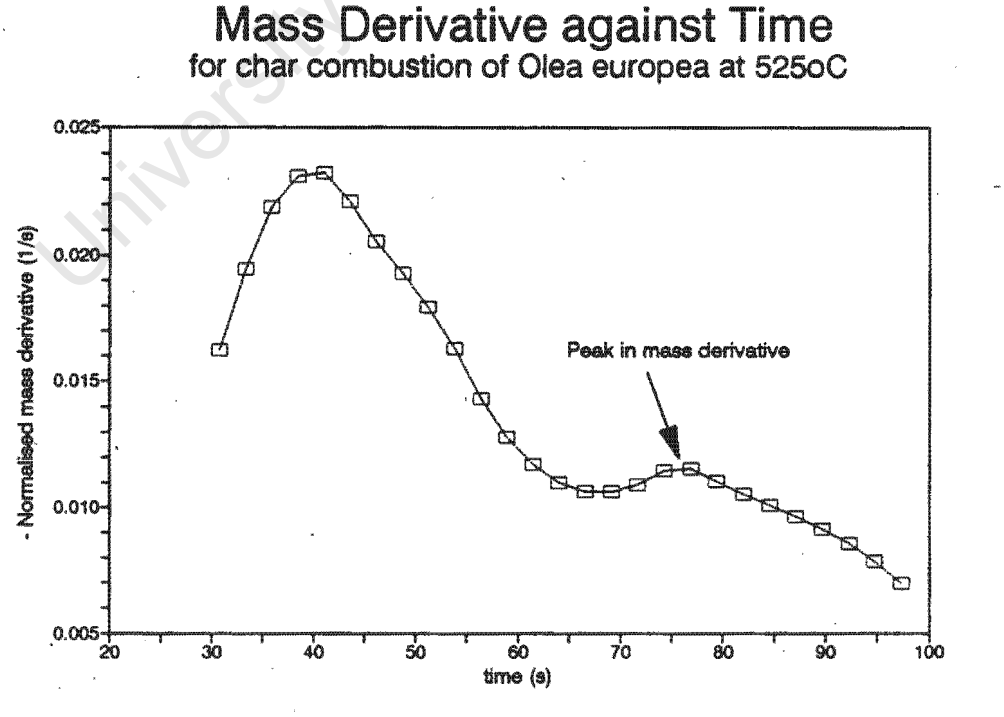

Figure 7.3: Rate of Mass Loss during Devolatilisation

"Equal slopes" tests were applied to these data sets to determine whether significant differences in devolatilisation rate constants between hard and soft woods could be distinguished. This type of statistical test is described in appendix F. The results of these tests showed the variation within a species is as great as that between different species.

The form of the reactivity vs time curves for devolatilisation indicate that a two component reaction mix is occurring. Figure 7.3 shows a reactivity curve for a Grevillea robusta heartwood sample which exhibits the peak in reactivity during the devolatilisation process. This peaking is characteristic of many of the samples tested. Attempts to apply a two component model as described in section 5.2.1 were unsuccessful as the data sets, particularly for softwoods where devolatilisation occurred so quickly, were too small to give reliable results.

7.4 Char Combustion Data and Models

The char combustion phase lasts considerably longer than the devolatilisation phase and the mass loss is a slower, steadier process. The end of char combustion is defined as being when no further mass loss occurs.

The different char combustion models involved performing three correlations. For the overall rate constant model, a fit between the normalised rate of mass loss and the normalised mass was required. The shrinking core model involved a multiple regression with four transformed variables, and the progressive conversion model required a simple fit between mass and time to obtain an average rate of mass loss.

The average number of data points involved in these correlations was over one hundred and for this size of data sets, the critical value for the correlation co-efficient is only 0.305. All correlations had coefficient considerably larger than this.

7.4.1 Overall rate constant model

For the overall rate constant model typical correlation coefficients were of the order of 0.95. Figure 7.4 shows a plot of the data for this regression and indicates the best fit line. (In this graph, there are too many data points to represent each one by a discreet point, so they have been represented by a line).

"Equal slopes" tests were performed on the repeated data sets, comparing a hardwood to a softwood at three different temperatures. These tests showed that highly significant differences could be distinguished between the species. The same tests were performed on the three Eucalypt species. These tests also showed that significant differences could be measured between the rate constants of different species.

7.4.2 The shrinking core model

Applying the shrinking core model to the species for which repeated tests were performed resulted in highly successful fits. Generally, a more complex model with more variables will result in a better statistical fit. For this three parameter model correlation coefficients were of the order of 0.98. However, the regressions consistently gave negative values for a_1 and a_3. These correspondingly gave negative values for the effective diffusivity and the rate constant. This indicates that although the mathematical model fits the data well, the underlying theory is inappropriate.

7.4.3 Average rate of mass loss

The last correlation performed on the char mass data was the calculation of the average rate of mass loss. This involved a plot of mass against time and calculation of the slope using standard least squares correlation techniques. Again the fits were good with correlation coefficients to the order of 0.96. Figure 7.5 shows an example of this fit, plotting mass against time and the best fit straight line. The mass data is reasonably linear with time, although non-linearity occurs both at the start and at the end of char combustion.

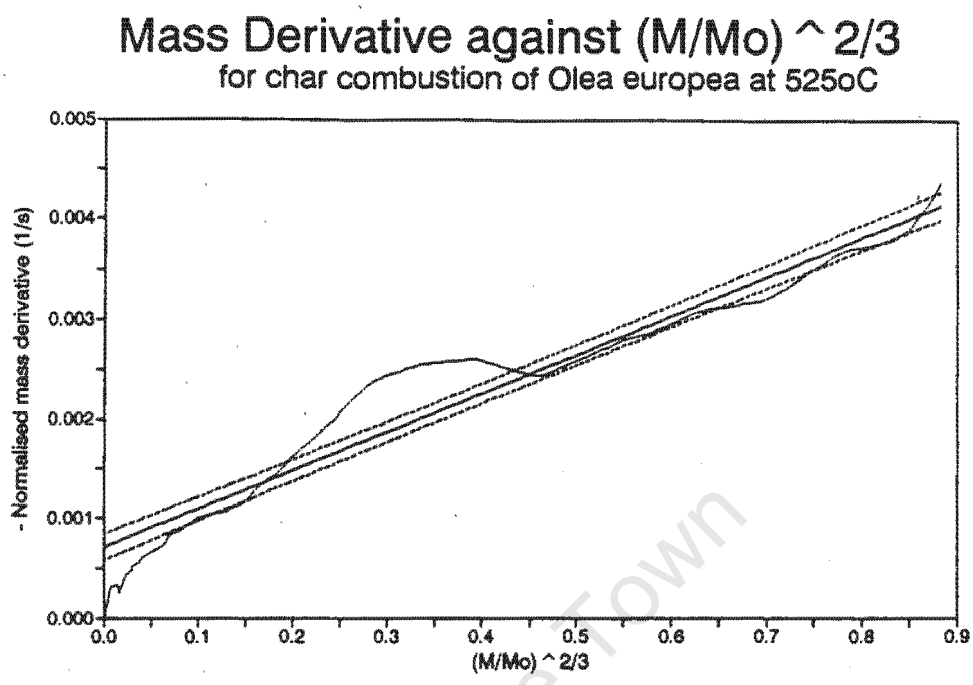

Figure 7.4: Regression Plot for Char Combustion Rate Constant Model

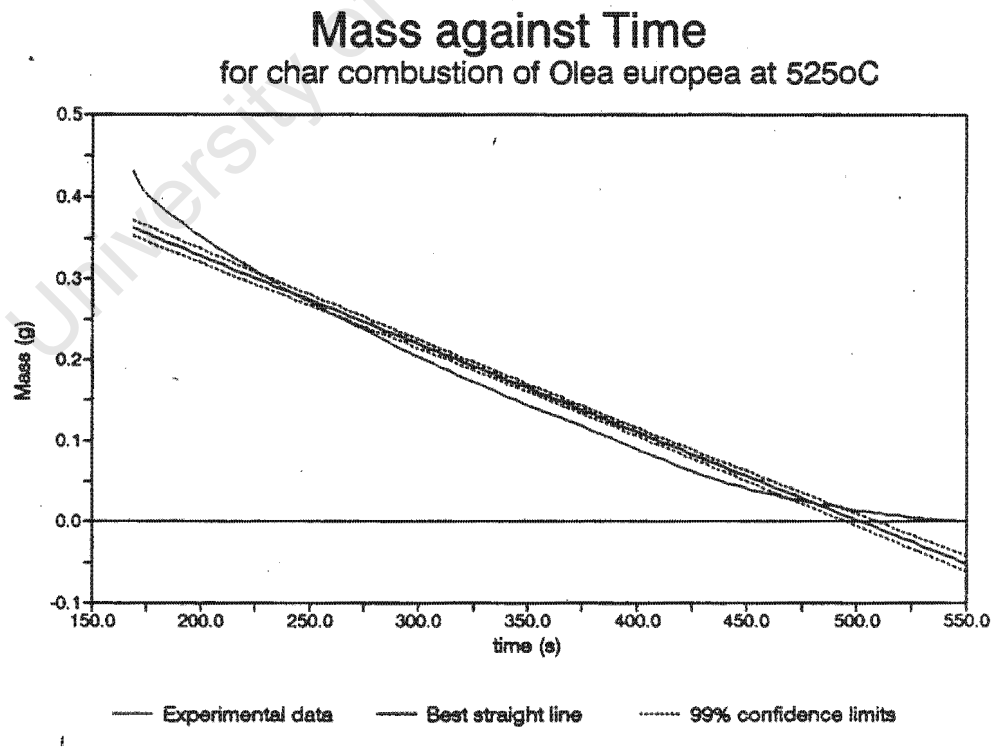

Figure 7.5: Regression Plot for Char Combustion Mass vs Time

"Equal slopes" tests were performed to determine whether there were significant differences between species. These tests were performed on those species for which repeated tests were performed as well as on the three Eucalypt species. The results of these tests showed that highly significant differences existed between the species.

Using the approximate form of the progressive conversion model suggested in section 5.4.6 together with reported values for the intrinsic rate constant allows one to estimate the effective diffusivity and the effectiveness factor from the average rate of mass loss. For this calculated value of D_e to have meaning (i.e. $D_e > 0$), the average rate of mass loss at in the temperature range 450 - 650°C is constrained by:

for T = 450°C: $dm/dt < -0.0179$ g/s

for T = 650°C: $dm/dt < -1.928$ g/s

The average mass loss rates calculated were in the range from - 0.00035 to - 0.0012 g/s at 450°C and from - 0.00095 to - 0.0038 g/s at 650°C. This indicates that the progressive conversion model, or at least this simple form of it, does not fit the experimental data.

7.4.4 The Arrhenius equation

To calculate the activation energy for a reaction requires a fit of the Arrhenius equation to a set of rate constants calculated at different temperatures. The overall rate constant derived for char combustion combines the effects of boundary layer diffusion, intra-particle diffusion and intrinsic kinetics. If intrinsic kinetics are dominant or rate limiting, then the overall rate constant will approximate the intrinsic rate constant and will have an Arrhenius dependence on temperature.

Examining the graphs of rate constants against temperature presented in appendix G shows that an Arrhenius equation can not be applied to the rate constants for char combustion derived in this way.

7.5 The Useful Parameters

The discussion above indicates that not all the parameters are useful for comparing species. For devolatilisation, although the first order overall rate constant model fits the experimental data, there are no significant differences in rate constants between the species. This indicates that devolatilisation occurs in a similar manner for all species. For char combustion, the shrinking core model and the progressive conversion model are not appropriate. Thus the parameters derived from these models could not be used for comparative purposes.

In addition, although an overall rate constant could be calculated for char combustion, this rate constant does not conform to an Arrhenius dependence on temperature. Thus activation energies could not be calculated for the individual species.

The parameters that are of use then are firstly the descriptive ones: the ignition time, the normalised devolatilisation time, the normalised char burnout times and the percentage char formed. Secondly, for char combustion the overall rate constants can be compared as can the average rates of mass loss. Graphs of these parameters are presented for the complete set of twenty species in appendix G.

The purpose of this discussion has been to identify the parameters which can be used to compare species. Chapter eight will take this analysis further by using these parameters to compare the full twenty species.

Chapter 8

Discussion

The discussion in this chapter will have two foci: one to identify the trends evident in the experimentally determined characteristics; and two to attempt to relate these characteristics to the value of a wood species as a fuel.

The first section of this chapter will take each parameter in turn and discuss the variation in values among the species. Attention will be focussed on temperature dependence, density dependence and overall differences between hardwood species and softwood species. The next two sections will examine the differences and similarities firstly between the three species of equal density and secondly between the three Eucalypt species.

The rest of the chapter will attempt to make the connection between experimentally determined parameters and fuel value. Firstly the species will be ranked according to the values of the different parameters in an attempt to identify patterns and consistencies among the species, and to test correlation with information on fuelwood preferences. The next section will discuss the influence of internal structure of the wood on its combustion properties. This will include a discussion around the relationship between micro properties, as determined by the types of experiments conducted here, and the macro properties of a cooking fire. Lastly a summary of the results will be presented.

8.1 The Combustion Parameters

This section will examine the temperature and density dependence of the experimentally determined parameters. It should be noted that no consistent differences could be established between heartwood and sapwood samples. For this reason, the values of the properties for the heartwood and the sapwood sample for each species and each temperature were averaged to give a value for the species at that temperature.

Graphs for each species displaying the values of these parameters plotted against temperature are presented in appendix G.

8.1.1 Ignition time

Ignition time is defined as the time taken for the sample to ignite into a flame after the hot air has been turned on. During this period, heat transfer across and within the sample is occurring to raise the temperature level of the sample. Ignition will occur when sufficient volatiles are flowing out of the sample. Devolatilisation may be occurring prior to ignition, but not sufficiently enough to provide the necessary air/fuel mix in the boundary layer.

The ignition time will be dependent on a number of factors. Firstly the rate of heat transfer will determine the internal temperature of the sample, and so the rate of pyrolysis. This heat transfer is a complex process with a number of secondary factors affecting the average rate of transfer (Murty Kanury & Blackshear, 1970[a]). Clearly, the properties of the external environment (such as bulk temperature and air flow) will affect the transfer across the boundary layer. Internally, the heat transfer will be strongly dependent on the physical structure of the wood. Wood is a good insulator due to the presence of air spaces. This means that a denser wood will conduct heat faster (Desch, 1968: p189). However, a denser wood has a higher heat capacity which will tend to reduce the rate of heat transfer. The convection effect discussed in chapter three will also be influenced by the structure of the wood.

As volatiles form inside the wood, they will move towards the surface. This movement will again depend on the wood type as a more closely packed denser structure will inhibit this motion. This affects the ignition time as flaming will only occur when sufficient quantities of volatiles are leaving the sample.

Temperature dependence

The form of the temperature dependence is consistent for all species. At high temperatures (above 625°C), the ignition is virtually instantaneous for all samples. As the temperature decreases, the ignition time increases in an exponential manner. Figure 8.1 shows the effect of temperature on ignition time for three species of different densities. As mentioned above, the bulk gas temperature determines the sample surface temperature and so affects the rate of heat flow into the sample. This controls the rate at which pyrolysis is occurring.

Density dependence

The general trend is that ignition time at lower temperatures increases with density. Figure 8.1 shows this effect where a high, a medium and a low density species is represented. Figure 8.2 plots the ignition temperature at 500°C (obtained for each species by fitting an exponential curve to the five discrete points and calculating the ignition time at 500°C on this curve). This graph shows that lower density species have on average a lower ignition time. However, the trend is not rigid and species pairs of close density may not conform to the trend. This is particularly so in the case of softwoods where as a group they conform to this density trend, but within the group do not show any clear dependence on density.

Hardwood/softwood differences

The softwoods are of a lower density than hardwoods and thus exhibit a faster ignition time, except in cases where the hardwood is particularly light, for example Erythrina lysistemon and Gmelina arborea.

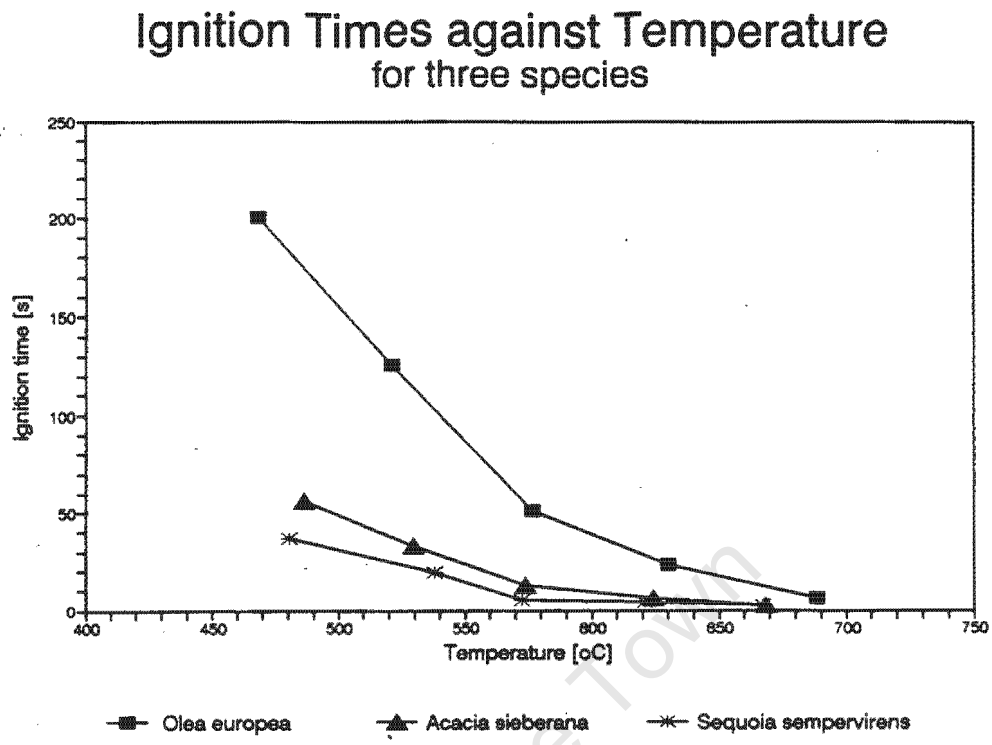

Figure 8.1: Ignition Time against Temperature

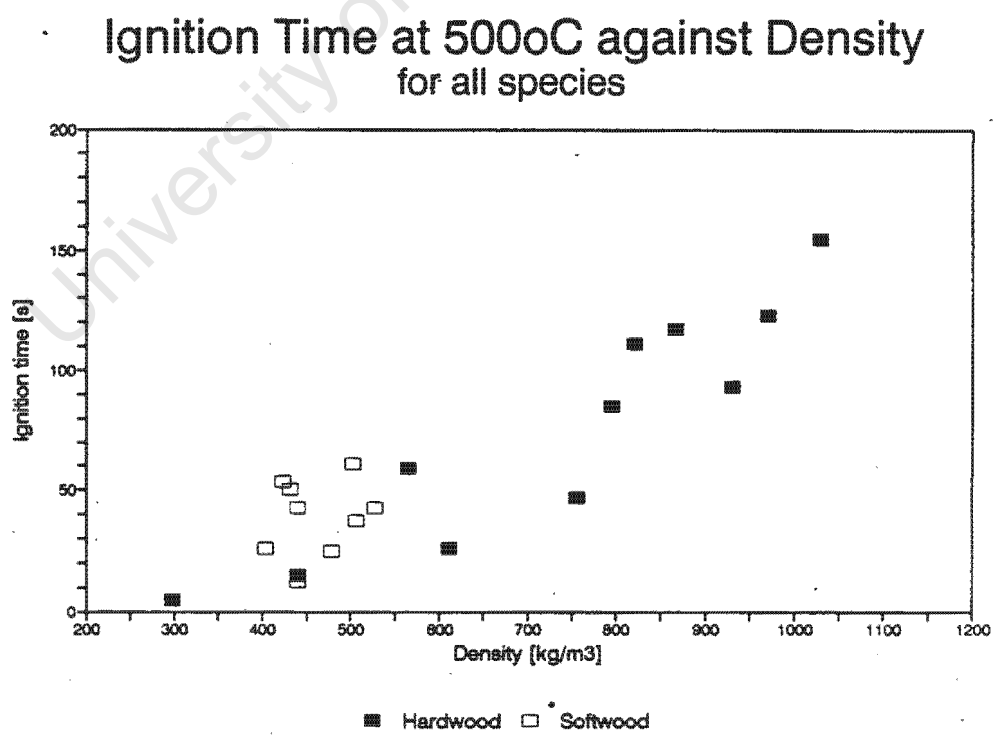

Figure 8.2: Ignition Time against Density

The hardwoods show a reasonably consistent dependence on temperature whereas the softwoods do not show any clear distinctions based on density.

This relationship at low temperatures between ignition time and density can be explained in terms of the effect of internal structure. Both internal heat transfer and permeability to outward flowing pyrolysis products will be determined by the wood structure. However, although there will be a correlation between density and permeability, this will not be a strict dependence. It is quite possible for a denser sample to have a structure which more easily facilitates the flow of gases.

8.1.2 Devolatilisation time

This parameter is defined as the total time taken for devolatilisation (from ignition to end of flaming) divided by the total mass of volatiles released from the wood.

Temperature and density dependence

The devolatilisation time is reasonably constant over the temperature range tested.

Figure 8.3 shows devolatilisation time against temperature for three species of widely different densities. The denser species has the lowest devolatilisation time and the lighter species has the highest. This trend is borne out in figure 8.4 where there is a general increase in average devolatilisation time as density decreases.

Hardwood/softwood differences

Again, since most of the hardwoods are denser than the softwoods they tend, as a group to have a lower devolatilisation time.

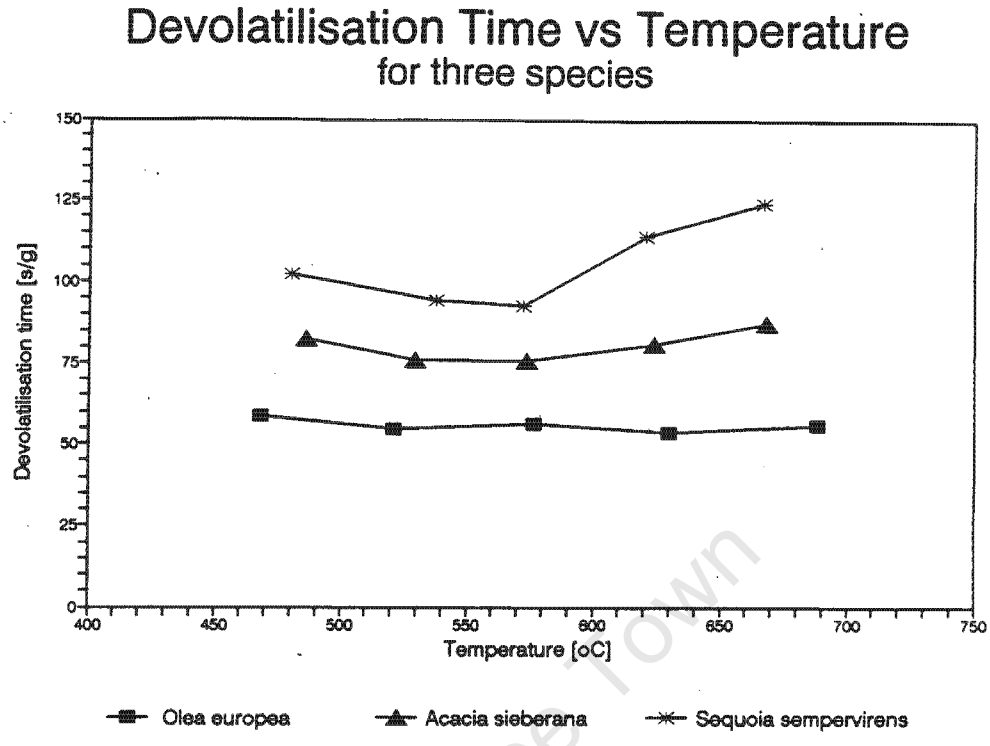

Figure 8.3: Devolatilisation Time against Temperature

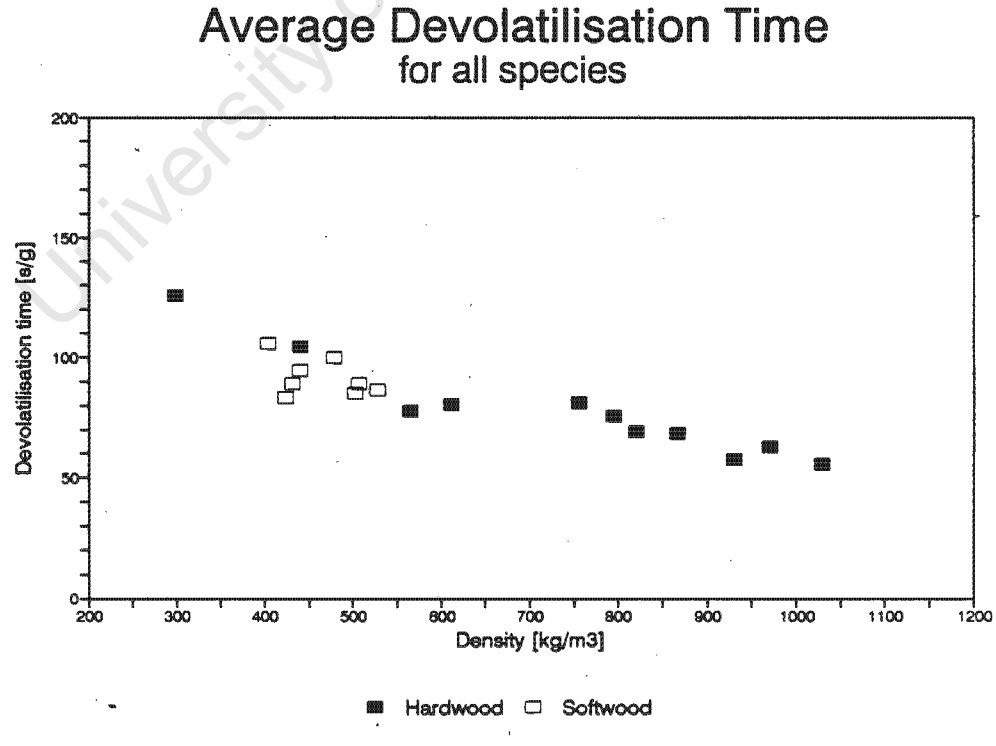

Figure 8.4: Average Devolatilisation Time for All Species

The processes involved in devolatilisation are heat transfer into the sample, pyrolysis reactions and outward flow of gases from the sample. The first and last of these processes are likely to be influenced by wood structure in the same way that ignition time is affected. That is, devolatilisation time per gram of volatiles will be slower for denser woods. The experimental results agree with this.

8.1.3 Char burnout time

This property is defined as the time taken from the end of pyrolysis to the end of char combustion, divided by the original mass of char. The end of char combustion is located as the time at which no further mass loss is experienced.

Temperature dependence

There is a trend of decreasing char burnout time with increasing temperature. Figure 8.5 presents char burnout time against temperature for three species of widely different densities.

This relation is explained by the fact that a higher temperature is likely to speed up both the diffusion of oxygen into the sample and the kinetics of combustion.

Density dependence

The magnitude of the dependence of char burnout time on temperature seems to vary with density. At higher densities, this effect is less pronounced. This is illustrated for three species in figure 8.5. If a straight line is fitted to the char burnout time against temperature for each species, the magnitude of the slope of the line increases with decreasing density.

Figure 8.6 shows the char burnout time at a low (475°C), medium (575°C) and a high (675°C) temperature for each species. This plot shows that for lower densities, the range in char burnout times is greater.

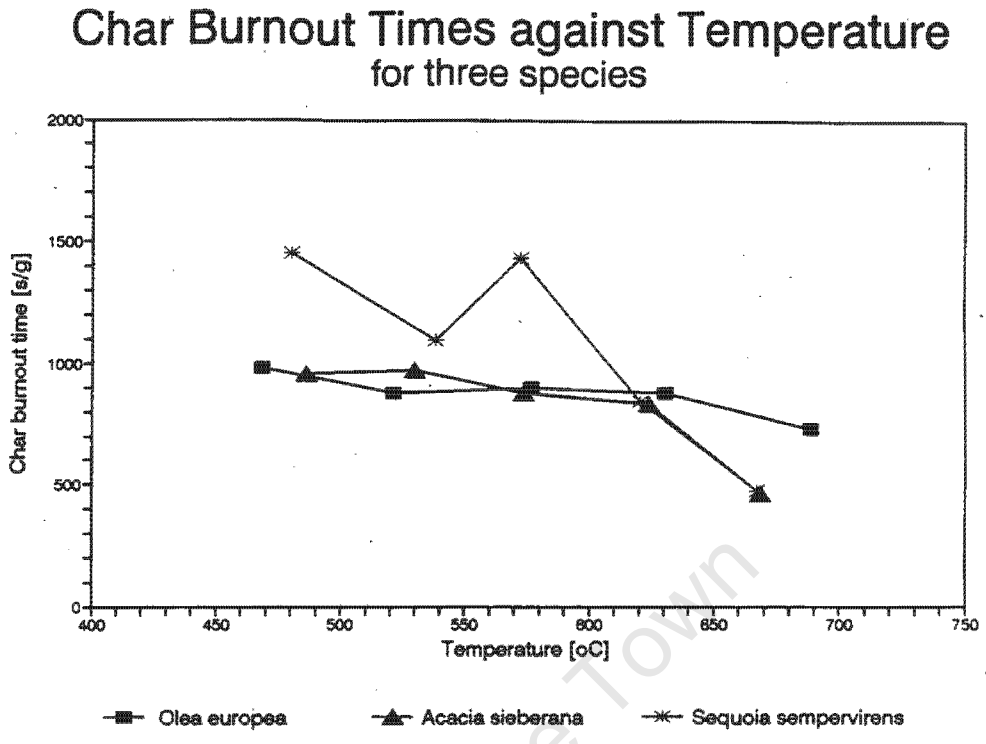

Figure 8.5: Char Burnout Time against Temperature

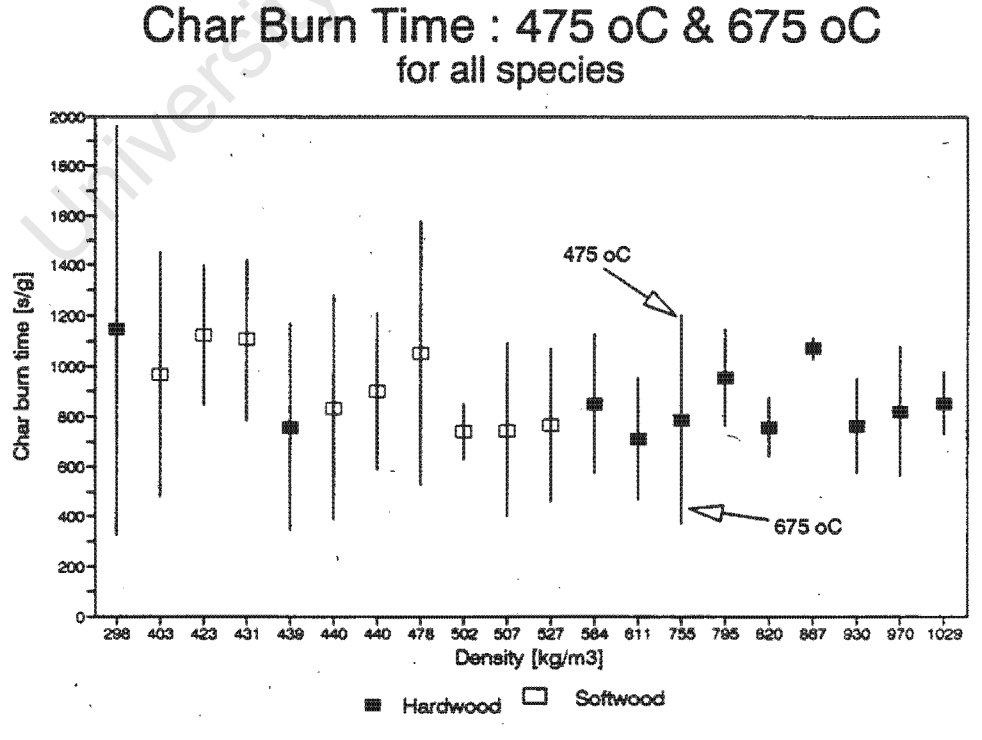

Figure 8.6: Char Burnout Times for All Species

Hardwood/softwood differences

Again, the softwoods tend to have a stronger dependence on temperature. This is probably due to the fact that they have a lower density than the hardwood species.

Within the softwood group, there is no clear density trend, whereas within the hardwood group which spans a greater range of densities, there is a clearer relationship with density.

8.1.4 Percentage char formed

The percentage char is defined as the ratio between char mass at the end of devolatilisation and total mass of volatiles released (including those released before ignition), expressed as a percentage.

Graph 8.7 shows that hardwoods form slightly more char than softwoods. The hardwoods form on average 4% more char than the softwoods.

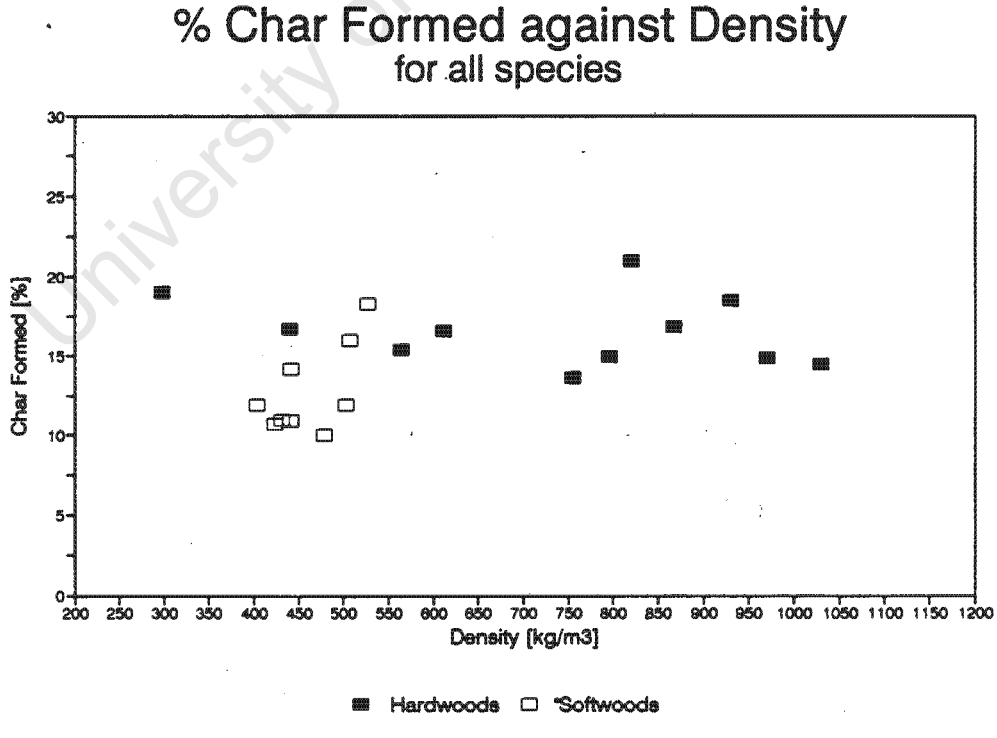

Figure 8.7: Average % Char Formed for All Species

The mechanism of char formation lies in the pyrolysis reactions. The different constituents of wood, cellulose, hemicellulose and lignin produce different quantities of char. Lignin produces around 45% - 55% char (Simmons, 1983: p15) whereas cellulose only produces around 15% (Roberts, 1970: p264). Softwood contains on average more lignin than hardwood (23% - 33% as opposed to 16% - 25%) (Simmons, 1983: p6). However, this difference would only mean that softwoods produce about 3% more char than hardwoods.

Of more importance is the effect of secondary pyrolysis reactions on char formation. Secondary pyrolysis can follow different reaction paths which result in different levels of char production. A wood with a lower permeability favours a reaction path which results in less char being formed (Eberhard, 1987: p20). Since softwoods have a lower longitudinal permeability than hardwoods, this would tend to decrease their level of char formation. This is borne out by the slight differences in char production between hardwoods and softwoods observed in this investigation.

8.1.5 Rate constants

This parameter is derived from correlations between the normalised rate of mass loss and (normalised mass)$^{2/3}$ as outlined in chapters six and seven. The rate constant is an over-all "lumped" value including the effects of all the different processes in char combustion.

Temperature dependence

The general trend is for the rate constant to increase slightly with temperature. However, figure 8.8 which plots the rate constants for three species against temperature, illustrates that this relationship is not of an Arrhenius form.

There are exceptions to this general observation. Olea europea, Araucania angustifolia and Sequoia sempervirens have a more or less constant rate constant with temperature. Maytenus acuminata and Erythrina lysistemon show a steeper increase with temperature than the other species.

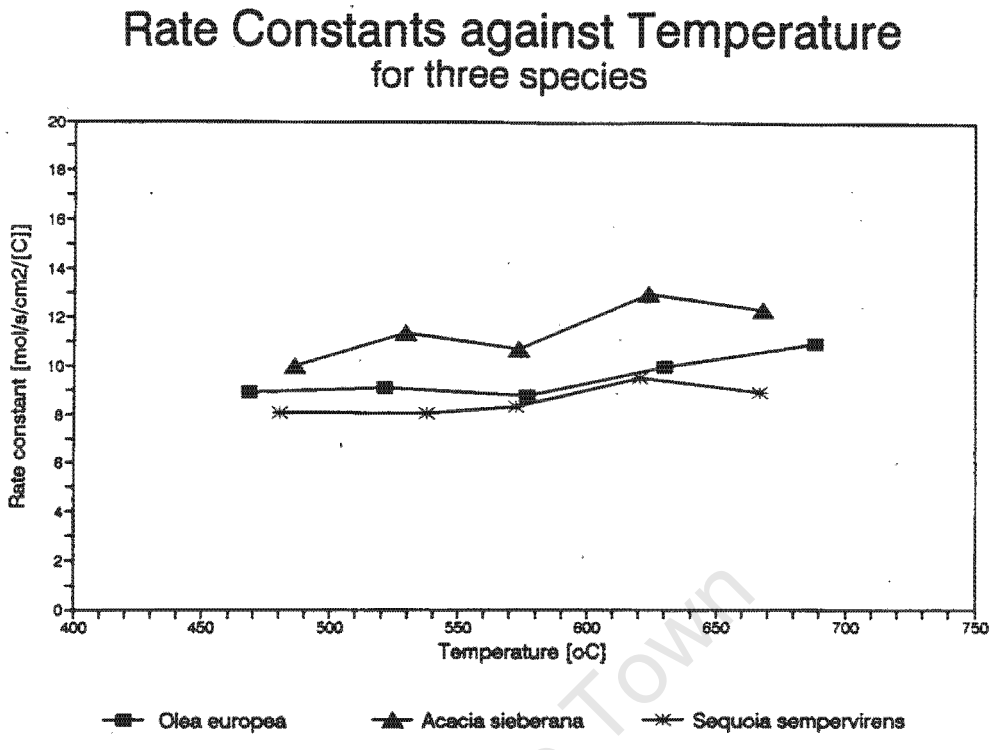

Figure 8.8: Char Rate Constants against Temperature

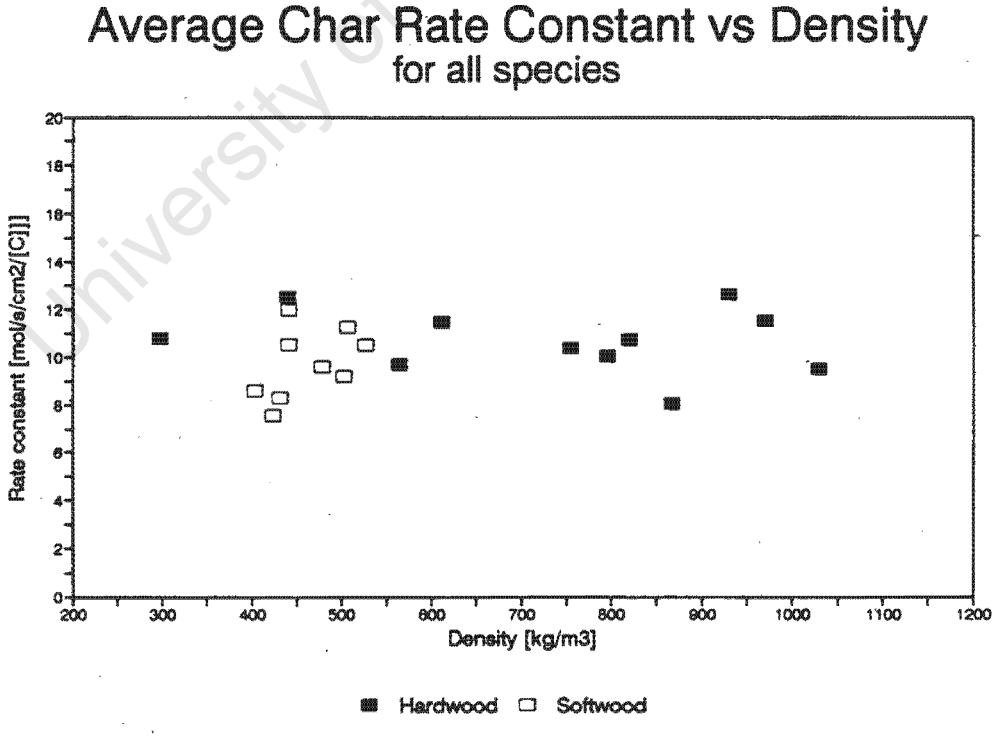

Figure 8.9: Char Rate Constants for all Species

In most cases no clear distinctions can be made between the heartwood and sapwood samples of a species. However for the three species Podocarpus latifolius, Cupressus torulosa and Cupressus lusitanica, the rate constants for the sapwood samples are higher than those of the heartwood samples.

Density dependence

There are no consistent trends in the rate constant with density. Figure 8.9 plots the char rate constant for all species in order of increasing density.

The dependence on temperature does not follow an Arrhenius dependence. Recall that this is a lumped rate constant and so includes boundary layer and intra-particle diffusion effects as well as the intrinsic char combustion kinetics. Clearly only the intrinsic rate constant will have an Arrhenius dependence on temperature and the diffusion components will disturb this relationship. It is possible that at the high temperatures of these experiments, the diffusion processes become rate limiting and the intrinsic kinetics are no longer significant.

8.1.6 Mass loss rates

The mass loss rate is the magnitude of the slope of the straight line fitted to the plot of mass against time. It has units of g/s and represents the average rate of mass loss during char combustion.

Temperature dependence

The mass loss rate tends to increase with temperature (see figure 8.10). For the more dense species this relationship is approximately linear, whereas for less dense woods the mass loss rate increases sharply in the higher temperature range.

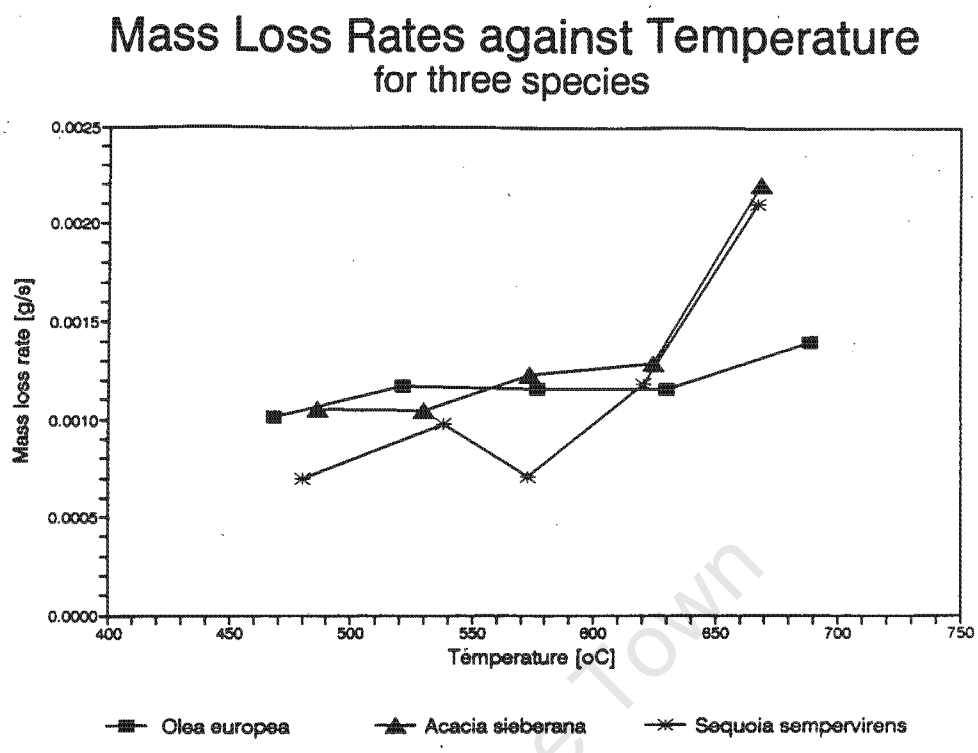

Figure 8.10: Mass Loss Rates against Temperature

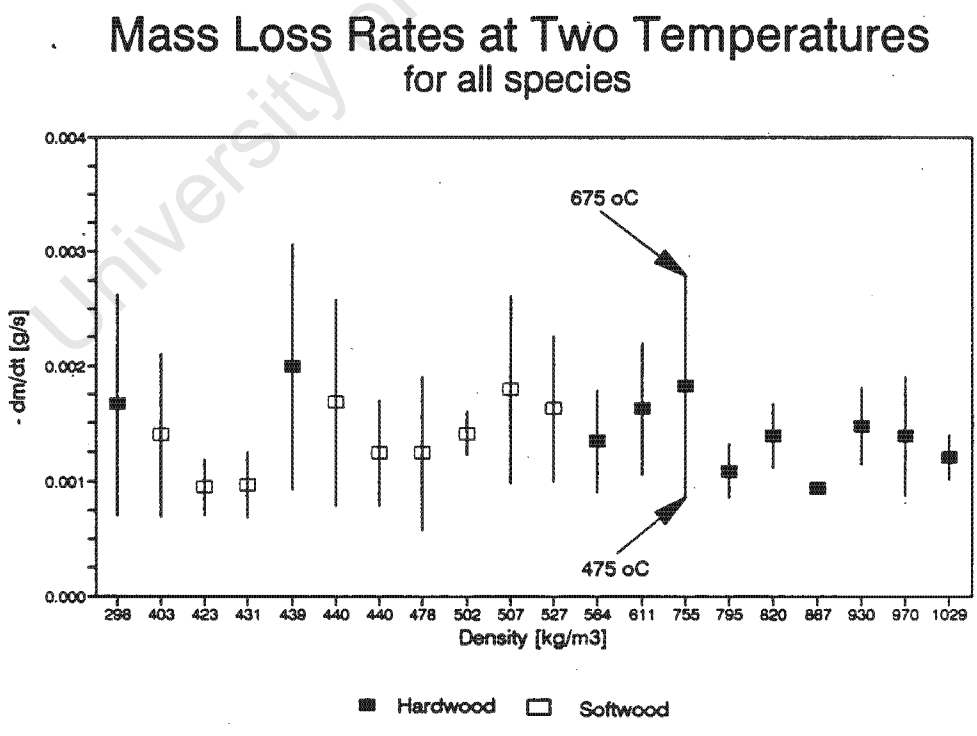

Figure 8.11: Mass Loss Rates for All Species

Density dependence

For the hardwoods there is a trend that the lower the density, the sharper the increase in mass loss rates with temperature (see figure 8.11). Eucalyptus is the notable exception to this trend. For the softwoods, there is no such obvious dependence on density.

8.2 Three Species of Equal Density

Three of the species chosen for experimentation had identical densities of 440 kg.m^{-3}. Two of these species, Cupressus lusitanica and Albies religiosa are softwoods and the third, Gmelina arborea is a hardwood. What follows is a brief discussion of their differences and similarities.

All three species have ignition times (at 500°C) which conform more or less to the density trend discussed above. However, Cupressus lusitanica has a noticeably higher ignition time than the other two (see figure 8.12).

Figure 8.13 shows devolatilisation times for all three species against temperature. All have a very similar devolatilisation time, although Gmelina arborea has a value that increases at high temperatures.

All three species exhibit a similar range of char burnout times with temperature (see figure 8.14). However Cupressus lusitanica has the highest average value and Gmelina arborea the lowest. The percentage char formed is in the range 11% - 17% with the softwood Cupressus lusitanica having the lowest value. Figure 8.15 shows that although Gmelina arborea is in the same density range as the softwoods, it produces more char than most softwoods.

All three species have very similar average mass loss rates at low temperatures. However, figure 8.16 shows that at higher temperatures the hardwood Gmelina arborea has the highest value and Cupressus lusitanica the lowest value. Similarly, the three species show a similar trend in the char combustion rate constant (see figure 8.17) with Cupressus lusitanica having the lowest value.

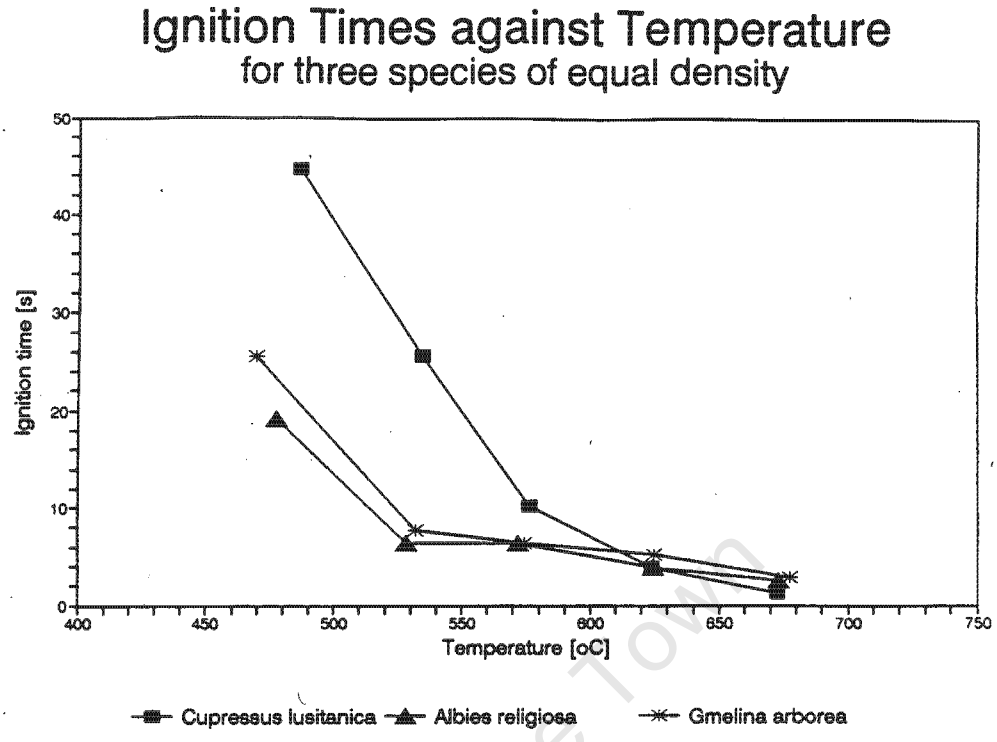

Figure 8.12: Ignition Time against Temperature: Equal Densities

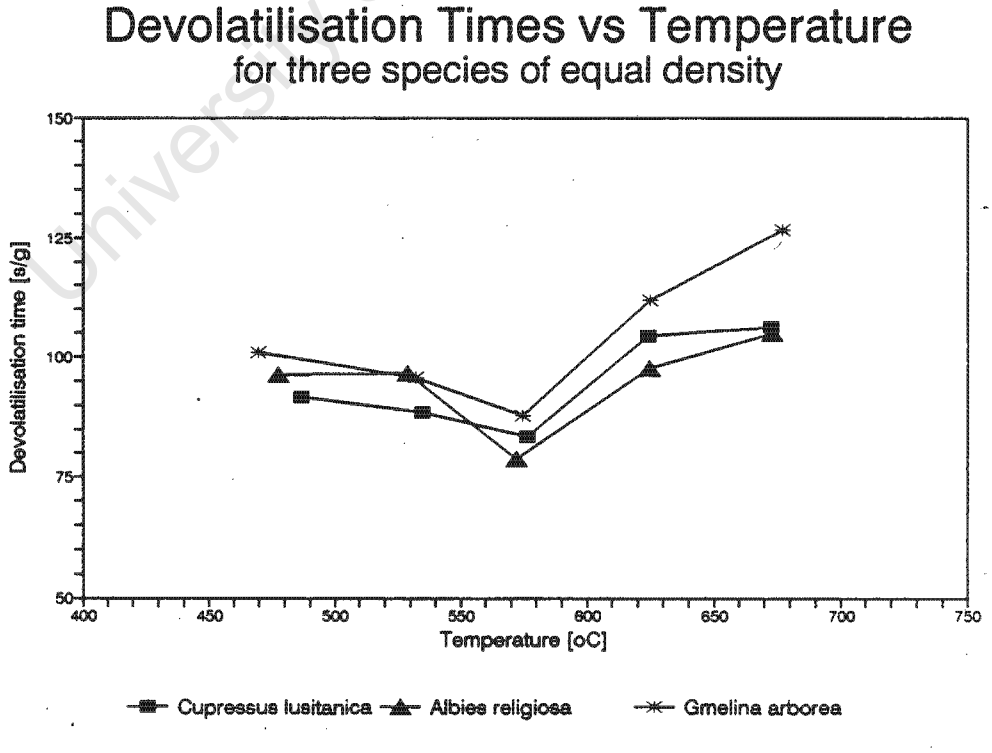

Figure 8.13: Devolatilisation Time against Temperature: Equal Densities

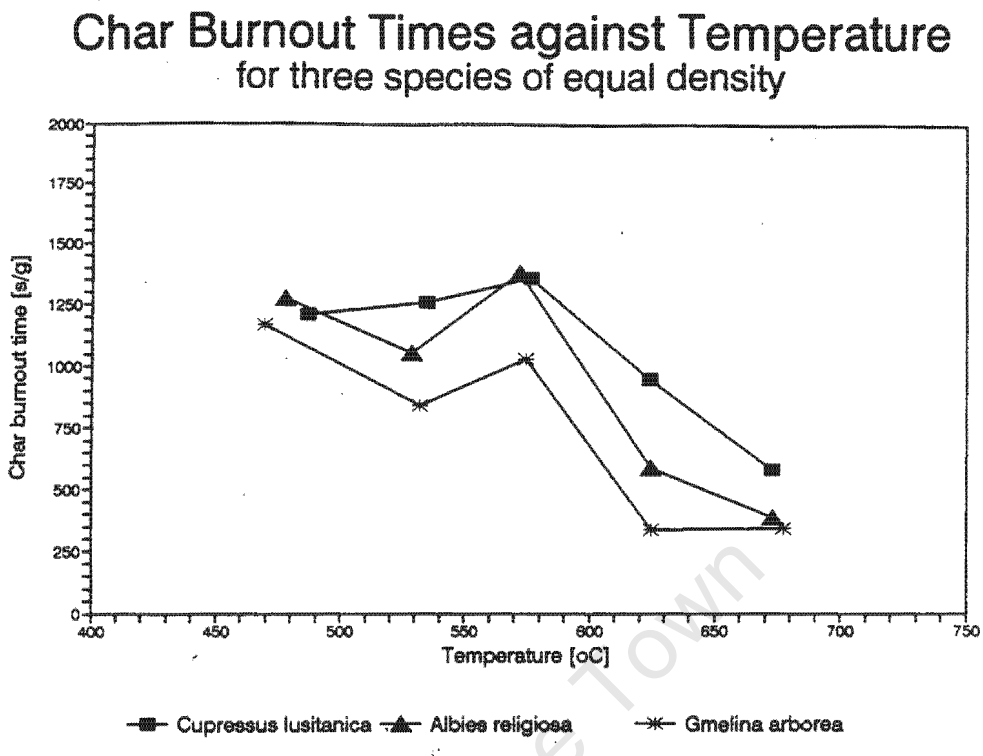

Figure 8.14: Char Burnout Times against Temperature: Equal Densities

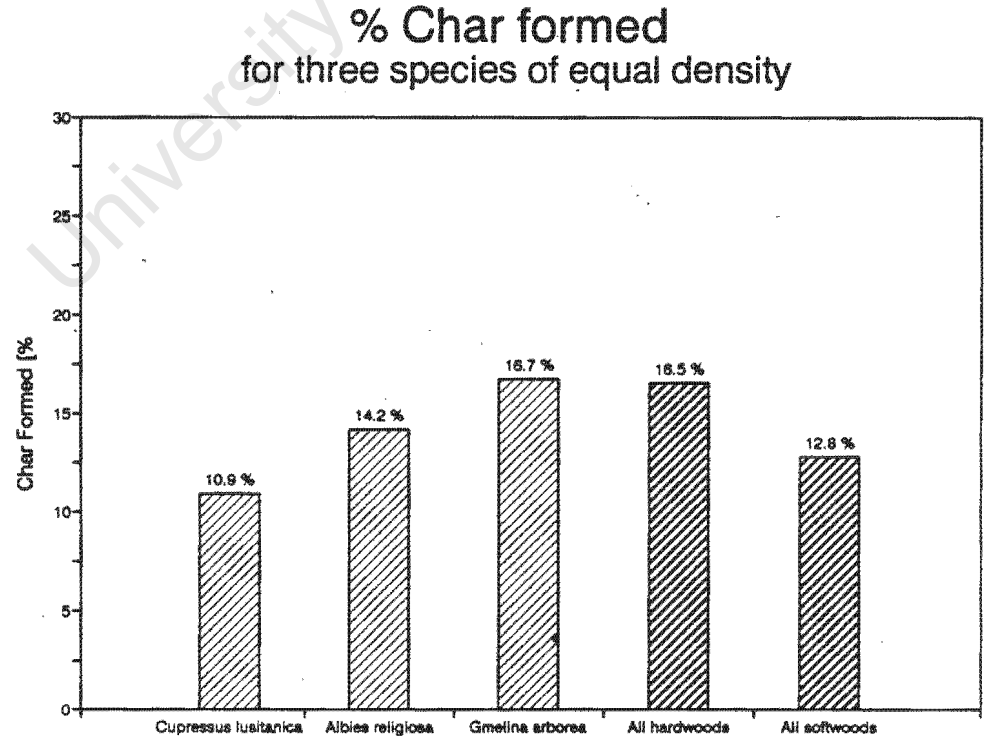

Figure 8.15: Percentage Char Formed: Equal Densities

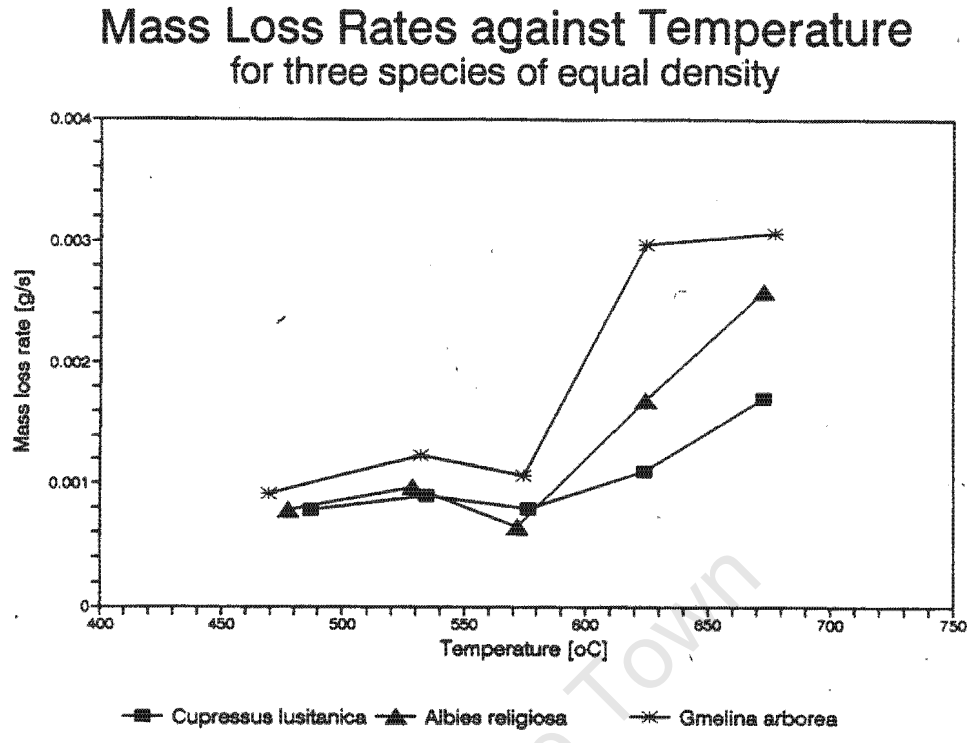

Figure 8.16: Mass Loss Rates against Temperature: Equal Densities

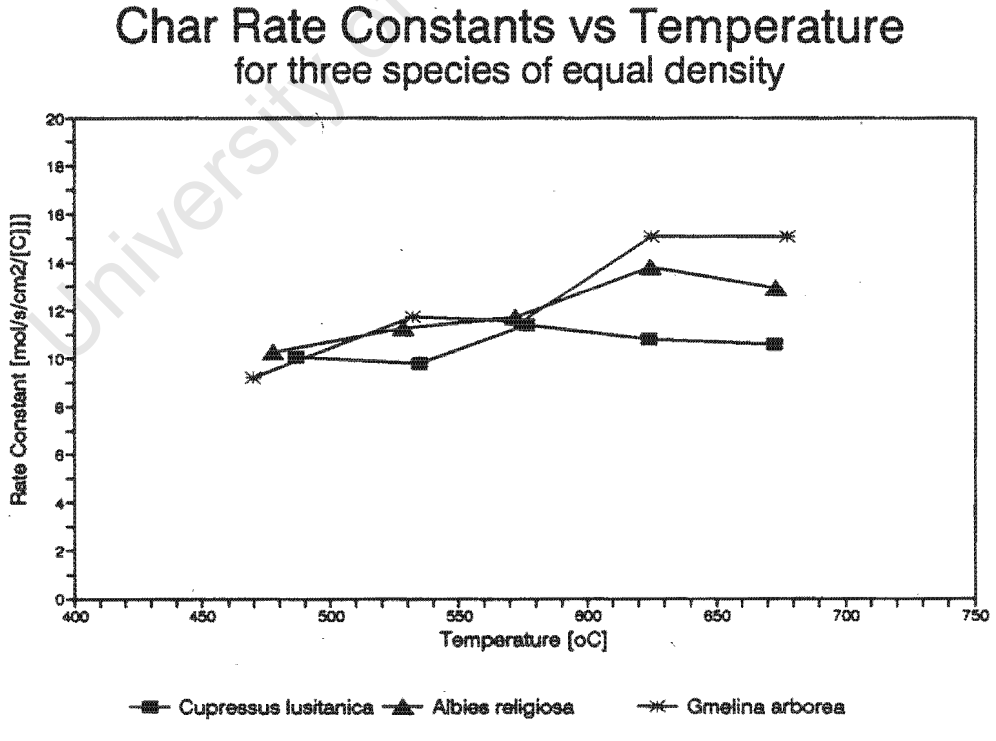

Figure 8.17: Rate Constants against Temperature: Equal Densities

Despite the fact that these species all have very similar densities, there are certain differences between them. In general, Gmelina arborea and Albies religiosa behave similarly, whereas Cupressus lusitanica is usually an exception. Although the devolatilisation times and char rate constants are similar for all three, Cupressus lusitanica ignites sooner, produces less char and burns the char at a lower rate than the others, taking longer to combust one gram of char.

8.3 Three Eucalypt Species

Three Eucalypt species were included in the species set: E. maidenii (867 kg.m^{-3}), E. maculata (795 kg.m^{-3}) and E. delegatensis (755 kg.m^{-3}).

The three species show an ordering of their ignition times that is consistent with their density ordering. Considering devolatilisation time and char burnout time, they again show an order that is consistent with their density differences. However, figures 8.18, 8.19 and 8.20 show that although E. maçulata has a density closer to that of E. delegatensis, it has an ignition time, a devolatilisation time and a char burn out time that is closer to that of E. maidenii. Figure 8.21 shows that Eucalyptus maculata produces the least amount of char.

E. maidenii and E. maculata have very similar mass loss rates for all temperatures. Figure 8.22 shows that E. delegatensis has a considerably higher value at higher temperatures. As before, the difference fits in to the density order, but is out of proportion to the density differences. Figure 8.23 plots the rate constants for the three species against temperature. Eucalyptus maculata and E. delegatensis exhibit very close values for the rate constant and E. maidenii has lower values.

This comparison has shown that for three species from the same family there are distinct differences in their combustion properties. E. delegatensis as the lowest density species ignites more quickly than the other two and the devolatilisation and char combustion reactions proceed at a higher rate.

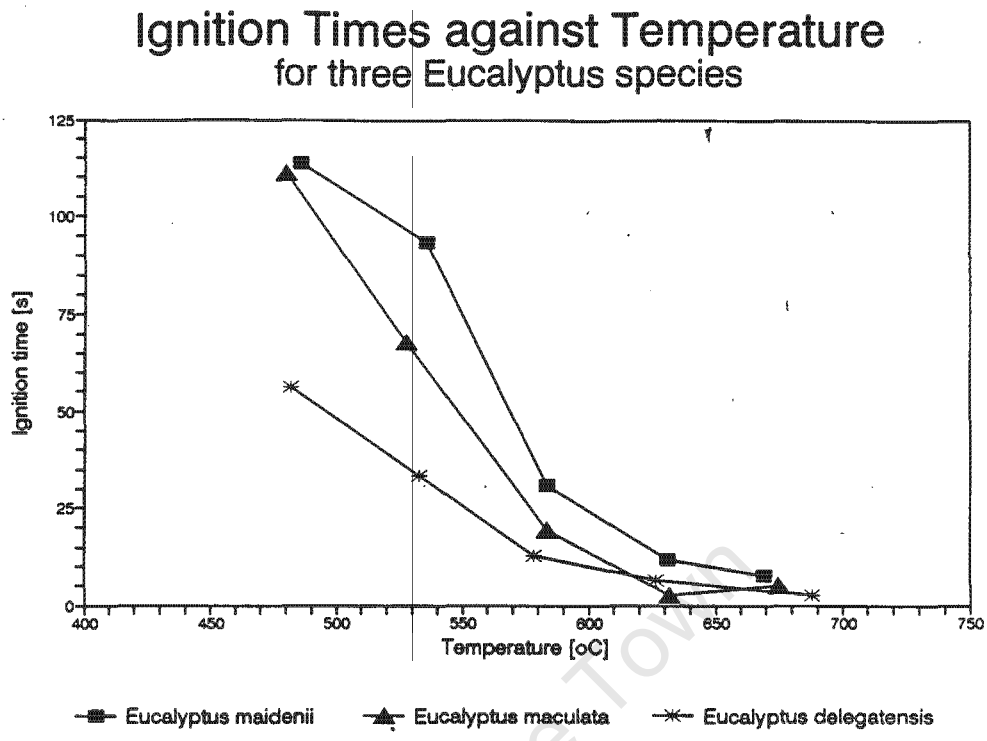

Figure 8.18: Ignition Time against Temperature for Three Eucalypts

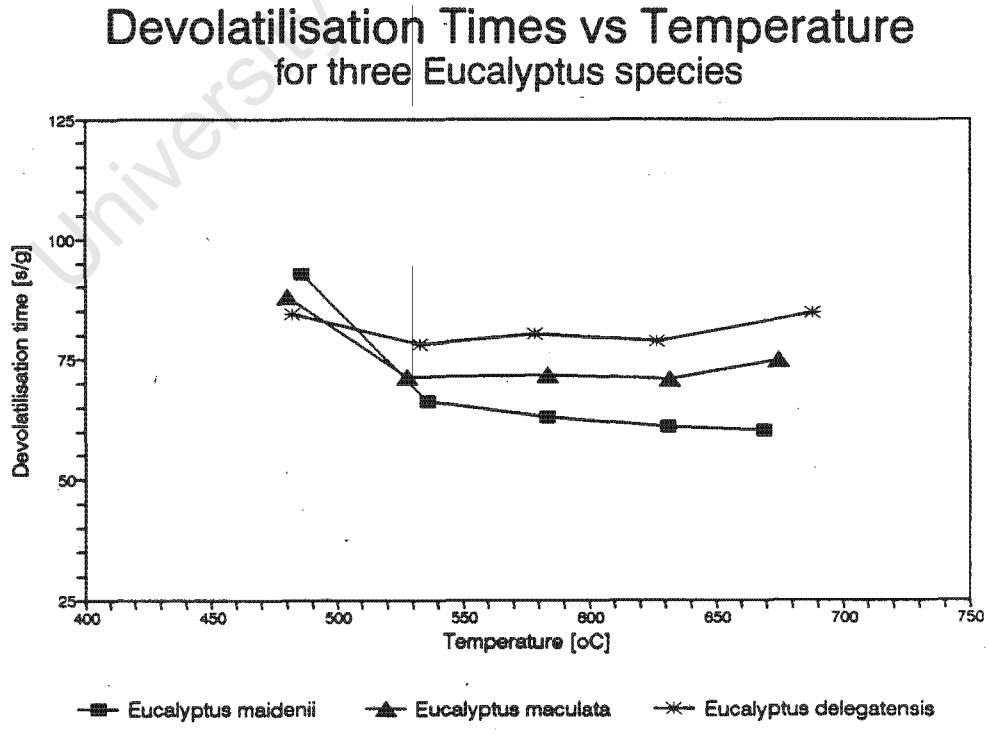

Figure 8.19: Devolatilisation Time against Temperature for Three Eucalypts

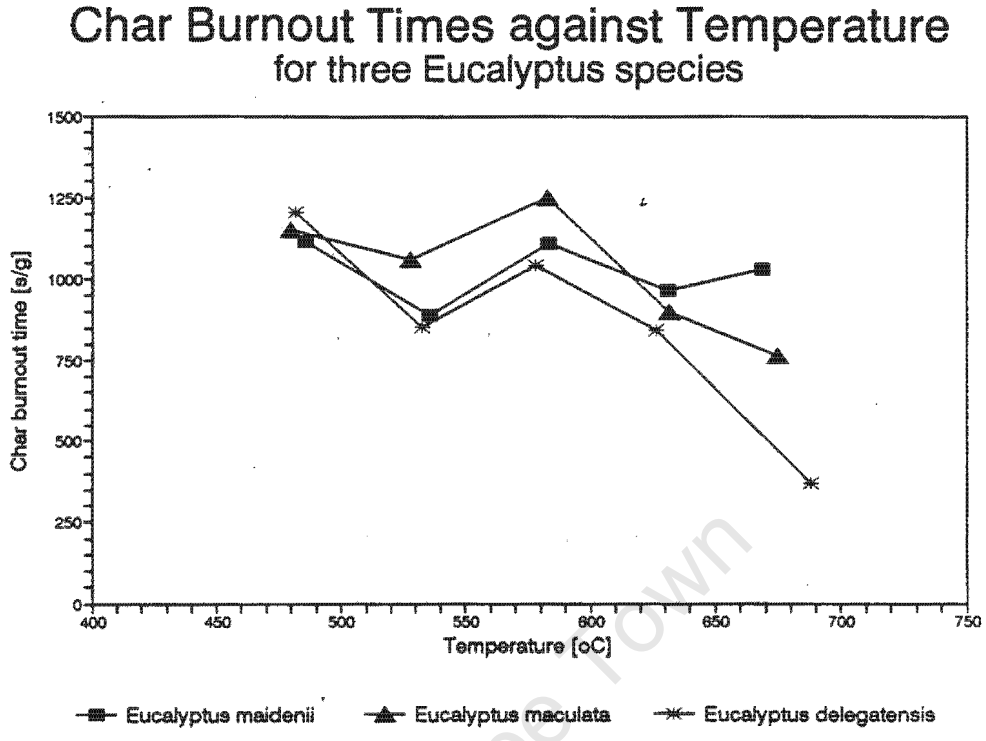

Figure 8.20: Char Burnout Times against Temperature for Three Eucalypts

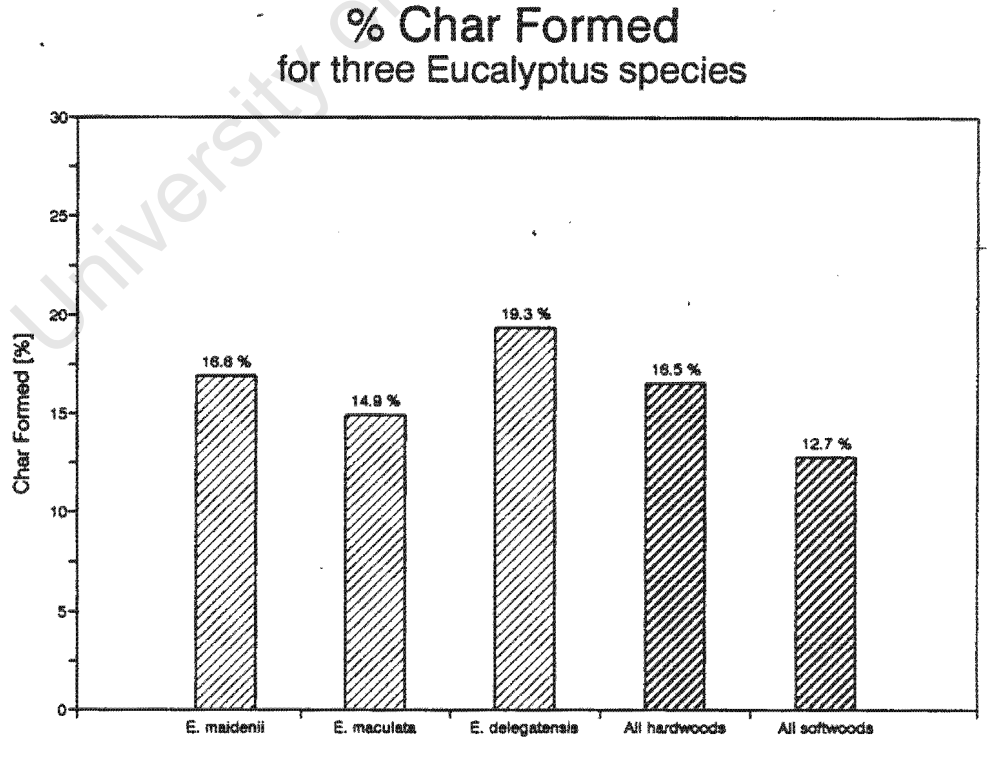

Figure 8.21: Percentage Char Formed for Three Eucalypts

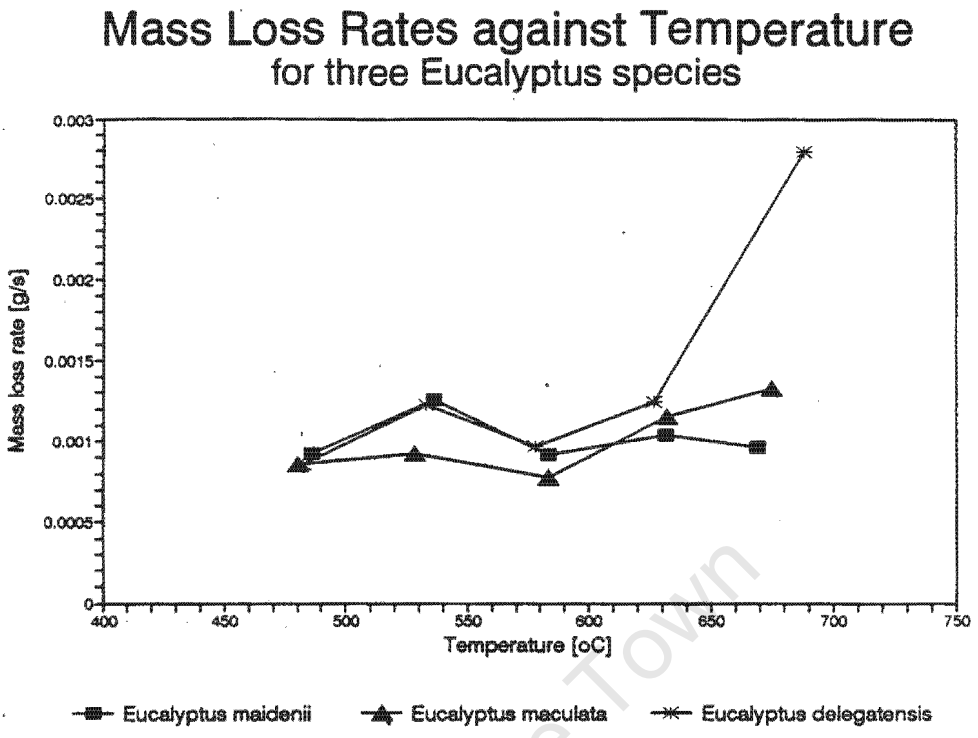

Figure 8.22: Mass Loss Rates for Three Eucalypts

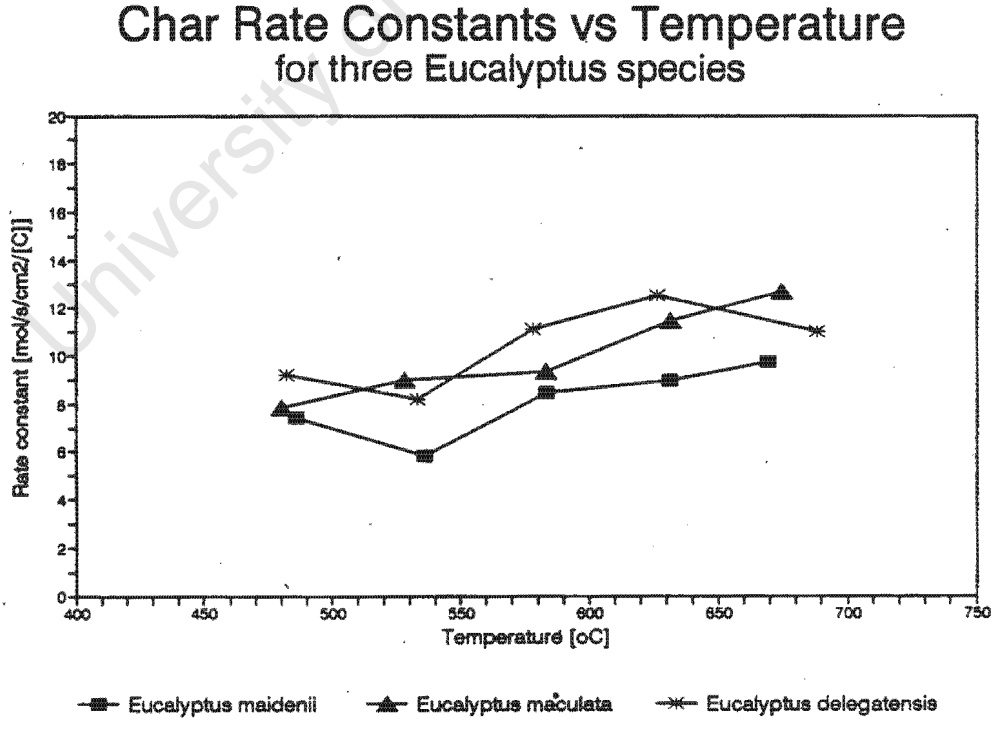

Figure 8.23: Rate Constants for Three Eucalypts

8.4 Ranking of Parameters

The aim of this analysis technique is to determine whether a consistent ranking exists among the species. This will establish whether there is an ordering of the species that holds for all or some of the parameters derived. If such a consistent ranking does exist, it might be possible to match this against the available information on fuelwood preferences.

The method involved taking each parameter and sorting the values into ascending or descending order. The positions of the different species were then recorded. Hardwood and softwood species were treated independently.

The parameters that were used in this analysis were restricted to the following:

i) ignition time at 450°C,
ii) average normalised devolatilisation time,
iii) normalised char burnout time at 600°C,
iv) average rate constant for char combustion and
v) average rate of mass loss at high temperatures (600°C).

These parameters were selected as they showed the greatest degree of differentiation among the species. Other parameters did not exhibit a large enough spread in values to be able to accurately rank the species. Percentage char formed, for example, did show general differences between hardwoods and softwoods, but could not reliably be used to distinguish between the species.

For ignition time and char burn out time, the species were arranged in descending order, whereas for devolatilisation time, rate constant and average rate of mass loss, the species were arranged in ascending order. The different rankings obtained are presented in table 8.1.

Species	ignition time	devol time	char time	K ave	- dm/dt
Hardwoods					
Olea europea	1	2	2	2	2
Ptaeroxylon obliquum	2	3	5	5	5
Maytenus acuminata	5	1	6	7	6.5
Eucalyptus maidenii	3	5	1	1	1
Terminalia sericea	4	4	4	3	4
Eucalyptus maculata	6	7	3	4	3
Eucalyptus delegatensis	8	9	8	8	9
Acacia sieberana	9	8	9	9	8
Grevillea robusta	7	6	7	6	6.5
Gmelina arborea	10	10	10	10	10
Erythrina lysistemon	11	11	11	11	11
Softwoods					
Podocarpus latifolius	5	2	6	5	7
Podocarpus falcatus	6	4	7	7	8
Cedrus libani	1	5	3	6	4
Cupressus torulosa	9	7	4	4	3
Albies religiosa	4	6	8	8	9
Cupressus lusitanica	9	7	4	4	3
Araucania angustifolia	3	3	2	2	2
Pinus patula	2	1	1	3	1
Sequoia sempervirens	7	9	9	9	6

Table 8.1: Species Ranking

For the hardwood species there is a reasonable degree of consistency in the rankings. For the three char properties listed (char burnout time, K at 600°C and dm/dt at 600°C), the species showed a consistent ranking. This ranking is only broadly dependent on density in that the six species with the highest densities are the top six in the ranking. However, there is no clear ordering on the basis of density. Table 8.2 lists the average rankings obtained from these parameters, with the corresponding densities of the species.

The column labelled "rating" in table 8.2 gives the fuelwood rating for that species listed by Poynton (1976). This rating gives three stars for a very good fuelwood, two for a moderately good fuelwood and one for a "somewhat indifferent" wood. Poynton comments that information on firewood quality is rather meagre and not all species are given a rating. The two single star woods tested are at the bottom of the ranking table, although Eucalyptus maidenii

which is a two star rating wood, appears at the top of the list. The rating given by Poynton includes a strong bias towards denser woods.

Position	Species	Density (kg/m^3)	Rating
1	Eucalyptus maidenii	867	**
2	Olea europea	1029	***
3	Eucalyptus maculata	795	***
4	Terminalia sericea	820	
5	Ptaeroxylon obliquum	970	***
6	Maytenus acuminata	930	
7	Grevillea robusta	564	***
8	Eucalyptus delegatensis	755	*
9	Acacia sieberana	611	*
10	Gmelina arborea	439	
11	Erythrina lysistemon	298	

Table 8.2: Overall Rankings for Hardwoods

The other two parameters listed in table 8.1, viz. ignition time and normalised devolatilisation time provide rankings which correspond to those for char properties for seven of the eleven species. Exceptions are Ptaeroxylon obliquum, Maytenus acuminata, Eucalyptus maidenii and Eucalyptus maculata.

For softwoods the rankings gave less consistent results. The char combustion properties provided an average ranking as shown in table 8.3. The ignition time and devolatilisation time rankings only corresponded to these for two species, namely Pinus patula and Sequoia sempervirens. The ranking presented in table 8.3 shows no relation to density. In particular Pinus patula and Sequoia sempervirens are the top two and have the lowest densities. However, the spread of densities for the softwoods tested is considerably smaller than that of the hardwoods. Poynton (1976) only provides firewood ratings for three of the softwood species tested, namely Podocarpus latifolius, Podocarpus falcatus and Pinus patula. These ratings are all single stars.

Position	Species	Density (kg/m^3)
1	Pinus patula	423
2	Araucania angustifolia	431
3	Cupressus lusitanica	440
4	Cupressus torulosa	478
5	Cedrus libani	502
6	Podocarpus latifolius	527
7	Podocarpus falcatus	507
8	Sequoia sempervirens	403
9	Albies religiosa	440

Table 8.3: Overall Rankings for Softwoods

8.5 Influence of Composition and Structure

The differences between woods stem from differences in chemical composition and physical structure. This section will firstly discuss the influences on combustion of variations in composition. This will be followed by a consideration of the effects of the physical structure of the wood. Lastly, the influence of sample size will be considered.

8.5.1 Chemical composition

The differences in composition lie primarily in variation of the proportions of lignin, cellulose and hemicellulose in the wood. Other differences lie in the presence of resins and inorganic salts. Resins are likely to increase the calorific value of wood and promote flammability (Dadkhah-Nikoo, 1987). Inorganic salts could act as catalysts to further reactions of pyrolysis products, especially in the case of lignin (Roberts, 1970: p270).

The residue of pyrolysis is carbonaceous char whose combustion is obviously independent of the original composition. However, since devolatilisation involves a thermal decomposition of these compounds, this stage might be affected by differences in chemical composition.

The temperature ranges in which these organic compounds thermally decompose are given below (Simmons, 1983: p13):

Cellulose : 320°C - 370°C
Hemicellulose : 220°C - 320°C
Lignin : 200°C - 500°C

Softwoods contain more lignin and less cellulose then hardwoods. Lignin is less reactive than cellulose and tends to produce larger quantities of char. This might be expected to result in differences during the devolatilisation stage of wood combustion.

The fact that lignin produces more char might be expected to imply that softwoods would produce greater quantities of char. However a simple calculation shows that this difference could only be expected to be in the order of 3% by mass. In fact the experiments show that softwoods produce less char than hardwoods which can be attributed to the influence of secondary pyrolysis reactions.

The temperatures at which these experiments were conducted, and the temperatures which might be expected in a cooking fire, are above 475°C. This means that all components will be reacting simultaneously. The implication of this is that differences in composition will not significantly affect the flaming process. If experiments were to be conducted in a lower temperature range, then the differing reactivities of these substances would certainly result in different devolatilisation characteristics.

The results of the experiments conducted here indicate that no clear distinctions could be made between the devolatilisation processes of different species. Where composition does make a difference is in the flammability of wood. A species with a high resin content will ignite easily, even if the wood is damp.

8.5.2 Physical structure

The internal structure of different wood species can vary considerably. Hardwoods as a group have a completely different structure from softwoods and within the hardwood group there exists considerable variation. The spread of density among the species is an indication of the different internal structures.

The heat transfer properties of wood are influenced by wood structure. A denser wood will have a higher thermal diffusivity but also a higher heat capacity. This will impact on both the ignition time and the rate of devolatilisation. The experimental results indicate that a denser wood takes longer to ignite, yet has a slightly faster rate of devolatilisation.

The physical structure of wood will affect its permeability. The initial phase of combustion, which involves drying of the sample will be sensitive to this property. A less permeable wood will take longer to dry and hence longer to ignite. Similarly, during devolatilisation the product gases must flow out of the sample. A permeability will restrict this. Another influence of permeability is on the extent and form of secondary pyrolysis reactions. A less permeable wood will favour reactions that produce more char (Eberhard, 1987: p20).

The influence of physical structure on char formation is important since the structure and quantity of char formed is critical. Although the internal structure of the wood has been destroyed by the time the char is formed, the original form of the wood can affect the quality of the char. All woods produce approximately the same amount of char by mass, although a denser wood will clearly produce more char on a volumetric basis. A light char will burn quickly as oxygen can penetrate easily and the area to volume ratio is increased. A weak char that crumbles will also burn quickly for similar reasons. The structure of the char is probably determined by two things. Firstly the density of the original wood will determine the density of the char formed. Secondly the level of splitting and cracking will affect the form of the char. The factors that determine cracking are complex and relate to the stresses that the burning sample is subjected to during the drying and devolatilisation phases, and the strength of the wood in resisting these stresses.

8.5.3 Sample size

The size of the samples that are burnt in a fire is of considerable importance. Woodchips that are used for industrial purposes have a critical size which optimises their combustion.

A larger sample of wood will have a lower surface area to volume. This will affect the penetration of oxygen and heat and the outflow of product gases. The size of the pieces of wood that are used in cooking fires will affect the size of coals formed, the flammability of the wood and the heat retention.

The behaviour of large sample combustion will be significantly different from that of small samples. The devolatilisation and char combustion phases of small samples will be sequential and the amount of overlapping of the different processes will be restricted. Large samples on the other hand will burn in layers. The outer region of the wood may have turned to ash while the inner layers may still be undergoing char combustion, pyrolysis and even drying.

These considerations raise the important question of the relation between combustion properties of small samples and those of large samples. Experiments in this investigation were conducted on small samples and the parameters derived apply to this size of particle. For the significance of these results to be extended to larger particles with any confidence requires further investigation.

8.6 Summary

Table 8.4 summarises the effects of temperature and density on each of the different parameters.

Parameter	Temperature dependence	Density dependence
Ignition time (s)	Immediate at high temperatures Increases exponentially as temperature decreases	Lower densities have higher ignition times at low temperatures
Devolatilisation time (s/g)	Constant with temperature	Lower densities have a higher devolatilisation time
Char burnout times (s/g)	Decreases with increasing temperature	Lower densities a stronger dependence on temperature, although the average value is constant
Char formation (%)	Constant with temperature	Hardwoods form a higher percentage of char
Char rate constant (mol/s/cm^2/[C])	Increases slightly with temperature.	No clear relationship with density
Average rate of mass loss (g/s)	Increases with increasing temperature	Lower densities have a higher mass loss rate at higher temperatures

Table 8.4: Summary Table

This chapter has presented and discussed the experimental results. The influence of chemical composition, physical structure and sample size has been considered an attempt has been made to identify a consistent ranking of the different species. The last chapter will attempt to draw these results and discussion together and will present the conclusions of this investigation.

Chapter 9

Conclusions and Recommendations

The principle objective of this research was to establish a methodology to compare and rank fuelwoods. This chapter will extract the major findings of the investigation and will assess whether such a methodology has been achieved.

Firstly the usefulness of the theoretical models and the experimental work conducted in this investigation will be examined. The main findings of this empirical work will be presented. In an attempt to relate these findings to fuelwood rankings, a summary of anecdotal information on good fuel characteristics and the factors affecting these characteristics will be given. The connections between the empirical work and this information will be discussed. Finally, recommendations for further work will be made.

9.1 Theoretical Models and Empirical Results

The experiments that were conducted in this investigation determined properties of small samples and looked at the intrinsic kinetics of the reactions involved. Different models were used to describe the reactions and to determine the kinetic parameters.

For the devolatilisation phase an overall pseudo rate constant analysis was applied. Two forms of this model were applied: one used a single solid

reactant and the other used a two component solid reactant scheme. The experimental data for this phase did not permit successful use of the two component scheme as the time series did not cover a large enough sample of data points to allow reliable regressions. The single reactant scheme fitted the data well but showed that no significant differences could be established between the species.

For char combustion three models were used: namely a pseudo rate constant model, a shrinking core model and a progressive conversion model. The results showed that the latter two models did not fit the experimental data. The first model fitted the data well and allowed the calculation of rate constants for a range of temperatures. These rate constants did not conform to an Arrhenius dependence on temperature. The rate constants calculated in this way lump together the different effects of boundary layer diffusion, intra-particle diffusion and chemical kinetics. Since the rate constants did not conform to the Arrhenius equation, it indicated that chemical kinetics were not rate limiting.

A detailed examination of the different parameters derived from the experiments showed significant differences between species could be determined. There were general density related trends, particularly for the hardwood group which spanned a wide range of densities. Differences in behaviour between hardwoods and softwoods could be established, although this could be due to density differences. Table 8.4 summarises these differences.

In an attempt to relate these results to the usefulness as a fuel, a ranking analysis was performed. This revealed that for hardwoods there was a consistent ranking of the char combustion properties. For softwoods no such simple ranking could be determined, although particular species (Pinus patula and Araucania angustifolia) did consistently appear in the top of the ranking lists.

This ranking analysis points to the fact that although density does affect the combustion properties of wood, it can not be taken as the overall deciding factor.

The major difficulty in relating these experimental results to fuel usefulness lies in the fact they are properties relating to micro events in the combustion process and are valid for small samples. It is not possible to extrapolate the results of these tests to large particle combustion. When the sample exceeds a certain size, the individual processes in combustion (heating, drying, devolatilisation, char combustion) are not sequential and overlap. The interactions between these processes in a large sample can not be determined from small sample tests. In addition, the mechanical properties of larger samples are likely to be very different from small samples. The splits and cracks that occur in larger samples will facilitate heat and mass transfer into and out of the wood. Again the interactions between different combustion processes, for example volatile gas accumulation in inner regions whilst char combustion occurs on the outside, will affect the mechanical deformations that the wood will undergo.

The major conclusions to be reached from the experimental investigations are firstly that there are differences in the char combustion of wood species, but not in the devolatilisation phase (in the temperature range considered). Secondly, density plays an important but not over-riding role in the determination of these characteristics. The strongest differences between species were found in the descriptive parameters.

Ignition times were strongly dependent on density and temperature. Char burnout times were also found to vary with density and temperature. The average rate of mass loss can be viewed as an overall descriptive parameter for char combustion and was found to vary differently with temperature for different species. Differences in the actual kinetics of char combustion between species, i.e. the rate constants derived, were found not to be as significant.

For the devolatilisation phase of small sample combustion, it was difficult to identify significant differences. Although rate constants could be derived, statistical comparisons showed that there were no significant differences between species. Examining the average rate of devolatilisation time per gram showed that there was no significant trend with temperature and that lighter samples had a slower devolatilisation time than heavier samples. Again these results are valid for small samples. Devolatilisation is essentially a heat

transfer controlled process. For larger samples the temperature profile and heat flows inside the wood are significantly more complex. Cracks will allow easier penetration of heat into the wood structure. For small samples, the flaming boundary layer is an important heat source. For larger samples, the presence of a char layer undergoing combustion will provide a heat source in addition to flame interactions, and the possible presence of moisture inside the wood will act as a heat sink. Another effect of increasing sample size is to increase the relative importance of convection of outward flowing volatiles from the regions undergoing pyrolysis.

9.2 Summary of Useful Characteristics

Different characteristics are looked for in wood, depending on the way it will be used. Kindling must be in the form of small twigs or chips and must ignite easily even when wet. For cooking fires, wood must produce coals that burn slowly and release a lot of heat. If the wood is used in an open fire as opposed to a stove, the species selectivity becomes more important. Where a fire is made for warmth, large pieces of wood are required that burn slowly and last for hours.

The most important properties of wood that determine these burning characteristics are:

i) Density: a denser wood will release more heat per unit volume and produce denser coals that burn for longer.

ii) Moisture content: the presence of moisture in wood detracts from its use as a fuel since it makes ignition difficult and reduces the quantity of heat released. A tree with wood that dries quickly will be favoured because of this.

iii) Cracking and splitting: wood that cracks will produce smaller coals that crumble and burn quickly. This property of wood is probably related to its strength, permeability and the devolatilisation processes in large samples.

Considering the literature on anecdotal information, it appears that the most important fuel characteristics of wood stem from macro properties. The connections between kinetic properties and fuelwood usefulness are elusive, whereas it is easier to relate macro properties such as those listed above, to people's expectations of a good fuelwood. It is concluded that a methodology to compare and rank fuelwoods should not be based on the chemistry and kinetics of small sample combustion. Instead the properties listed above should be investigated in more detail and used, possible together with some small sample characteristics to construct a ranking technique.

9.3 Recommendations

The establishment of criteria on which to base comparisons between species is important in the field of woodlot species selection. The results of this investigation have shown (1) that a reasonably consistent ranking on the basis of small sample combustion properties can be achieved and (2) that more general, descriptive characterisations are more useful than kinetic rate constants. However, the differences between small and large samples make it difficult to relate this ranking to fuelwood usefulness.

Further investigation of small sample combustion should only be continued if it is linked to a characterisation of larger samples. It is recommended that further investigations should focus on the macro properties of wood combustion. The results of such work should be correlated with the rankings described in section 8.4 to ascertain whether small sample characteristics can be related to wood fuel usefulness.

Distinctions should be made between wood for kindling, cooking fires and space heating. Attention should focus mainly on char production. The tendency of wood char to crumble to fines should be investigated and an attempt made to characterise the quantity and density of solid coals formed. Wood sample sizes should be used that most closely resemble the sizes used

in real fires. This may vary with species as different trees produce different size branches.

The ease of ignition is an important property, especially for wood used as kindling. It is recommended that the methods used in this investigation are adequate to characterise this property of wood.

The work described above should be combined with information on drying rates, densities, speed of growth as well as branch size and dead wood production for different tree species. All these factors should then be considered together to assess the usefulness of a tree species as fuelwood.

References

Agrawal, R K (1985[a]). On the Use of the Arrhenius Equation to Describe Cellulose and Wood Pyrolysis. Thermochemica Acta, 91, pp343-349.

Agrawal, R K (1985[b]). Compensation Effect in the Pyrolysis of Cellulosic Materials. Thermochemica Acta, 90, pp47-51.

Alves, S S & Figueiredo, J L (1988). Pyrolysis Kinetics of Lignocellulosic Materials by Multistage Isothermal Thermogravimetry. Journal of Analytical and Applied Pyrolysis, 13, pp123-134.

Archer, F (1988). Planning with People: Ethnobotany and African Uses of Plants. Presented at the Twelth Plenary Meeting of AETFAT, Hamburg, 4-10 Sepetember, 1988.

Aron, J; Eberhard, A A & Gandar, M V (1989). Demand and Supply of Fuelwood in the homelands of South Africa. Post Conference Series No. 21. Second Carnegie Inquiry into Poverty and Development in Southern Africa. SALDRU, University of Cape Town.

Ausman, J M & Watson, C C (1962). Mass Transfer in a Catalyst Pellet during Regeneration. Chemical Engineering Science, 17, pp323-329.

Baldwin, S (1988). The Design of Fuel Efficient Woodstoves Appropriate for Underdeveloped Areas of South Africa. Chapter 18, Renewable Energy Resources and Technology Development in Southern Africa. Ed A Eberhard and A Williams. Elan Press. Cape Town.

Bamford, C H; Crank, J & Malan, D H (1946). The Combustion of Wood. Part 1. Proc. of the Cambridge Philosophical Society, 42(2), Cambridge University Press.

Becker, H A & Phillips, A M (1982). Burning of Pine: Wave Propagation models for Regimes of Well-Developed Heterogeneous Combustion. 19th Symposium (International) on Combustion. The Combustion Institute.

Becker, H A; Phillips, A M & Keller J (1984). Pyrolysis of White Pine. Combustion and Flame, 58, pp163-189. The Combustion Institute.

Belleville, P & Capart, R (1984). Pyrolysis of Large Wood Samples. Applied Energy, 16, pp223-237.

Beeston, G & Essenhigh R (1963). Kinetics of Coal Combustion: The Influence of Oxygen Concentration on the Burning-Out Times of Single Particles. ,67, pp1349-1355.

Bembridge, T J (1986). Aspects of Agriculture and Rural Poverty in the Transkei. Post Conference Series No. 261. Second Carnegie Inquiry into Poverty and Development in Southern Africa. SALDRU, University of Cape Town.

Best, M (1979). The Scarcity of Domestic Energy. A Study in Three Villages. Saldru Working Paper No. 27, Saldru, University of Cape Town, Cape Town.

Blackshear, P L & Murty Kanury, A (1970). On the combustion of Wood. I: A Scale Effect in the Pyrolysis of Solids. Combustion Science and Technology, 2, pp1-4.

Brown, D J (1982). The Questionable Use of the Arrhenius Equation to Describe Cellulose and Wood Pyrolysis. Thermochemica Acta, 54, pp377-379.

Burley, J (1978). Selection of Species for Fuelwood Plantation. 8th World Foorestry Congress, Jakarta. Food and Agriculture Organisation of the United Nations, Rome.

Capart, R; Falk, L & Gelus M (1988). Pyrolysis of Wood Macrocylinders under Pressure: Application of a Simple Mathematical Model. Applied Energy, 30, pp1-13.

Cornelissen, L H. Combustibility of Solid Fuels. Laboratory Project No. 16. Dept. of Mechanical Engineering, University of Cape Town, 1985.

Cunningham, T (1984). Indigenous Plant REsources: a Boffer Against Rural Poverty. Carnegie Conference Paper No 145, University of Cape Town.

Dadkhah-Nikoo, A & Bushnell, D J (1987). Analysis of Wood Combustion Based on the First and Second Laws of Thermodynamics. Journal of Energy Resources Technology. Transactions of the ASME, 109, pp129-141.

Desch, H E (1968). Timber, its Structure and Properties. St Martins Press, New York.

Dutta, S & Wen, C Y (1977). Reactivity of Coal and Char. 2: In Oxygen-Nitrogen Atmosphere. Industrial Engineering Chemistry: Process, Design and Development, 16(1), pp31-36.

Duvvuri, M S et al (1975). The Pyrolysis of Natural Fuels. Journal of Fire and Flammability, 6, pp468-477.

Eberhard, A A (1986[a]). Energy Consumption Patterns in Underdeveloped Areas in South Africa. Energy Research Institute, University of Cape Town. Cape Town.

Eberhard, A A (1986[b]). South African Energy Crisis: Some Suggested Strategies. Post Conference Series No. 13. Second Carnegie Inquiry into Poverty and Development in Southern Africa. SALDRU, University of Cape Town.

Eberhard, A A (1987). Calorific Values and Combustion Characteristics of South African Grown Fuelwoods. Energy Research Institute, University of Cape Town.

Eberhard, A A (1989). Energy consumption Patterns and Supply Problems in Underdeveloped Areas in South Africa. Energy Research Institute, University of Cape Town.

Eberhard, A A & Poynton, R J (1986). Fuelwood Calorific Values and Preferences as Criteria for the Choice of Tree Species for Planting in South Africa. Proc Renewable Energy Potential in Southern Africa, Energy Research Institute, University of Cape Town, 8-10 Sept 1986.

Eckholm, E (1975). The Other Energy Crisis, Worldwatch Paper 1.

Eckholm, E et al (1984). Fuelwood: the energy crisis that won't go away. Earthscan. London.

FAO (1981). Map of the Fuelwood Situation in Developing Countries. Food and Agriculture Organization of the United Nations. Rome.

Field, M A (1969). Rate of Combustion of Size Graded Fractions of Char from a Low Rank Coal Between 1200 K and 2000 K. Journal?, 13, pp237-252.

Financial Times (1986). World Status: Fuelwood (1986). Financial Time Energy Economist, 52, p7-10.

Findley, W P K (1975). Timber Properties and Uses. Crosby Lockwood Staples, London.

Gandar, M (1983). The Utilisation of Trees and the Impact on the Environment: A Study in Mahlabatini District, Kwazulu. Institute of Natural Resources, University of Natal, Pietermaritzburg.

Gandar, M (1988). The History of Woodlot Development for Fuelwood Production in Southern Africa. Chapter 16, Renewable Energy Resources and Technology Development in Southern Africa. Ed A Eberhard and A Williams. Elan Press. Cape Town.

Glassman, I (1977). Combustion, Academic Press, New York.

Goldenberg, J et al (1987). Energy for Development. World Resources Institute. Washington.

Goldstein, R J (1983). Fluid Mechanics Measurements. Hemisphere Publishing Corporation, Washington.

Gwaitta-Magumba, D A (1983). Woodfuel and Other Energy Sources in Swaziland. Carnegie Conference Paper No 156, University of Cape Town.

Hines, A L & Maddox, R N (1985). Mass Transfer: Fundamentals and Applications. Prentice Hall, New Jersey.

Ishida, M & Wen, C Y (1968). Comparison of Kinetic and Diffusional Models for Solid-Gas Reactions. American Institute of Chemical Engineers Journal, 14(2), pp311-317.

Jones, P (1978). Choosing Efficient Fuelwood for Wood Burning. American Christmas Tree Journal, 22(1), p12.

Kansa, E J; Perlee, H E & Chaiken, R F (1977). Mathematical Model of Wood Pyrolysis Including Internal Forced Convection. Combustion and Flame, 29, pp311-324, The Combustion Institute.

Kgathi, D L (1984). Aspects of Firewood Trade between Rural Kweneng and Urban Gaborone: a Socio-economic Perspective. Working Paper No 46, NIR, University of Botswana, Gaborone.

Kung, H-C (1972). A Mathematical Model of Wood Pyrolysis. Combustion and Flame, 18, pp185-195.

Laurendeau, N M (1978). Heterogeneous Kinetics of Coal Char Gasification and Combustion. Progress of Energy Combustion Science, 4, pp221-270.

Lee, C K; Chaiken, R F & Singer J M (1976). Charring Pyrolysis of Wood in Fires by Laser Simulation. 16th Symposium (International) on Combustion. The Combustion Institute: Pittsburgh.

Lewellen, P C; Peters, W A; Howard, J B (1977). Cellulose Pyrolysis Kinetics and Char Formation Mechanism. Fire and Explosion Research, pp1471-1481.

Liegme, C A (1983). A Study of Wood Use for Fuel and Building in an Area of Gazankulu. Bothalia, 14(2), pp245-257.

Marrero, T R & Mason, E A (1972). Gaseous Diffusion Coefficients. Journal of Physical Chemical Reference Data, 1(1).

Mulcahy, M F R & Smith I W (1969). Kinetics of Combustion of Pulverized Fuel: A Review of Theory and Experiment. Reviews of Pure and Applied Chemistry, 19, pp81-108.

Murty Kanury, A & Blackshear, A (1970[a]). Some Considerations Pertaining to the Problem of Wood Burning. Combustion Science and Technology, 1, pp339-355.

Murty Kanury, A & Blackshear P L (1970[b]). On the Combustion of Wood II: The Influence of Internal Convection on the Transient Pyrolysis of Cellulose. Combustion Science and Technology, 2, pp5-9.

Murty Kanury, A (1971). Burning of Wood - A Pure Transient Conduction Model. Journal of Fire and Flammability, 2, pp191 - 205.

Murty Kanury, A (1972[a]). Rate of Burning of Wood (A Simple Thermal Model). Combustion Science and Technology, 5, pp135-146.

Murty Kanury, A (1972[b]). Thermal Decomposition Kinetics of Wood Pyrolysis. Combustion and Flame, 18, pp75-83.

Nunn, T R; Howard, J B; Longwell, J P & Peters W A (1985). Product Compositions and Kinetics in the Rapid Pyrolysis of Sweet Gum Hardwood. Industrial and Engineering Chemical Process Des. and Development, 24, pp836-844.

NAS (1980). Firewood Crops - Shrub and Tree Species for Energy Production. Advisory Committee on Technology Innovation, National Academy of Sciences.

Otto, K P et al (1977). The Mechanical Properties of Timbers with Particular Reference to those Grown in the Republic of South Africa. Bulletin N. 48. The South African Forestry Research Institute. The Department of Forestry, Pretoria.

Petrella, R V (1980). The Mass Burning Rate of Polymers, Wood and Organic Liquids. Journal of fire and Flammability, 11, pp3-21.

Petrie, J. Private communication with the author.

Petrie, J (1987). Determination of Combustion Activation Energy for Pine Char Sample. Appendix B in Calorific Values and Combustion Characteristics of South African Grown Fuelwoods, A A Eberhard, pp36-39, 1987. Energy Research Institute, University of Cape Town.

Phillips, A M & Becker, H A (1982). Pyrolysis and Burning of Single Sticks of Pine in a Uniform Field of Temperature, Gas Composition and Gas Velocity. Combustion and Flame, 46, pp221-251. The Combustion Institute.

Poynton, R (1976). Characteristics and Uses of Trees and Shrubs obtainable from the Forest Department. Bulletin No. 39. The Government Printer, Pretoria.

Poynton, R (1984). Tree Species for Fuelwood Production in South Africa. South African Forestry Journal, p18-21, 131.

Pyle, D L & Zaror, C A (1984). Heat Transfer and Kinetics in the Low Temperature Pyrolysis of Solids. Chemical Engineering Science, 39(1), pp147-158.

Ragland, K W; Boerger, J C & Baker, A J (1988). A Model of Chunkwood Combustion. Forest Products Journal, 38(2), pp27-32.

Roberts, A F (1970). A Review of Kinetics Data for the Pyrolysis of Wood and Related Substances. Combustion and Flame, 14, pp161-272.

Roberts, A F (1971[a]). Problems Associated with the Theoretical Analysis of the Burning of Wood. Proc. 13th International Symposium on Combustion, pp893-903, Combustion Institute, Pittsburgh.

Roberts, A F (1971[b]). The Heat of Reaction During the Pyrolysis of Wood. Combustion and Flame, 17, pp79-86.

Rogers, J et al (1986). Chemical Composition of Forest Fuels Affecting their Thermal Behavior. Canadian Journal of Forestry Research, 15, pp721-726.

Rubak, W; Karcz, H & Zembrzuski, M (1984). Evaluation of Intrinsic Kinetic Parameters of Coal Combustion. Fuel, 63, pp488-493.

Shafizadeh, F & Bradbury, A (1980). Chemisorption of Oxygen on Cellulose Char. Carbon, 18, pp109-116.

Shafizadeh, F & DeGroot, W (1977). Thermal Analysis of Forest Fuels. Tillman D A, Sarkanen K V, Anderson L L (eds.), Fuels and Energy from Renewable Resources, Academic Press, New York.

Shen, J & Smith, J M (1965). Diffusional Effects in Gas-Solid Reactions. Industrial Engineering Chemistry Fundamentals, 4, p293.

Siau, J F (1971). Flow in Wood. Syracuse Wood Science Series. Syracuse University Press, New York.

Simmons, W W (1983). Analysis of Single Particle Wood Combustion in Convective Flow. Ph.D. Dissertation. The University of Wisconsin-Madison.

Simmons, S M & Gentry, M (1986). Particle Size Limitations Due to Heat Transfer in Determining Pyrolysis Kinetics of Biomass. Journal of Analytical and Applied Pyrolysis, 10, pp117-127.

Simmons, W W & Ragland, K W (1986). Burning Rate of Millimeter Sized Particles in a Furnace. Combustion Science and Technology, 46, pp1-15.

Simmons, G & Sanchez, M (1981). High-Temperature Gasification Kinetics of Biomass Pyrolysis. Journal of Analytical and Applied Pyrolysis, 3, pp161-171.

Smith, I W (1982). The Combustion Rates of Coal Chars: A Review. Nineteenth Symposium (International) on Combustion. pp1045-1065. The Combustion Institute.

Steward, F R; Richard, E & O'Donnell (1980/81). Measurement of the Burning Rate of a Single Fuel Particle in a Fire Environment. Fire Safety Journal, 3, pp139-147.

Streeter, V L (1961). Handbook of Fluid Dynamics, McGraw Hill, New York.

Tillman, D A (1981). Review of Mechanisms Associated with Wood Combustion. Wood Science, 13(4), pp177-184. Forest Products Research Society. 1981.

Timberlake, L (1985). Africa in Crisis. The Causes, the Cures of Environmental Bankruptcy. Earthscan, London.

Tinney, E R (1965). 10th Symposium (International) on Combustion, p925. The Combustion Institute: Pittsburgh.

Todd, J J (1981). The Combustion of Wood in Domestic Appliances. Centre for Environmental Studies, University of Tasmania. Proc 2nd Applied Physics Conference of the AIP, RMIT Melbourne, 30 Nov - 4 December 1981.

van Vuuren, N J J; Banks, C H & Stohr, H P (1978). Shrinkage and Density of Timbers Used in the Republic of South Africa. Bulletin No. 57.

Vovelle, C; Mellottee, H & Delbourgo, R (1982). Kinetics of the Thermal Degradation of Cellulose and Wood in Inert and Oxidative Atmospheres. 19th Symposium (International) on Combustion. The Combustion Institute, pp797-805.

Walpole, R E & Myers R H (1978). Probability and Statistics for Engineers and Scientists (2nd edition). Macmillan, New York.

Ward, S M & Braslaw, J (1985). Experimental Weight Loss Kinetics of Wood Pyrolysis under Vacuum. Combustion and Flame, 61, pp261-269.

Williams, A T (1986). The Potential for the Production of Energy from Biomass in Southern Africa. MSc(Eng) thesis. Energy Research Institute, University of Cape Town, Cape Town.

Williams, A T & Eberhard, A A (1988). The Potential for the Production of Energy from Biomass in South Africa. Chapter 15, Renewable Energy Resources and Technology Development in Southern Africa. Ed A Eberhard and A Williams. Elan Press. Cape Town.

Wilson, F & Ramphele, M (1989). Uprooting Poverty. The South African Challenge. David Phillip. Cape Town.

World Bank (1983). The Energy Transition in Developing Countries. Washington.

Zayed, R S; Oren, M J & MacKay, G D (1987). Mechanism of Wood Combustion: 2. Weight Loss Analysis. Fuel, 66, pp1166-1167.

Appendix A

Sherwood Number Calculations

Sherwood numbers can be used to obtain an estimate for the diffusion co-efficient h_D. This co-efficient describes the diffusion of air across the boundary layer surrounding the spherical sample.

The Sherwood number is defined by:

$$Sh = h_D\, d / D_A \quad \ldots\ldots\ldots\ldots\ldots\ldots \text{A.1}$$

where Sh = Sherwood number
h_D = diffusion co-efficient [cm/s]
d = diameter
D_A = binary diffusion co-efficient for species A

For a sphere, the Sherwood number can be approximated by (Laurendeau, 1978: p247):

$$Sh = 2(1 + c\, Re^{1/2}\, Sc^{1/3}) \quad \ldots\ldots\ldots\ldots\ldots \text{A.2}$$

where Re = Reynolds number
Sc = Scmidt number
c = a constant, $0.30 < c < 0.35$.

The Reynolds number is given by:

$$Re = d\,v / \upsilon$$

where υ is the kinematic viscosity.

The Scmidt number is given by:

$$Sc = \upsilon / D_A$$

At high temperatures, the Schmidt number can be approximated by Sc = 1.

The binary diffusion co-efficient (D_A) can be obtained from published tables (Marrero & Mason, 1972). Alternatively, D_A can be estimated by a calculation techniques outlined by Hines (1985) and corrected for temperature.

Appendix B

Data Capture and Processing Software

B.1 The Main Menu

B.1.1 Available functions and operations

The functions available on the main menu are:

i) choose a file,
ii) choose an operation,
iii) run,
iv) quit.

If "choose a file" is selected, then the user is prompted for a path to search. All files on that path with extension ".ful" will be listed and the user may select a file, using the arrow keys. The file name selected is then displayed at the bottom of the screen. A file must be selected before any file operations such as "view graphs" or "process data" can be performed.

If "choose an operation" is selected, the available options are displayed and the user may select one. The operations available are:

i) perform an experiment,
ii) process data,
iii) view graphs,
iv) view simultaneous graphs,
v) recreate the derivative.

The operation selected is displayed in the box at the bottom of the screen. Once an operation has been selected, the function "run" must be selected before it is executed. The operations are explained in greater detail below.

B.2 To Perform an Experiment

B.2.1 The hardware required

This operation performs certain data capture and hardware interfacing routines. The hardware configuration is shown below.

Instrument	Variable name	Interface
Ambient T.C.	Tamb	A/D PC-30 card
Heater T.C.	Theat	A/D PC-30 card
Air flow T.C.	Tair	A/D PC-30 card
Flue gas T.C.	Tflue	A/D PC-30 card
Pressure transducer	DPair	A/D PC-30 card
Mettler AE Scale	Mass	AE 100 interface - serial port

T.C. = thermocouple

The pressure transducer measures the square root of the pressure drop across an orifice plate located in the air supply line.

The configuration for the COM1 serial port (for interfacing with mass scale) must be set before the data capture is commenced. The file COMSETUP.EXE configures the serial port for interfacing.

B.2.2 To initiate data capture

Once the "perform an experiment" option has been chosen and run, a template appears with the experiment details of the last experiment, or of the default values. If these need to be altered, pressing the key "A" allows the user to make changes. The details required are: species name; sample code; sampling rate (sec) and experiment duration (min).

The A/D converter linearly transforms a 0 - 10 V signal to an integer in the range 0 - 4095. A scale factor must be used for each variable to convert to the appropriate units. To view and change these scalefactors, press the key "S" - a list of the current variables their channels and scale factors will be displayed. These can then be altered if required. It is important to use only the variable names listed above.

The Mettler scale sends a real number to four decimal places. The units are grammes and no scaling is required.

If the experiment details and scalefactors are correct, press <enter>. The option to save the data or not is then given. If data is to be saved, the last path used and the sample code are used to construct a file name. If this is not satisfactory, pressing <esc> once, twice, thrice allows the user to alter the filename, path and drive respectively. No extension to the filename is required as the program uses reserved extensions to construct different data files.

B.2.3 Data capture without saving

The display screen is set up showing the time, experiment details, air velocity and combustion chamber temperature.

When a key is pressed, the data capture will commence. The air velocity is calculated (see appendix D) and displayed with each data sample read.. The average temperature in the combustion chamber is computed as the average of Tair and Tflue. This is calculated with each data sample and displayed.

The data capture routine is terminated either when the time exceeds the experiment duration or when "E" is pressed.

B.2.4 Data capture with saving

The display screen is set up and the current air velocity and combustion chamber temperature are continuously updated and displayed (before the command to commence data saving has been given). When the air velocity and combustion chamber temperature have stabilised at the required values, pressing any key will commence data saving.

Two data files are set up: one with extension ".MAS" and the other with extension ".FUL". The former is in ASCII format and only contains the mass data. The latter is a structured turbo Pascal record file and contains all the data.

When the data capture is terminated, the user is prompted for the experiment duration. This is because the interfacing with the Mettler scale slows down the timing control. Thus, a 2 sec sampling rate is in fact about 2.56 sec. A stopwatch must be used to determine the true experiment duration. From this, the program calculates the true sampling rate.

B.3 Data Processing

This operation performs a number of routines:

i) determination of the different experimental stages,
ii) calculates the drag force on the particle and corrects the mass loss data,
iii) sets up an ASCII data file which can be imported into spreadsheet packages for analysis,
iv) computes the transformed variables to be stored in the ASCII file,
v) calculates the mass derivative,
vi) extracts descriptive information from the data and stores it in the ASCII file.

B.3.1 Stages of the experiment

Three graphs are displayed: mass loss, DPair and the mass derivative. From these graphs it is possible to determine at what times the different experiment stages started and finished.

Firstly the user is prompted for the time at which the air was turned on. Using tab, shift tab, left arrow and right arrow keys, the vertical line on the graphs can be moved to where the DPair values increases. Pressing <enter> selects this time as the time at which the air was turned on.

The next stage to mark is the onset of devolatilisation. This is marked by the start of a rapid decrease in the mass. The end of devolatilisation and the beginning of char combustion is marked by a change in the slope of the mass derivative curve from steep to relatively shallow.

The end of char burn is where the mass loss curve stops decreasing. The time at which the air is turned off is shown by the decrease in the DPair variable.

If a mistake is made in the selection of any of these times, <esc> allows the user to respecify the previous time.

B.3.3 Correcting for drag effects

The drag effect of flowing air on the mass variable must be corrected for. The drag when the air is turned on and off can be calculated from the instantaneous change in the mass reading. The drag force is than assumed to be linear with time, and so the drag at any stage can be interpolated from these two known variables.

The mass data in the "*.FUL" file is corrected, but not in the "*.MAS" file.

B.3.4 Calculating the derivative

This procedure calculates the derivative of the mass loss curve. The derivative is only calculated for the devolatilisation and char burn stages, and these two phases can be treated in different ways.

A choice of two routines is available. One routine fits a straight line to a certain number of data points centered around a point. The slope of this line is then taken to represent the mass derivative at the point in question. This procedure is repeated for every data point, and so the derivative for the complete data set is generated. The number of points (n) used in the least squares line fitting procedure can be specified up to 20 points. Similarly, the other routine fits a quadratic function to the n data points and computes the slope of the quadratic at the point in question.

The user also has the option to use a moving average routine to smooth the derivative. This can be useful for char combustion where the magnitude of the derivative makes it sensitive to slight fluctuations in the mass data.

B.3.5 Files and variables

The data processing routines store the transformed data in and ASCII file with extension ".ASC". The structure of the file is shown on the following page.

Variables for the devolatilisation phase are true time (sec) (corrected for error in sampling rate), mass (g), normalised mass (from 1 to 0) and normalised mass derivative (normalised by dividing by the amount of volatiles released during this phase).

Variables for the char combustion phase are: true time (s), mass (g), normalised mass (from 1 to 0), normalised mass derivative (normalised by dividing by the total mass of char formed) and variables for the pseudo rate constant model and the shrinking core model. The former requires normalised mass$^{2/3}$ and the latter requires the transformed variables y, x_1, x_2, x_3.

1: File name
2: Variable names for devolatilisation phase
3: Data for the devolatilisation phase time, mass, normalised mass, normalised mass derivative,
4: Average temperature for devolatilisation
5: Variable names for the char combustion phase
6: Actual data for char combustion time, mass, normalised mass, normalised mass derivative, (normalised mass)$^{2/3}$, y, x_1, x_2, x_3
7: Average temperature for char combustion
8: Descriptive information **ignition time, devolatilisation time,** **char combustion time, char mass,** **% char formed**

Figure B.1: Layout of ASCII Data File

B.4 Recreating the Derivative

The mass derivative may be recreated without having to respecify the experiment stages etc. The values are updated in the "*.FUL" file and the "*.ASC" file.

The program also gives the user the option to recreate the derivative of all the files on a certain path using the specified technique (straight line, quadratic, smoothed etc).

The figure below gives a functional structure of the data capture and processing program.

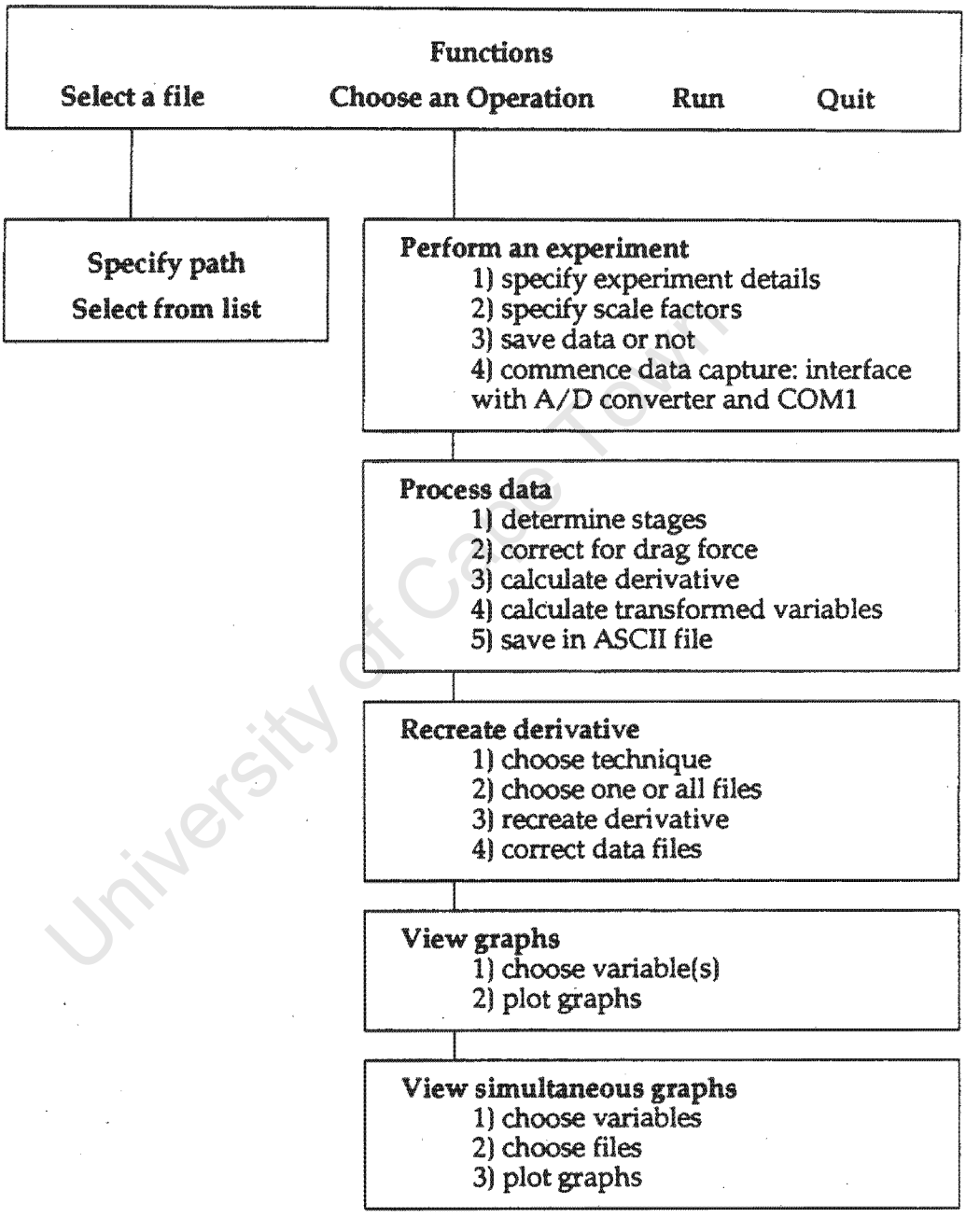

Figure B.2: Functional Structure of Data Capture Program

B.5 Graph Viewing

Choosing and running the "view graphs" option allows the user to view up to four graphs on the screen. The variables which may be viewed are mass, derivative, DPair and all the temperature variables. If only one graph is selected, the display will cover the whole screen.

Choosing "view simultaneous graphs" allows the user to view the same variable from up to four different files on one graph. Again up to four variables may be selected. After each set of graphs is displayed, the program waits for the user to press a key before displaying the next set.

Appendix C

Equipment Specifications

Mass meter:

AE 100 Mettler scale fitted with a bidirectional data interface unit (CL/RS232C).

Readibility:	0.1 mg
Reproducibility:	0.1 mg
Stabilisation time:	5 sec

Pressure transducer:

FC053 Pi low pressure transducer.

Range:	0 - 1000 mmH_2O
Output:	0 - 10 Vdc √
Linearity:	-0.2 at 60%
Zero stability:	0.02 %/°C

Thermocouples:

Two K-type thermocouples, one S-type, with amplifiers.

Range:	K-type:	0 - 1200 °C
	S-type:	0 - 1600 °C

Thyrister and element:

Altronics AM024 thyrister converter.

Kanthal silicon carbide electric element.

Appendix D

Air Velocity Calculations

From the pressure drop across the orifice plate it is possible to calculate the mass flow rate through the supply tube. The formula for this is given by (Goldstein, 1983: p250):

$$Q_p = A_o Y C_d \left[\frac{2\,dP}{\varrho(1-\beta^4)} \right]^{1/2} \quad \ldots\ldots\ldots\ldots D.1$$

$$= A_o Y K \left[\frac{2\,dP}{\varrho} \right]^{1/2} \quad \ldots\ldots\ldots\ldots D.2$$

where Q_p = mass flow rate in the pipe (m^3/s)
A_o = orifice throat area (m^2)
C_d = discharge co-efficient (non-dim)
dP = pressure drop over orifice (Pa)
ϱ = density of air (kg/m^3)
β = ratio of throat diameter to feed pipe diameter
K = flow co-efficient = $C_d/\sqrt{[1-\beta^4]}$ (non-dim)
Y[1] = expansion factor (non-dim)

This gives the mass flow inside the feed pipe at ambient temperature. Inside the combustion chamber, the air is that much hotter and so occupies a larger volume. Thus the flow in the combustion chamber is greater than that in the

1 the expansion factor Y is used to generalise the equations for incompressible flow to include compressible flow. It is common to use theoretical expansion factors ofr flow nozzles and venturi menters and experimentally determined ones for orifice plates. Values for Y are given by Streeter (p14-14, 1961).

feed pipe by a factor ($T_{chamber}/T_{amb}$) where $T_{chamber}$ and T_{amb} are the temperatures (K) inside the combustion chamber and the feed pipe. Since there are two thermocouples inside the chamber, T_{flue} and T_{air} (measuring temperature in degrees Centigrade), $T_{chamber}$ is approximated by:

$$T_{chamber} = (T_{flue} + T_{air}) / 2 + 273 \quad \ldots\ldots\ldots\ldots \text{D.3}$$

So if Q_c is the mass flow rate in the combustion chamber:

$$Q_c = \left[\frac{(T_{flue}+T_{air})/2 + 273}{T_{amb} + 273} \right] Q_p \quad \ldots\ldots \text{D.4}$$

Similarly, the density of air is temperature dependent, so:

$$\varrho_{T1} = (T_2/T_1)\, \varrho_{T2} \quad \ldots\ldots\ldots\ldots\ldots\ldots \text{D.5}$$

(where T_1 and T_2 are temperatures in degrees kelvin)

The density, ϱ in eqn D.1 is the density of air at T_{amb}. Since the density of air at 352.3 K is 1.00 kg/m^3, it is possible to write:

$$\varrho_{Tamb} = 352.3/(T_{amb} + 273) \quad \ldots\ldots\ldots\ldots \text{D.6}$$

Since the mass flow Q = A * v where A is the cross-sectional area of the flow and v is the velocity of the flow, the air velocity in the combustion chamber may be written:

$$V_c = Q_c / A_c \quad \ldots\ldots\ldots\ldots\ldots\ldots \text{D.7}$$

where V_c = velocity in the combustion chamber
A_c = cross-sectional area of the conbustion chamber

Then the velocity in the reactor is given by;

$$V_c = \frac{Y K A_o}{A_c} \left[\frac{2\, dP\, (T_{amb} + 273)}{352.3} \right]^{1/2} \left[\frac{(T_{air} + T_{flue})/2 + 273}{T_{amb} + 273} \right] \quad \ldots \text{D.8}$$

The specifications of the orifice plate, feed pipe and combustion chamber are:

Orifice plate:

$$K = 0.605$$
$$\text{throat diameter} = 10.4 \text{ mm}$$
$$Y = 0.96$$

Feed pipe:

$$\text{internal diameter} = 33.4 \text{ mm}$$

Combustion Chamber

$$\text{diameter} = 50 \text{ mm}$$

Thus

$$\beta = 0.31138$$
$$A_o = 8.495 \times 10^{-5} \text{ m}^2$$
$$A_c = 1.964 \times 10^{-3} \text{ m}^2$$

So equation D.8 reduces to:

$$V_c = 0.03553 \left[\frac{dP\,(T_{amb} + 273)}{352.3} \right]^{1/2} \left[\frac{(T_{air} + T_{flue})/2 + 273}{T_{amb} + 273} \right] \quad \ldots D.9$$

dP represents the true pressure drop across the orifice. This is given by

$$\sqrt{dP} = DPair + 1.95^2$$

where DPair is the reading from the pressure transducer. This is given by the output voltage from the transducer multiplied by the appropriate scale factor, i.e.

$$DPair = V_{out} \times 409.5 \times 0.0104^2$$

---

2 these figures are obtained from a callibration of the pressure transducer.

Appendix E

Common Names of Species

Scientific name	Common name
Acacia sieberana	Paperbark thorn
Albies religiosa	Sacred fir
Araucania angustifolia	Brazilian pine, Parana pine
Cedrus libani	Cedar of Lebanon
Cupressus luitanica	Lusitanica cypress, Mexican cypress
Cupressus torulosa	Himalayan cypress
Erythrina lysistemon	Transvaal tree, Kaffirboom
Eucalyptus delegatensis	Alpine ash, Gigantea gum
Eucalyptus maculata	Maculata gum, Spotted gum
Eucalyptus maidenii	Maiden's gum
Gmelina arborea	Gamari, White teak
Grevillea robusta	Silky oak
Maytenus acuminata	Silky bark, Sybas
Olea europea subsp. africana	Wild olive, Olienhout
Pinus patula	Patula pine, Spreading leaved pine
Podocarpus falcatus	Common yellowwood, Bastergeelhout, Outeniqua yellowwood, Kalandergeelhout
Podocarpus latifolius	Real yellowwood, Upright yellowwood, Opregte geelhout
Ptaeroxylon obliquum	Sneezewood, Nieshout
Sequoia sempervirens	Californian/coastal redwood
Terminalia sericea	Nkonola, Silver terminalia, Vaalboom, Sandvaalbos

Appendix F

Statistical Methods

Two statistical procedures were used to compare results from different species. The Wilcoxin (or Man-Whitney) two sample test was used to compare the descriptive parameters fron the repeated test samples. This statistical technique is commonly used for small samples and is described in Walpole (1978: p474). To compare rate constants and mass loss rates derived from regressions, the "equal slopes" test was used. The form of this test used is described below.

This test has as given two sets of data points: $\{(X_{1,i}, Y_{1,i})$: i = 1..n} and $\{(X_{2,i}, Y_{2,i})$: i = 1..n} whre there exist linear correlations between Y_1 and X_1 as well as between Y_2 and X_2. This test determines whether there are significant differences between the slopes of the regression lines fitted to the two data sets. Note that this test allows the two regression lines to have different intercepts. There are five steps to the test:

Step1:

Fit the equation $y = a + b\,x + c\,z$ to the data set:

$$\{(Y_{j,i}, X_{j,i}, Z_{j,i})\text{: } j = 1,2;\ i = 1..n_1+n_2;\ Z_{j,i} = \delta i_1\}.$$

This regression gives a value for $SS_{ERR}(1+2)$[1].

1 SSERR = Sum of the squares of the error terms.

Step 2:

Fit the equation $y = a + b\,x$ to the data set:

$$\{(Y_{1,i}, X_{1,i}): i = 1..n_1\}$$

This regression gives a value for $SS_{ERR}(1)$.

Step 3:

Fit the equation $y = a + b\,x$ to the data set:

$$\{(Y_{2,i}, X_{2,i}): i = 1..n_2\}$$

This regression gives a value for $SS_{ERR}(2)$.

Step 4:

Calculate the F factor:

$$F_{calc} = \frac{SS_{ERR}(1+2) - \{SS_{ERR}(1) + SS_{ERR}(2)\}}{\{SS_{ERR}(1) + SS_{ERR}(2)\}/(n_1 + n_2 - 4)}$$

Step 5:

Compare F_{calc} with $F_{table}(1, n_1 + n_2 - 4)$ at the required confidence level.

If $F_{calc} > F_{table}$ then the slopes of the two regression lines are significantly different.

Appendix G

Complete Data Graphs

This appendix presents in graphical form the complete results of the analysis on the twenty species. There are five sets of graphs. Each set contains twenty graphs, one for each species, and arranged in order of descending density. The variables plotted on the graphs are:

i) ignition time,
ii) normalised devolatilisation and normalised char burn out times,
iii) % char formed,
iv) rate constants for char combustion,
v) overall mass loss rates for char combustion.

All graphs have temperature on the X-axis and plot points for each experiment. The points plotted for ignition time, devolailisation time, char burn out time and % char formed are averages of the heartwood and sapwood samples. For the graphs showing char rate constants and overall mass loss rates, points are plotted for heartwood and sapwood samples independently.

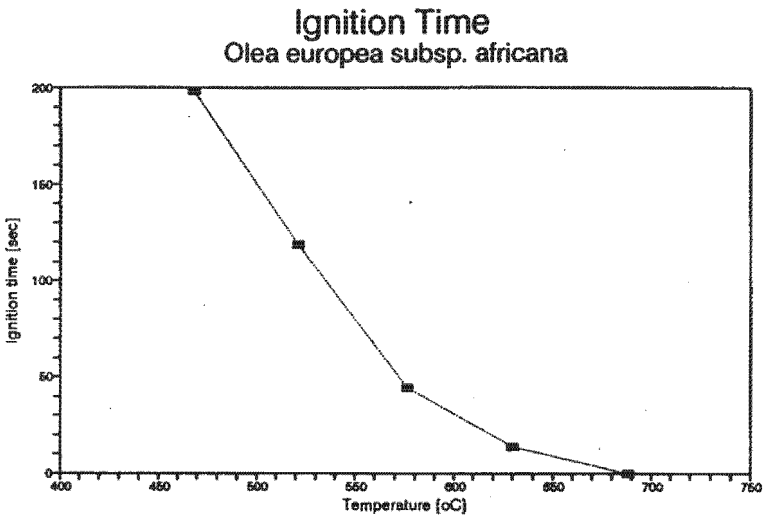

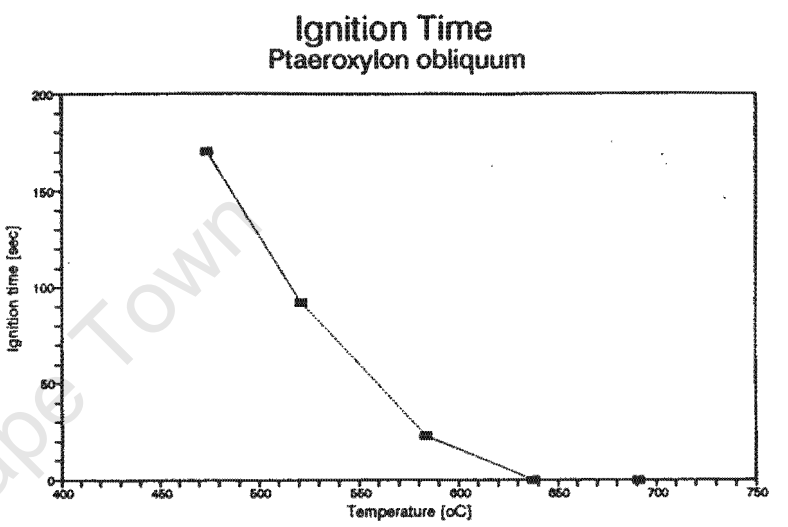

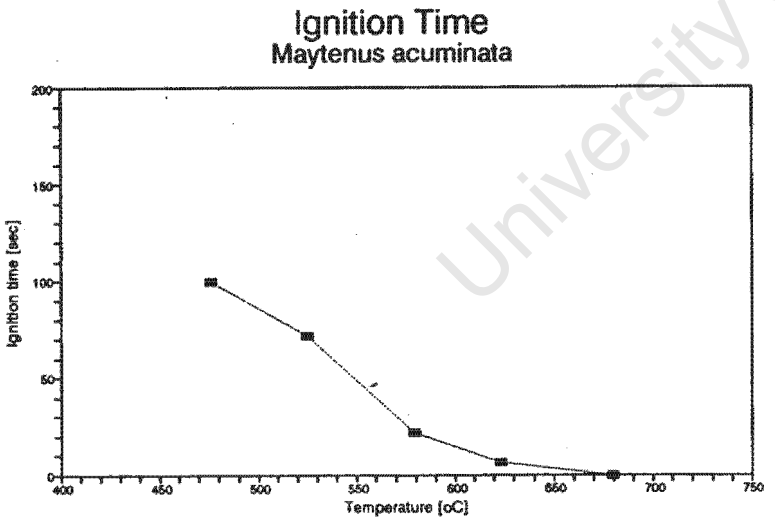

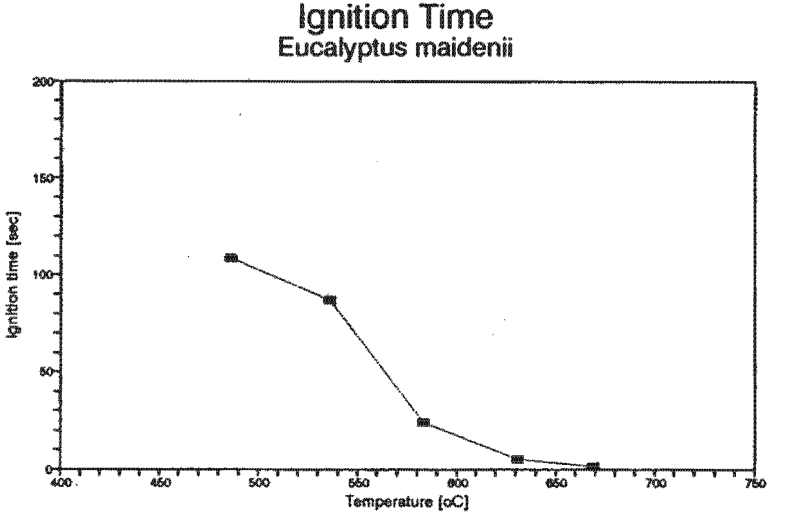

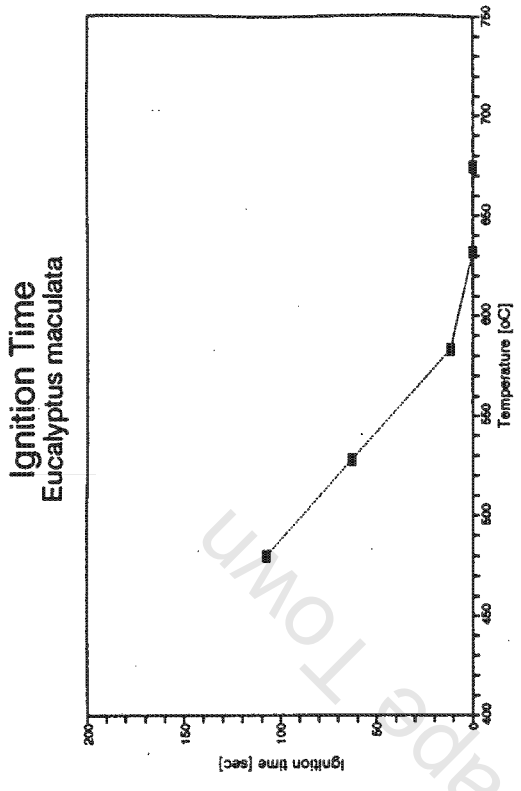

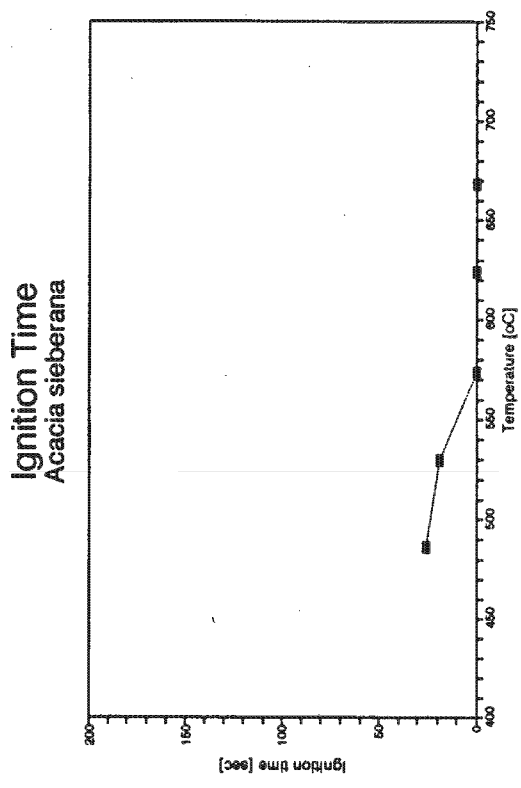

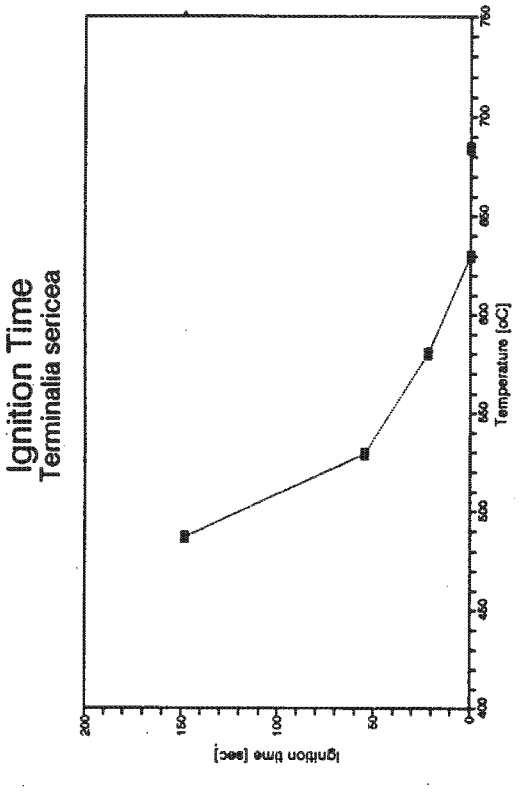

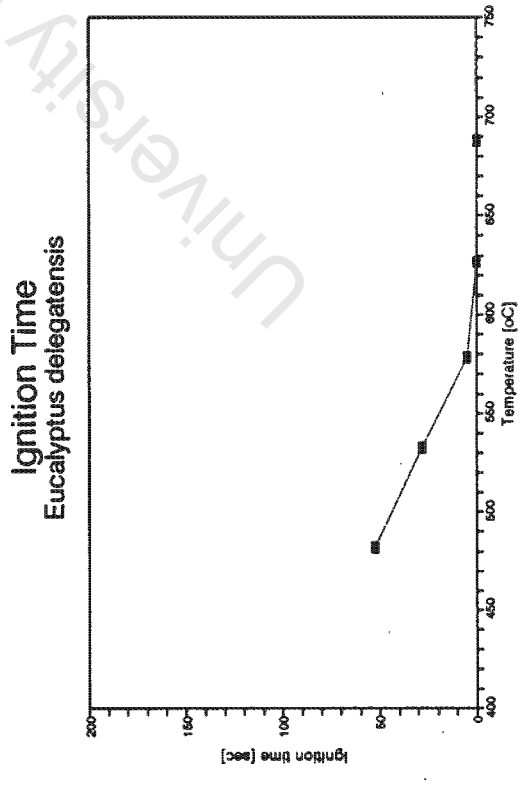

Appendix G: Data Graphs: Ignition time vs temperature

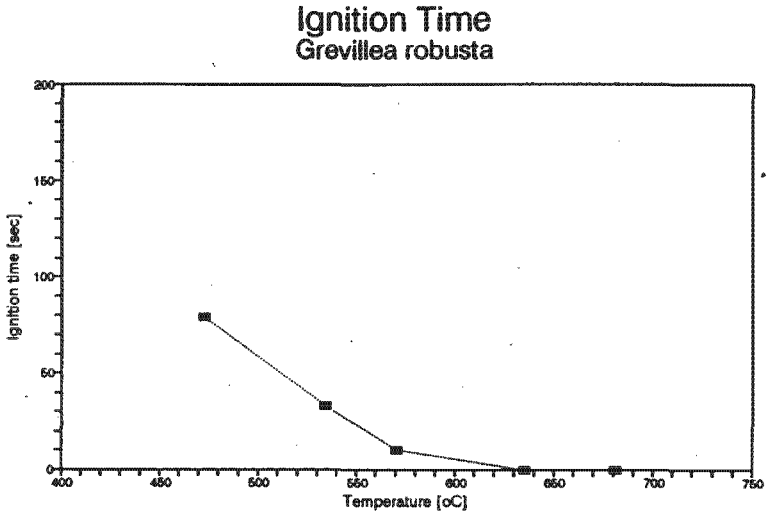

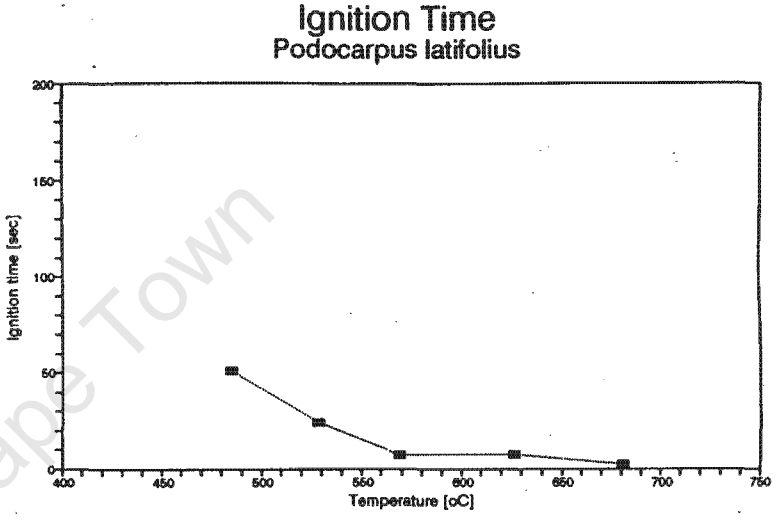

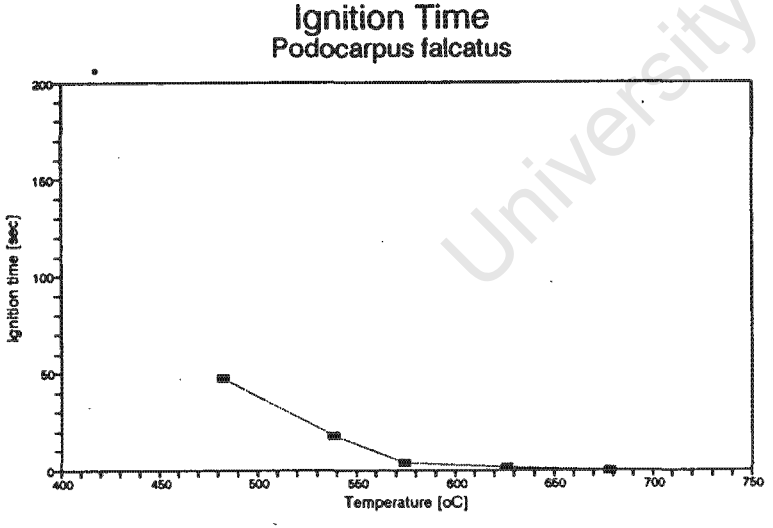

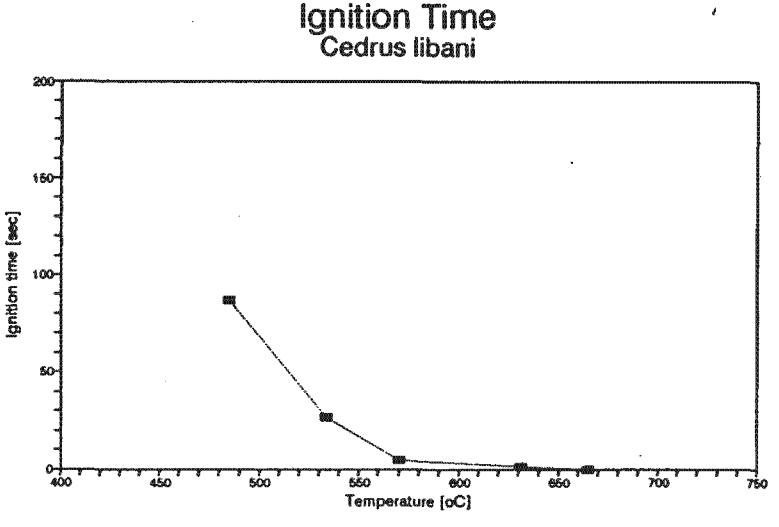

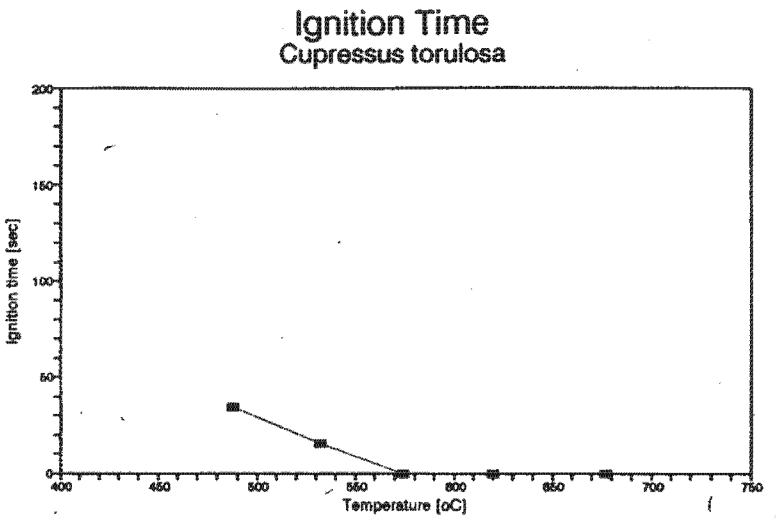

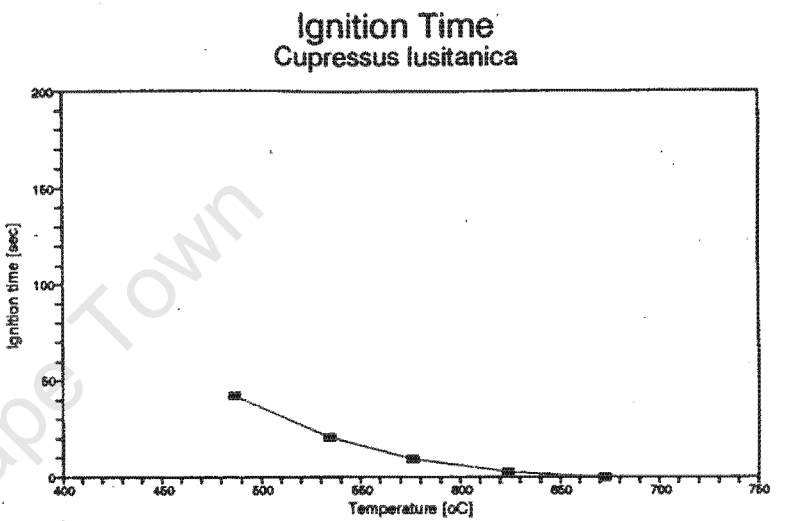

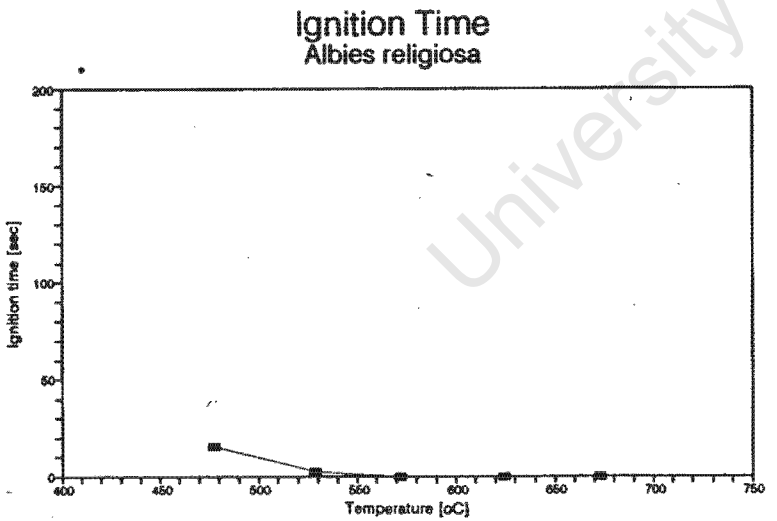

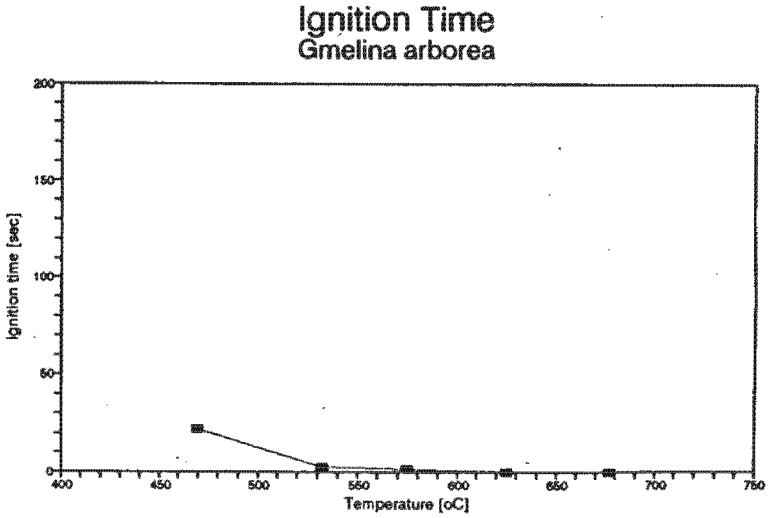

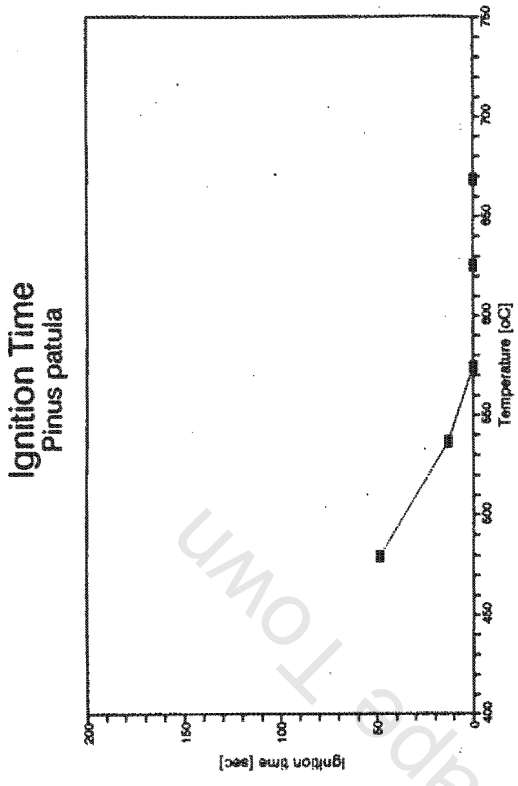

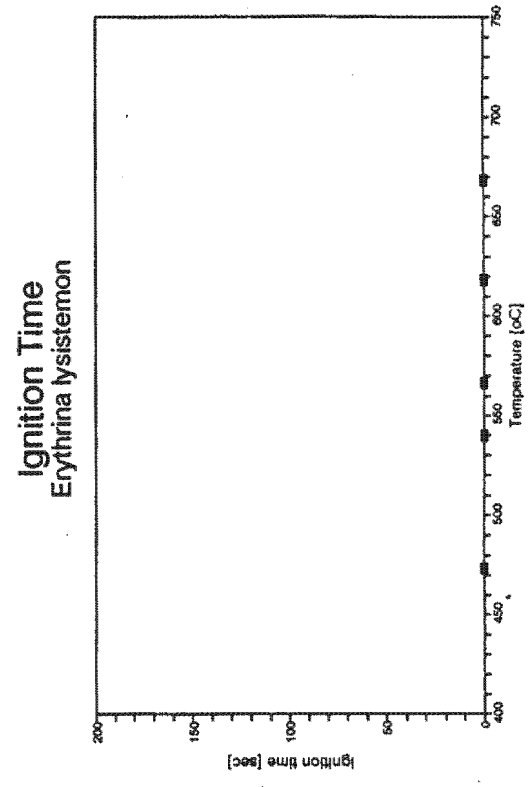

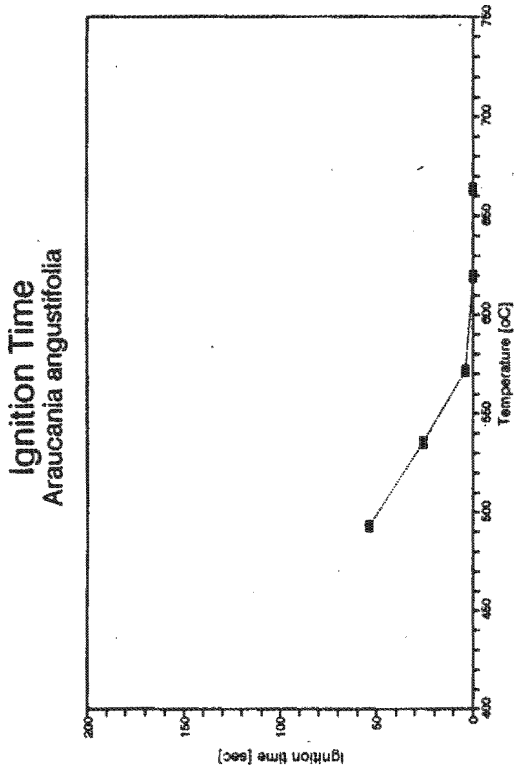

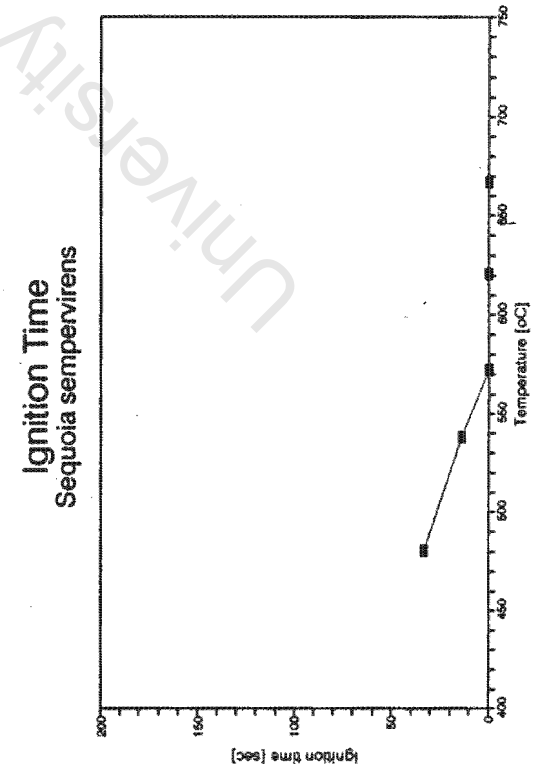

Appendix G: Data Graphs: Ignition time vs temperature

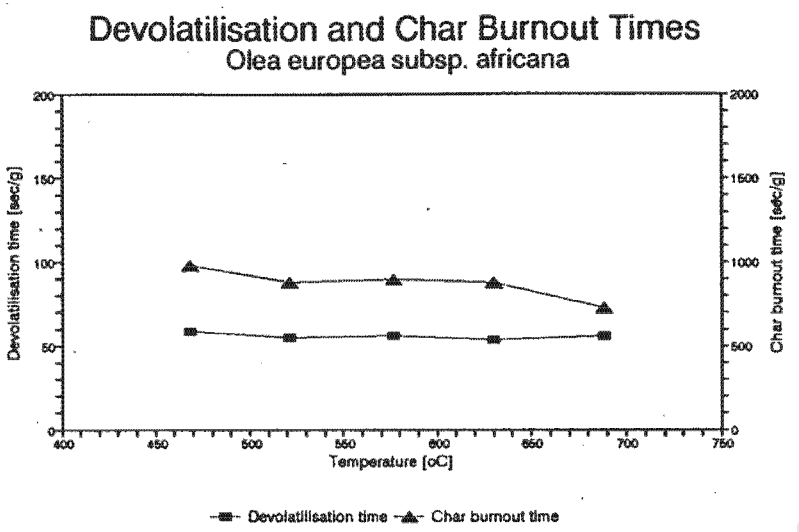

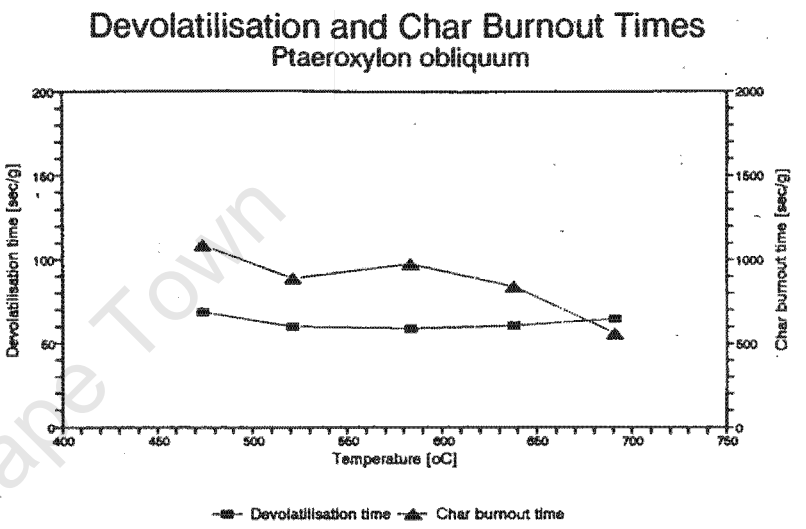

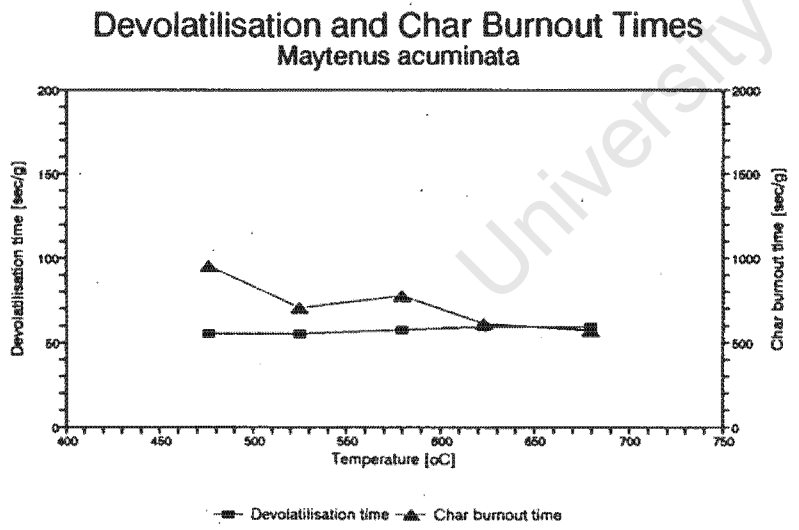

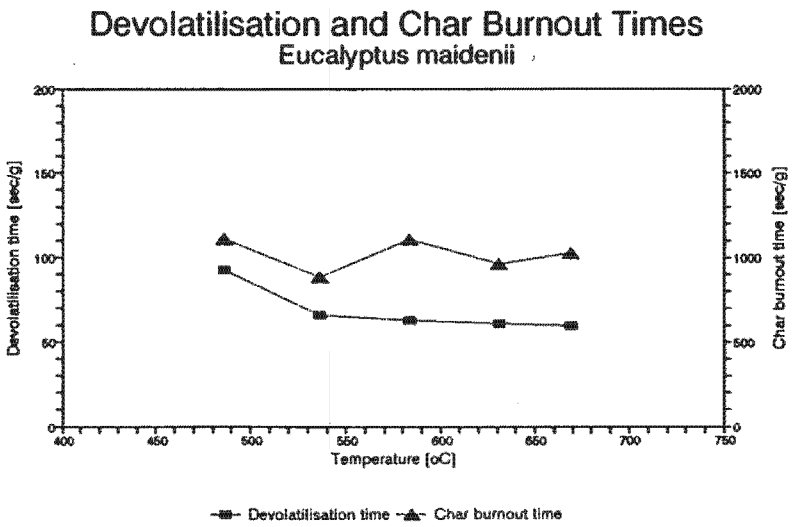

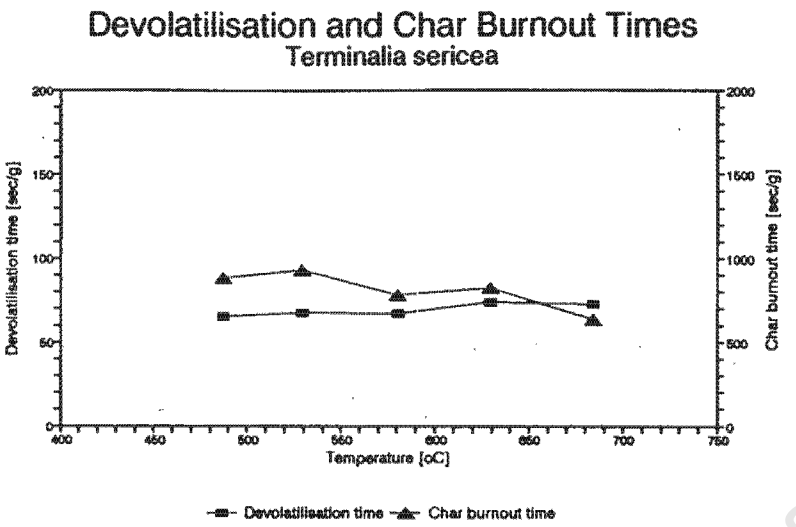

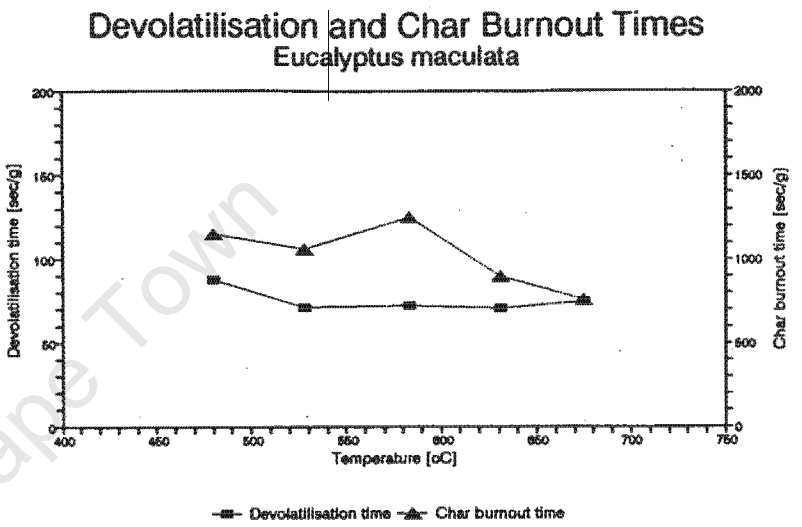

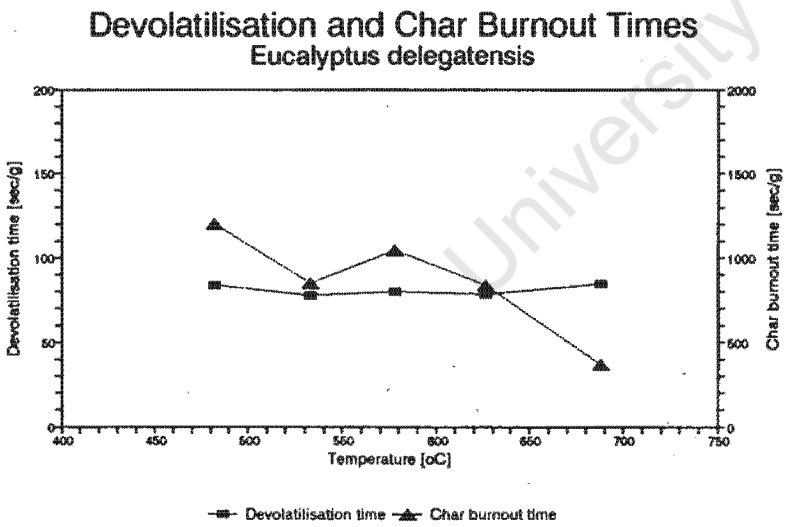

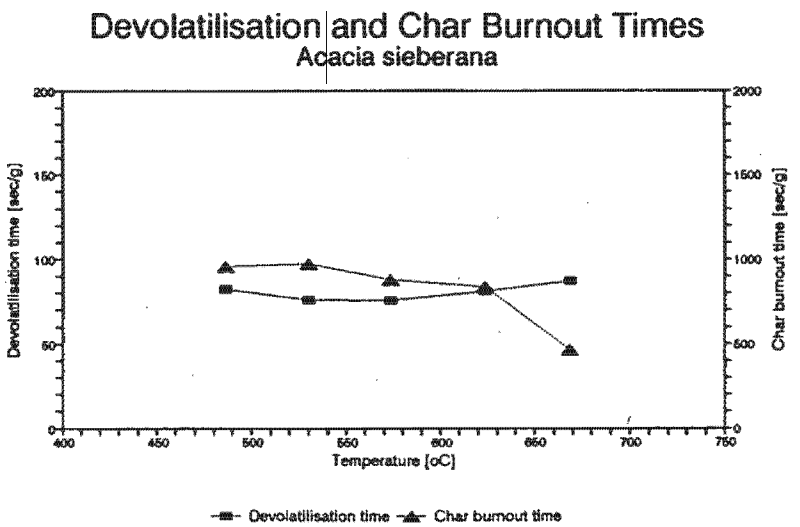

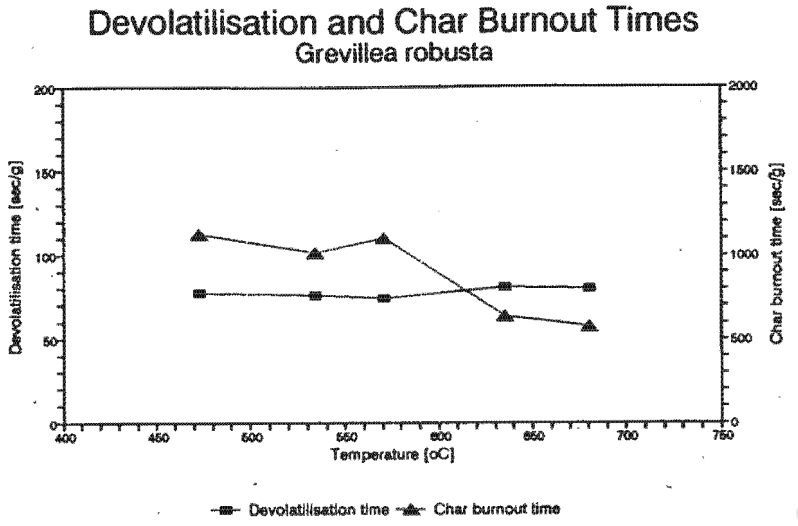

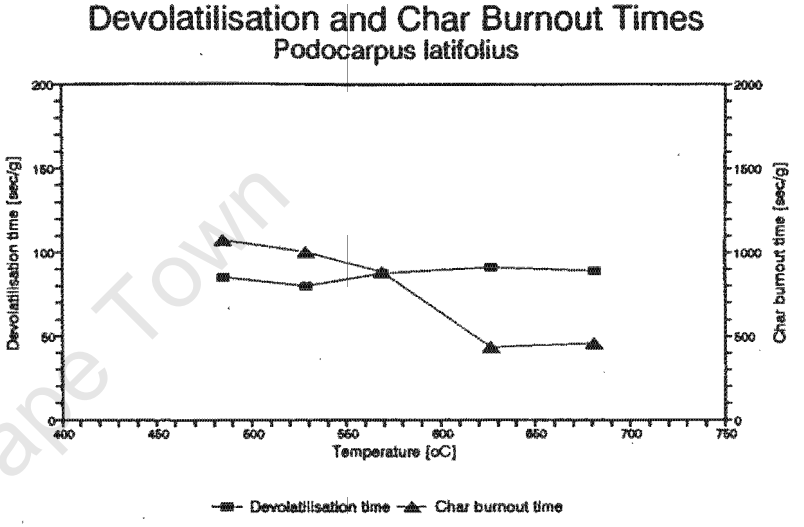

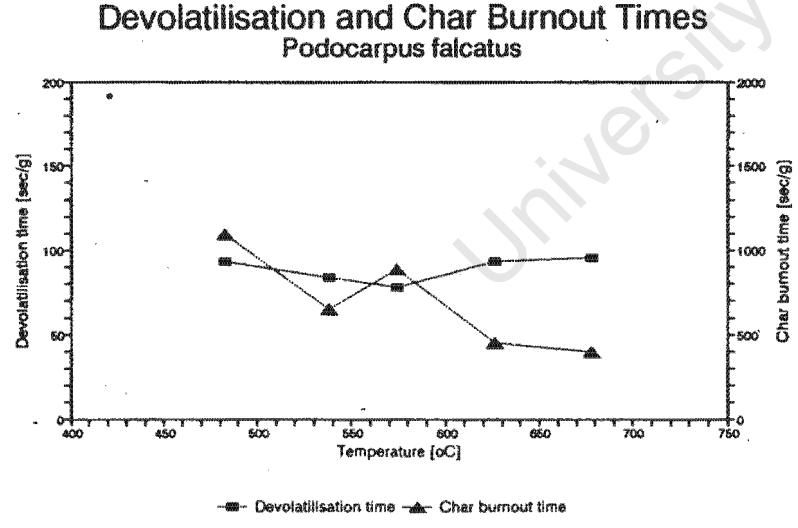

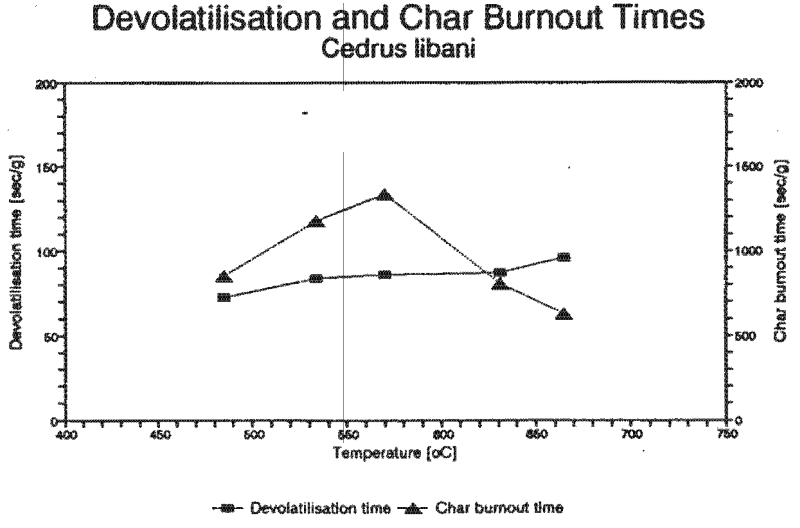

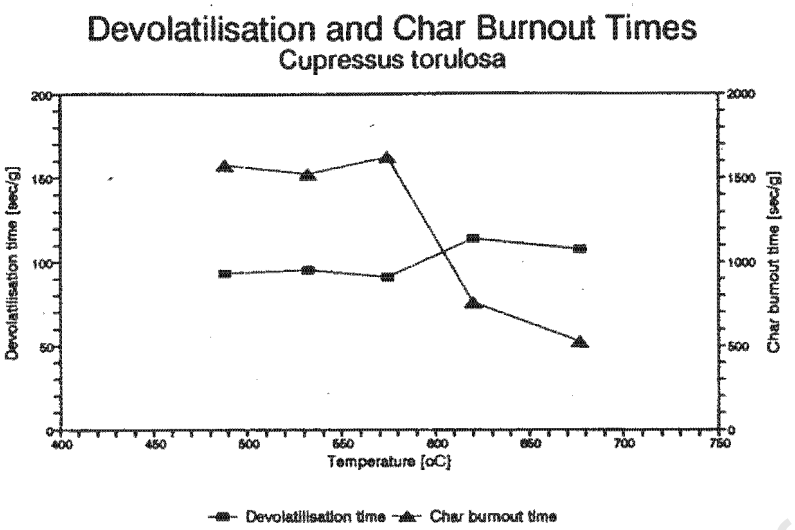

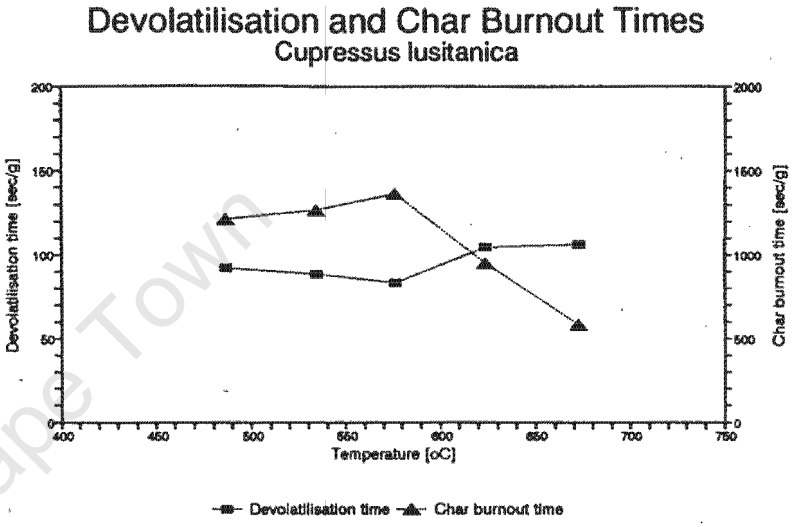

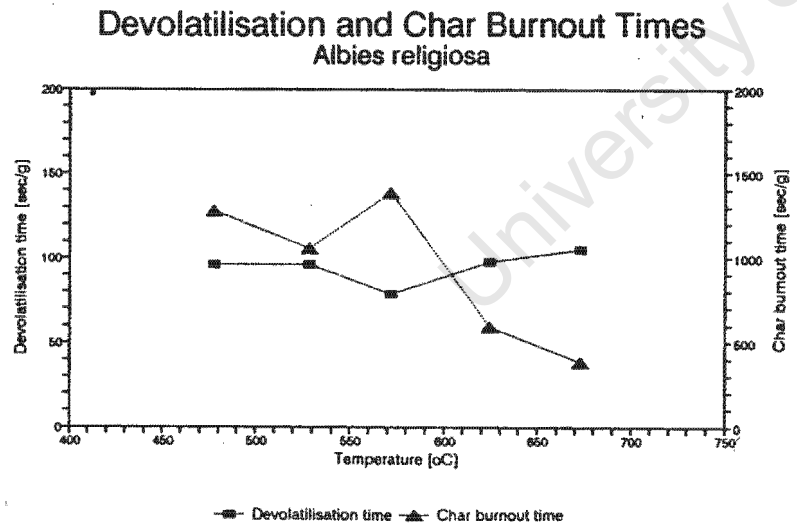

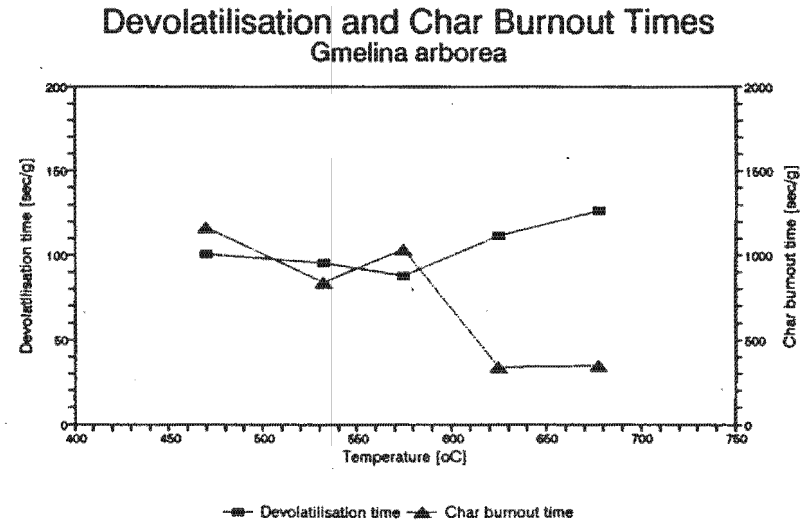

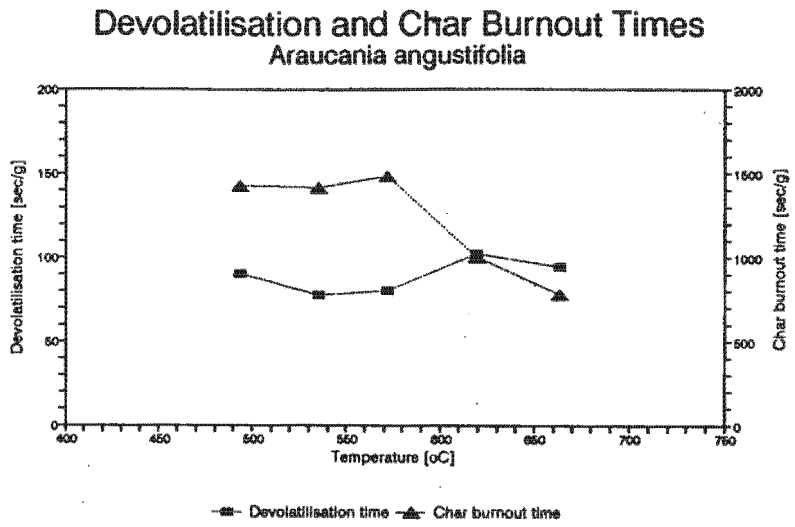

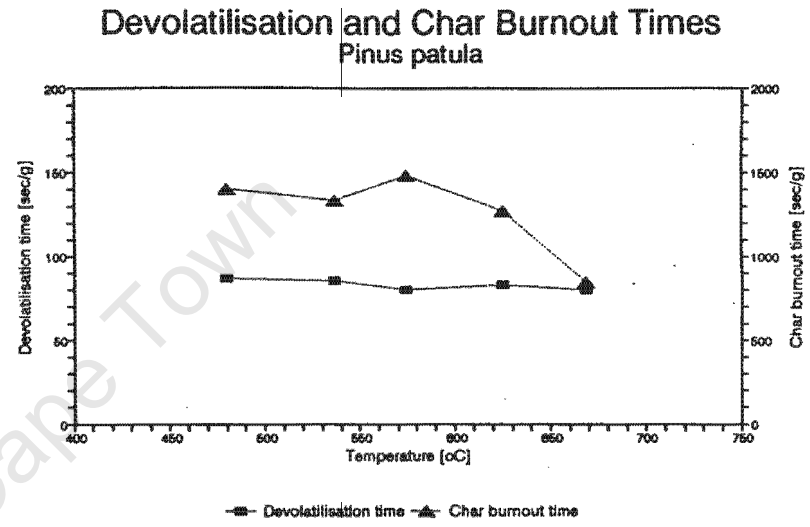

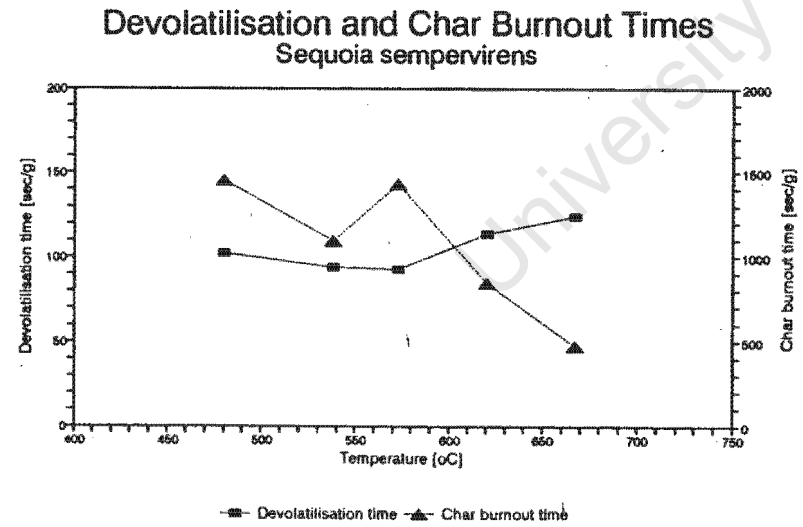

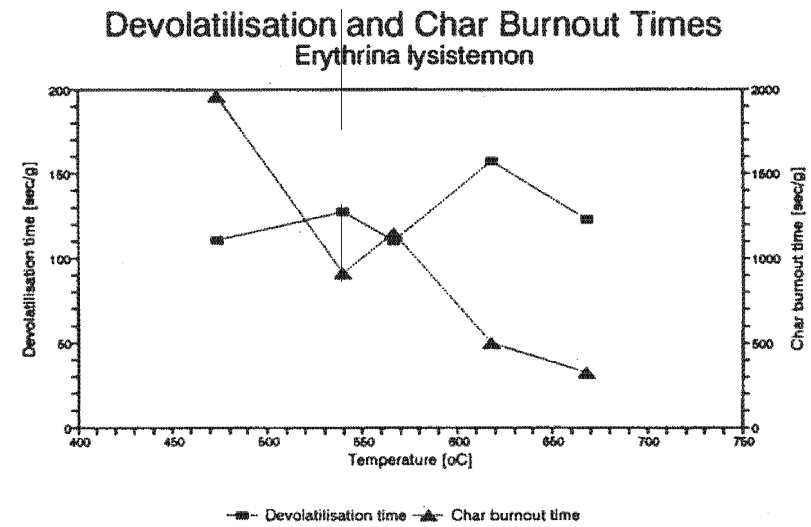

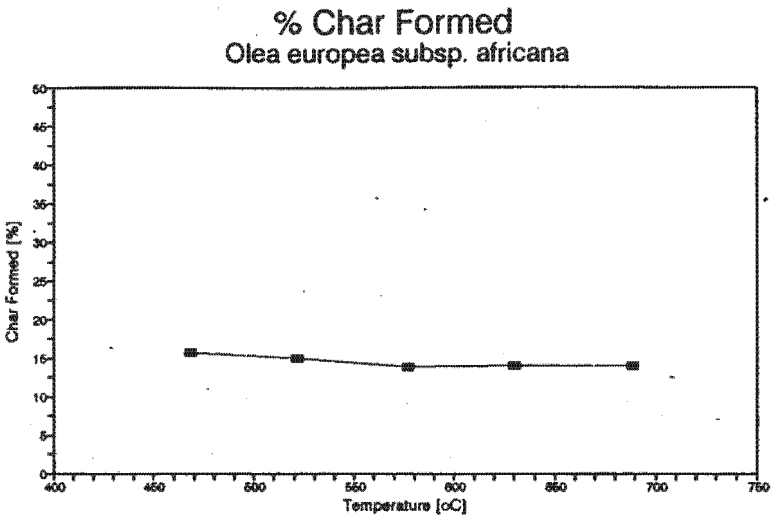

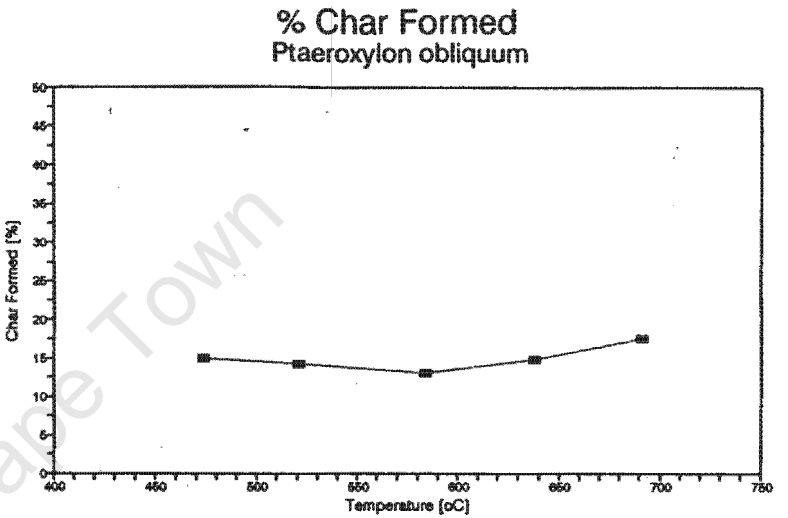

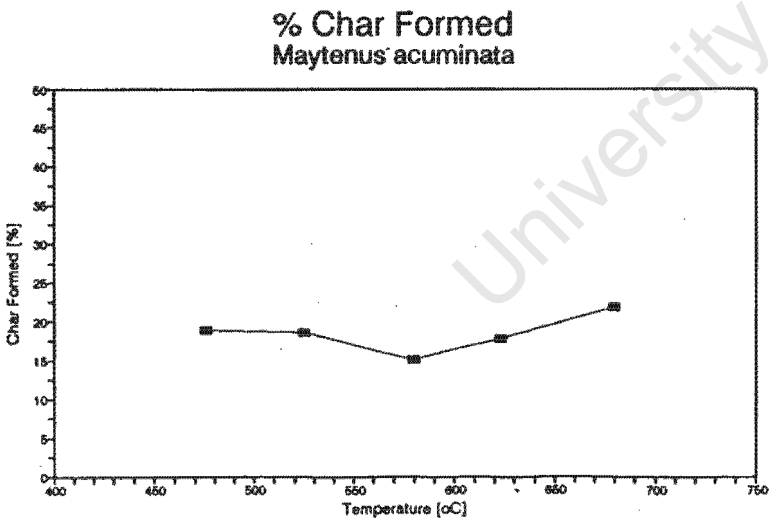

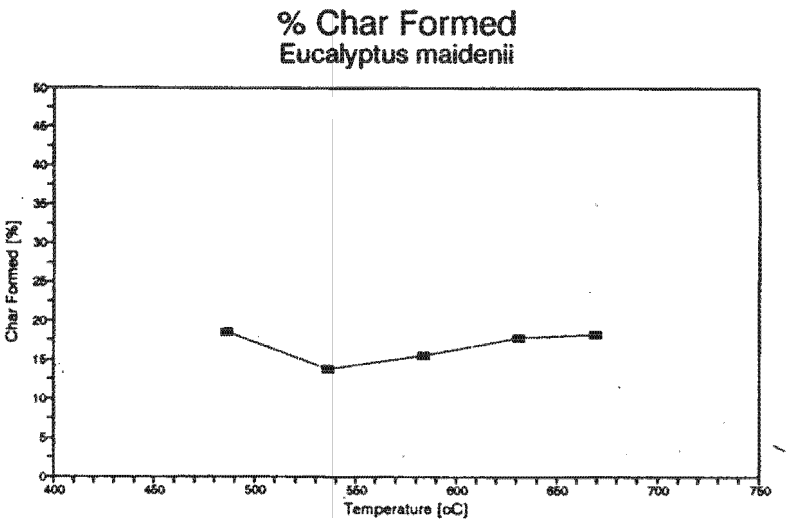

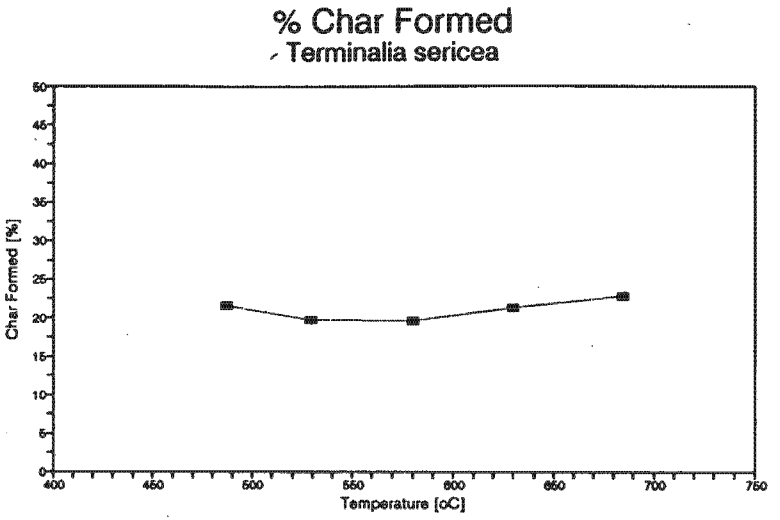

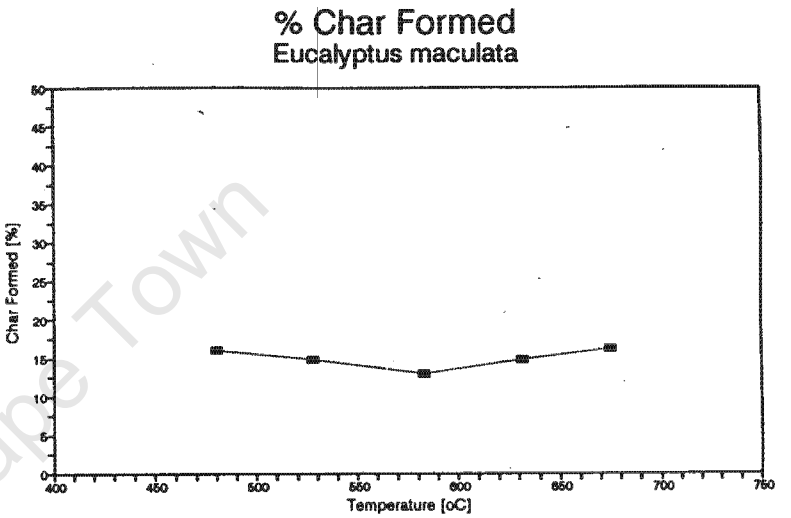

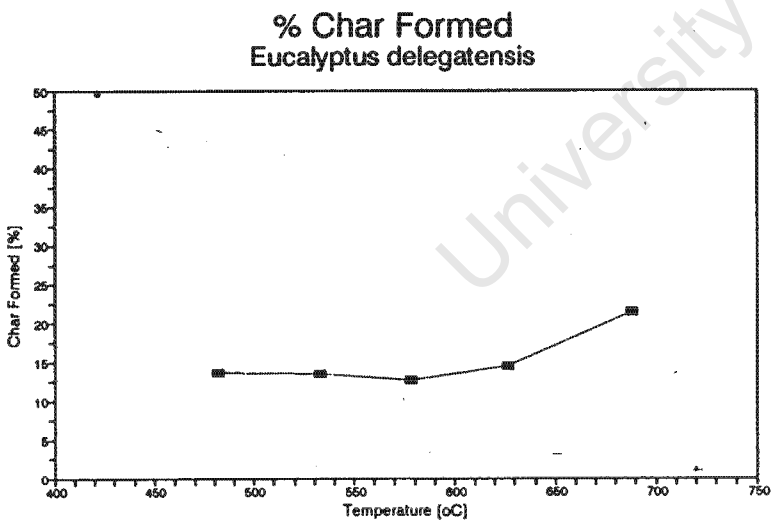

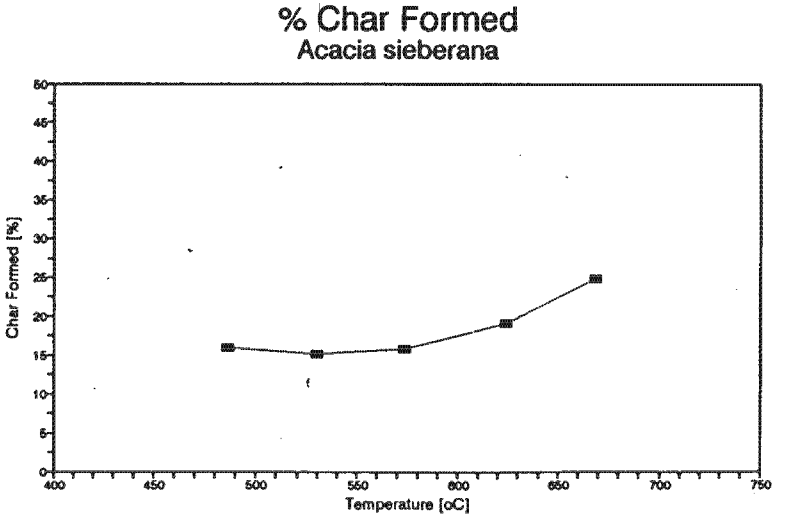

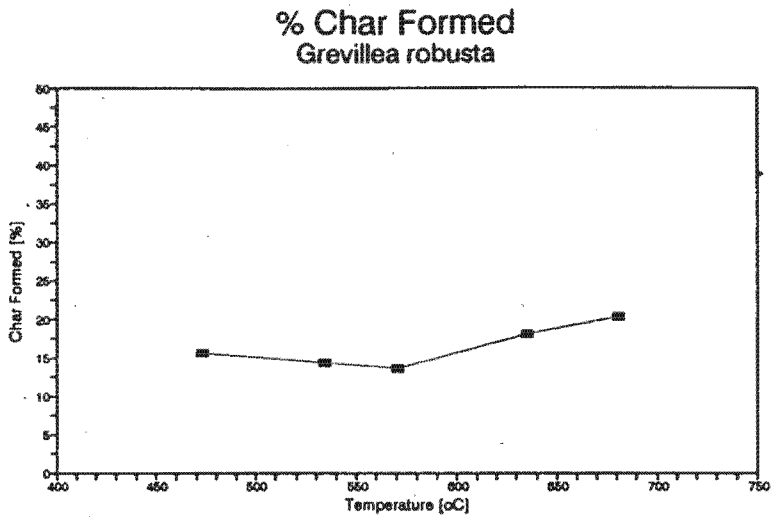

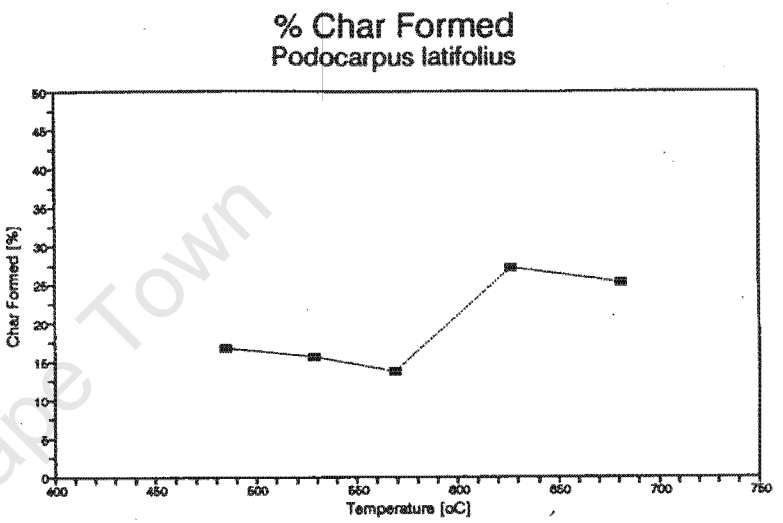

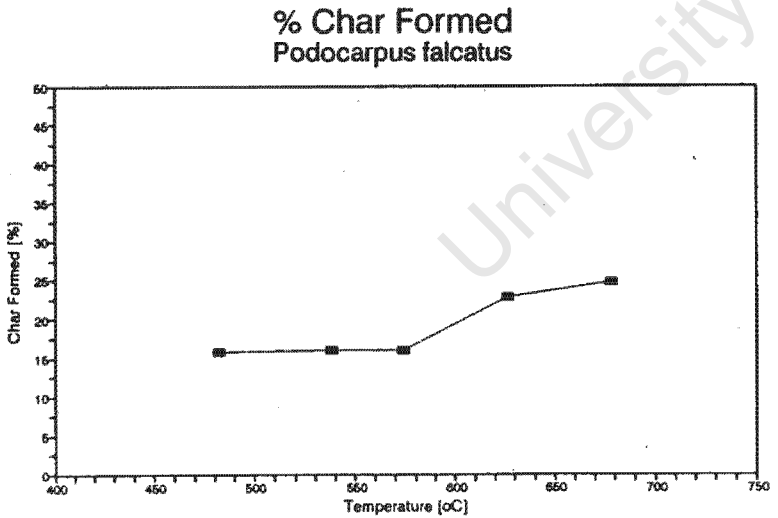

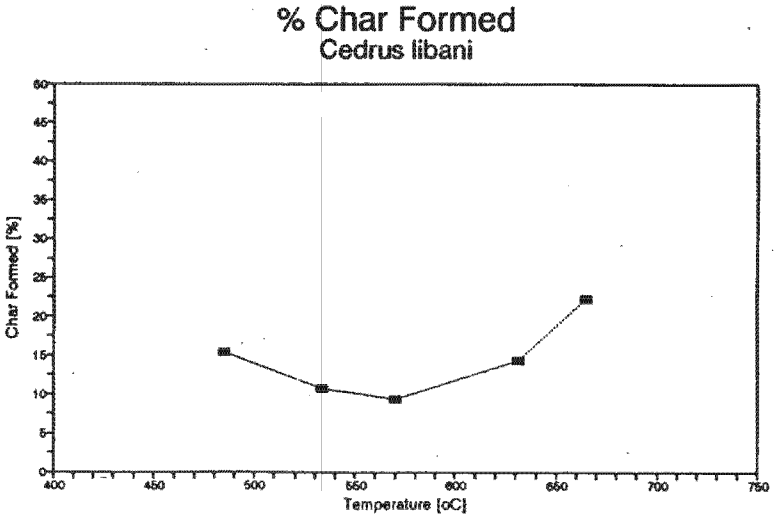

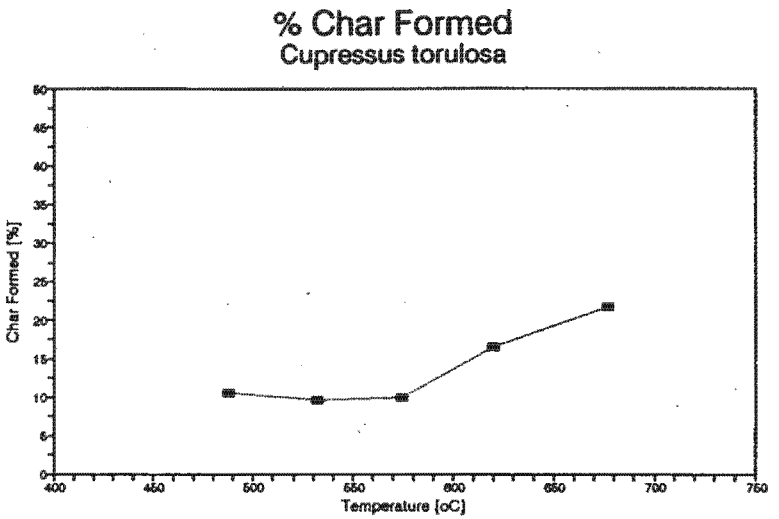

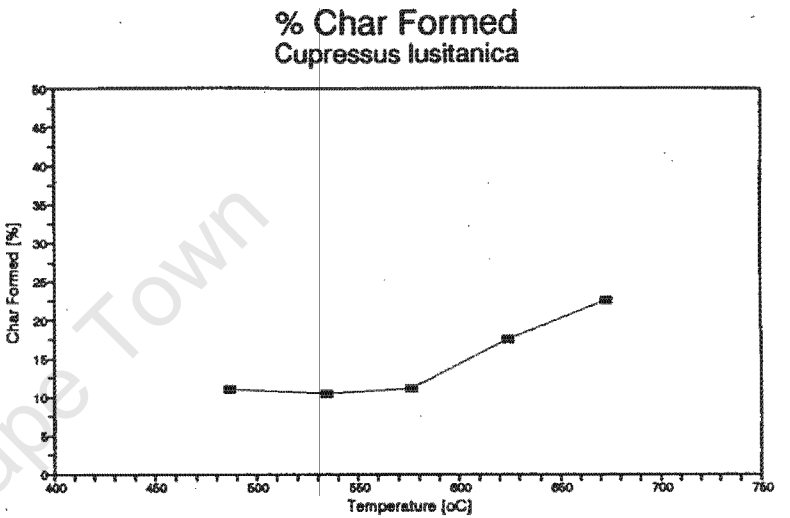

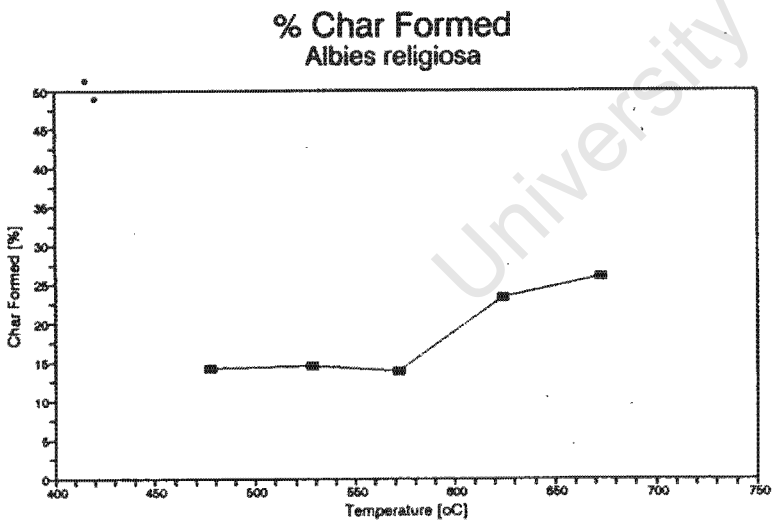

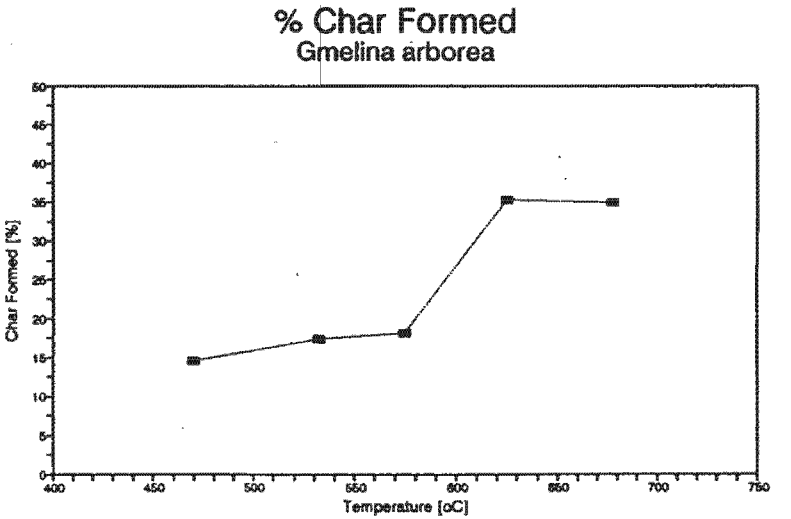

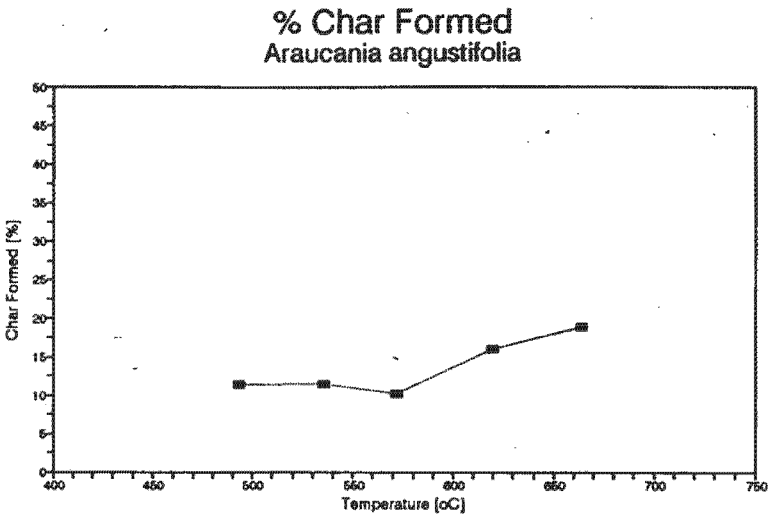

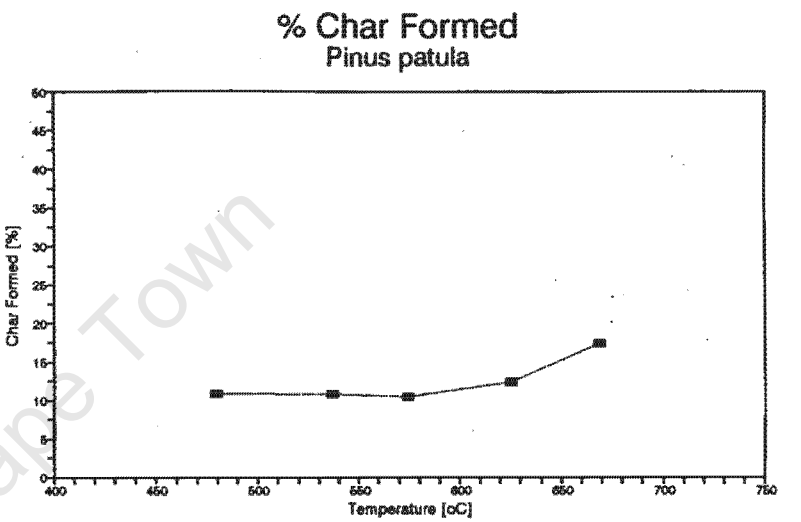

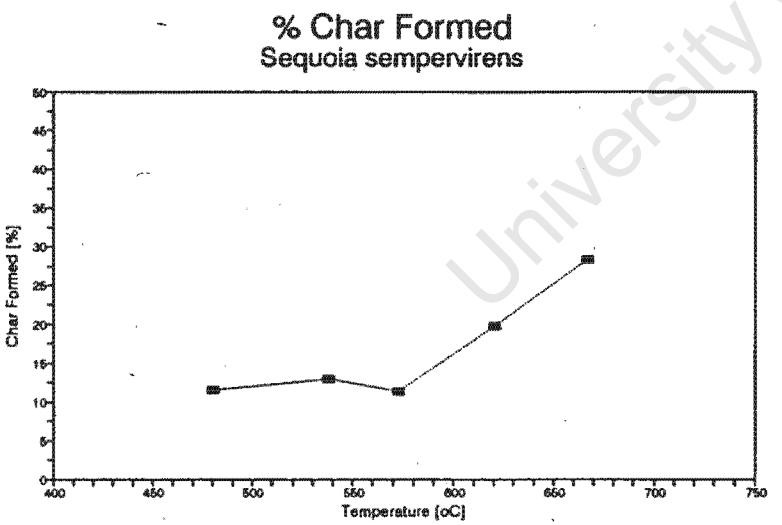

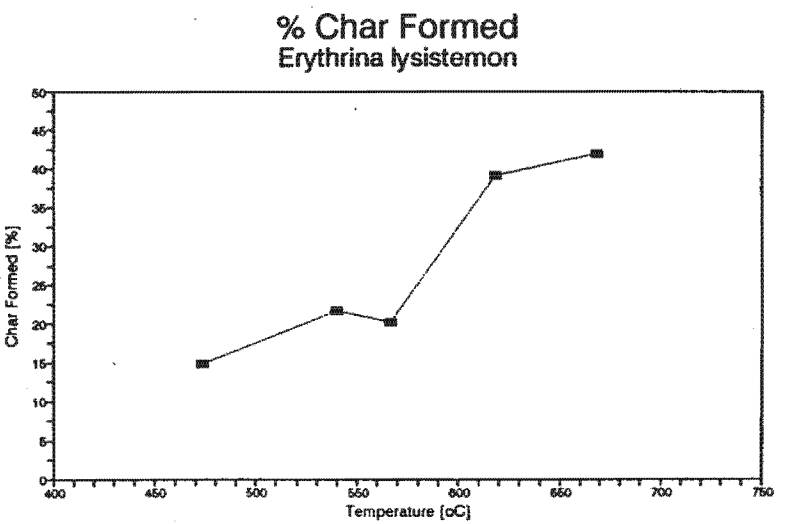

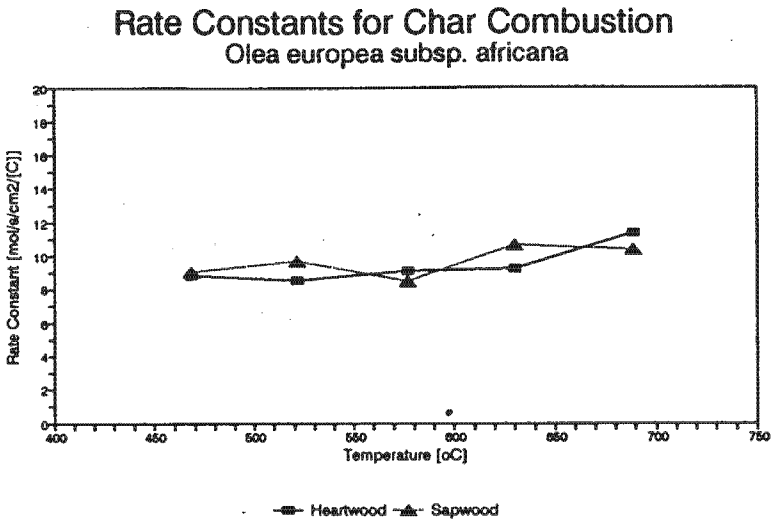

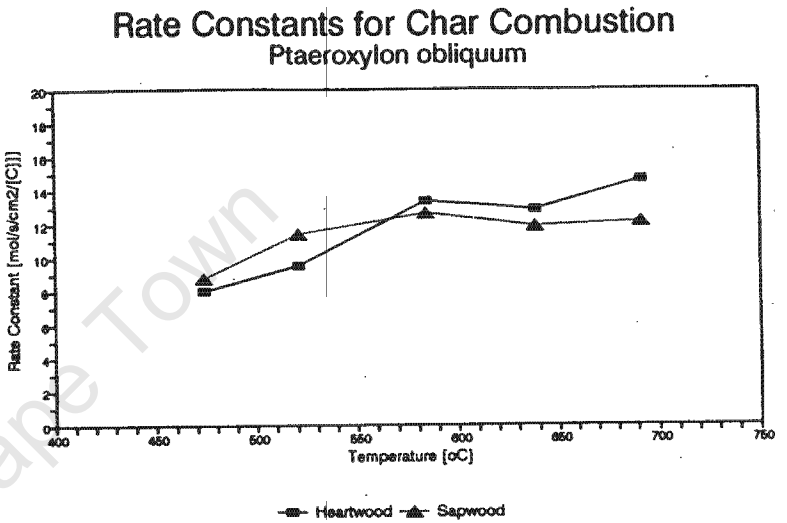

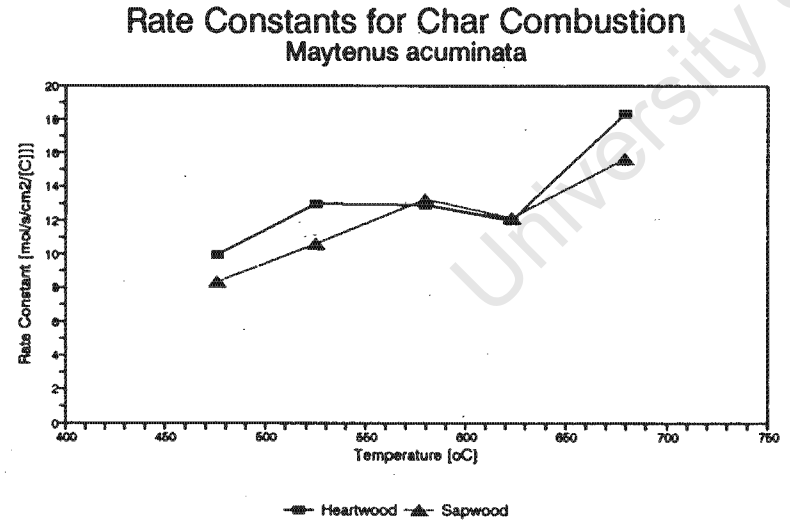

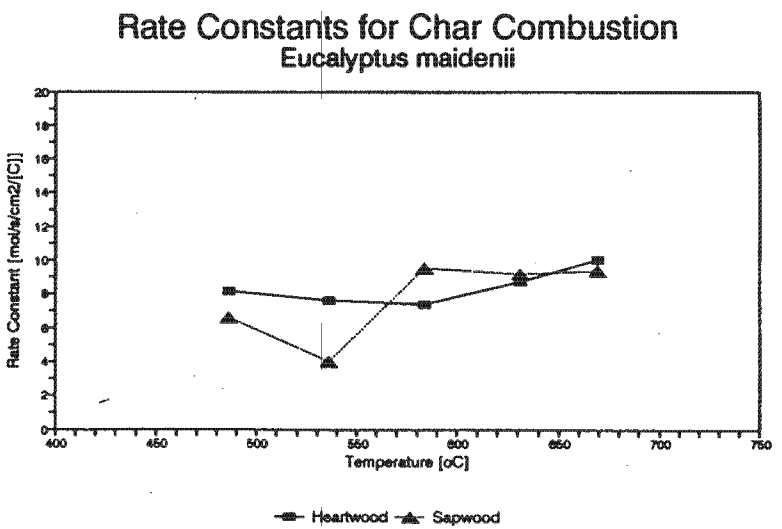

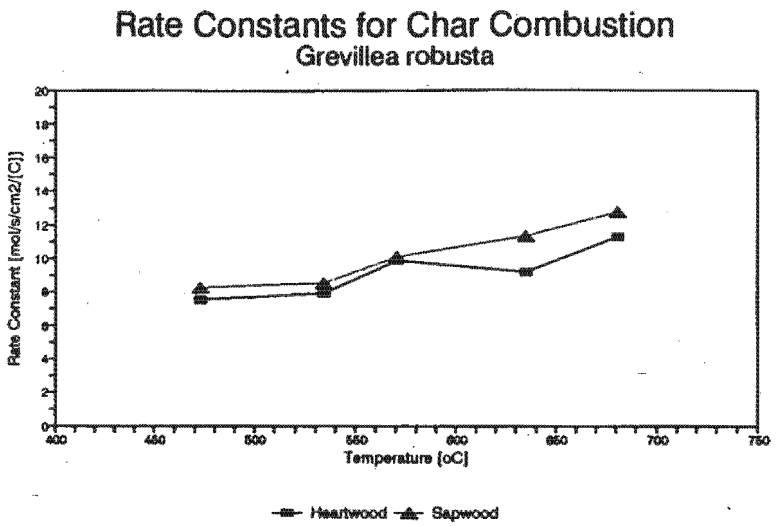

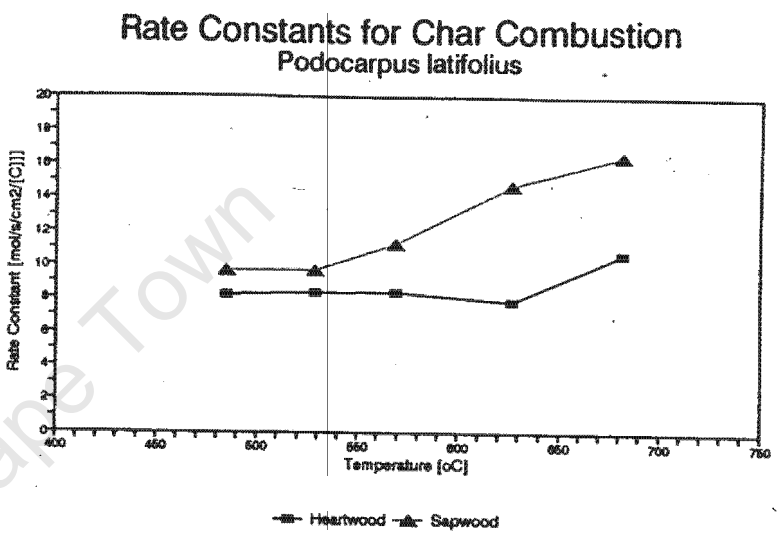

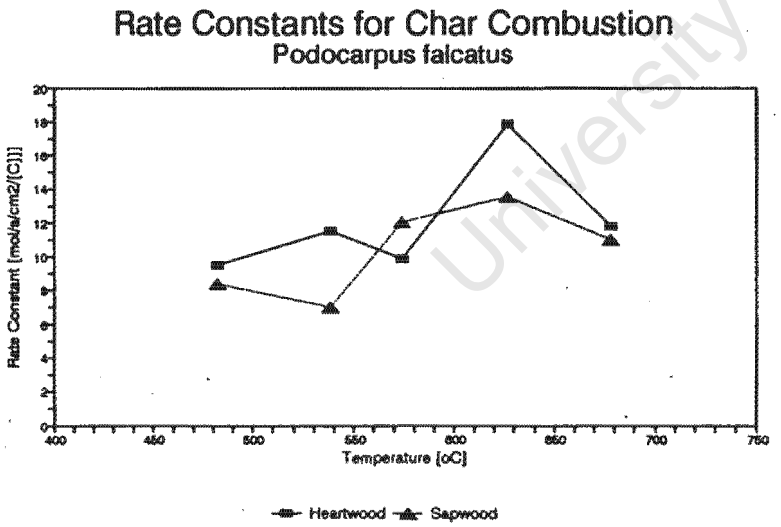

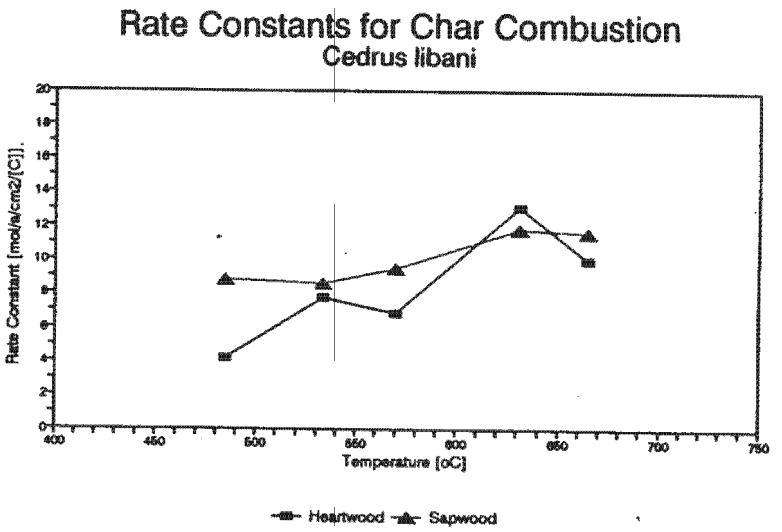

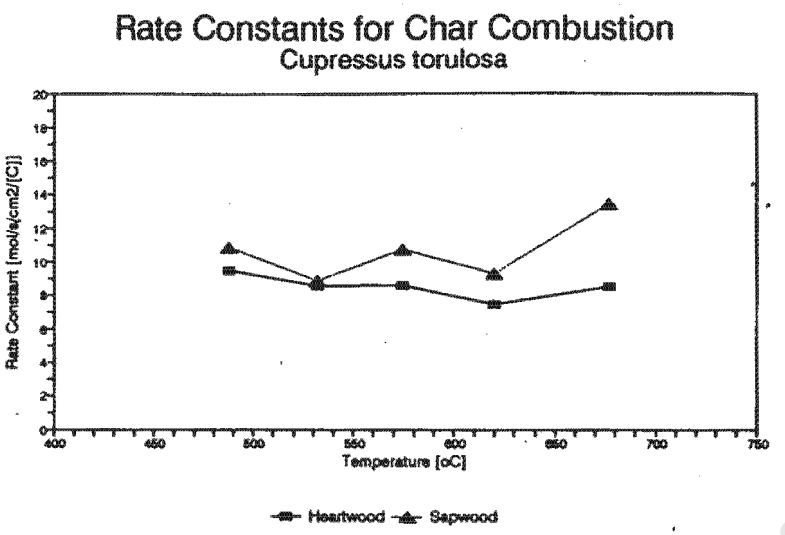

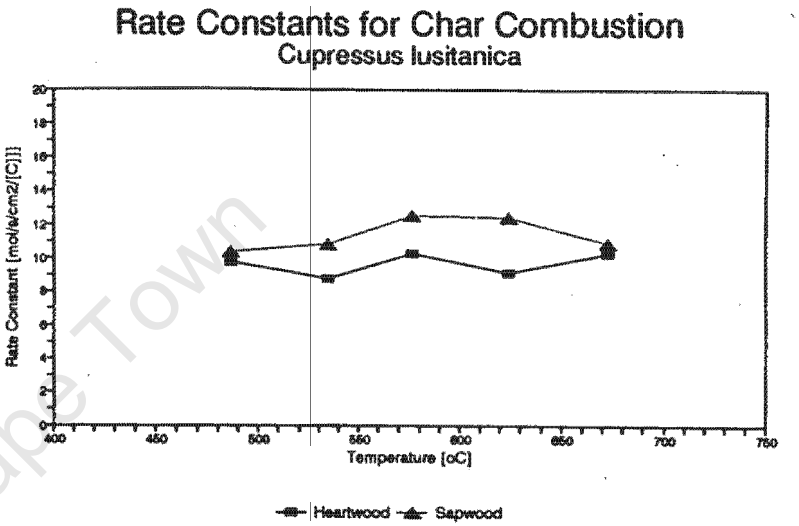

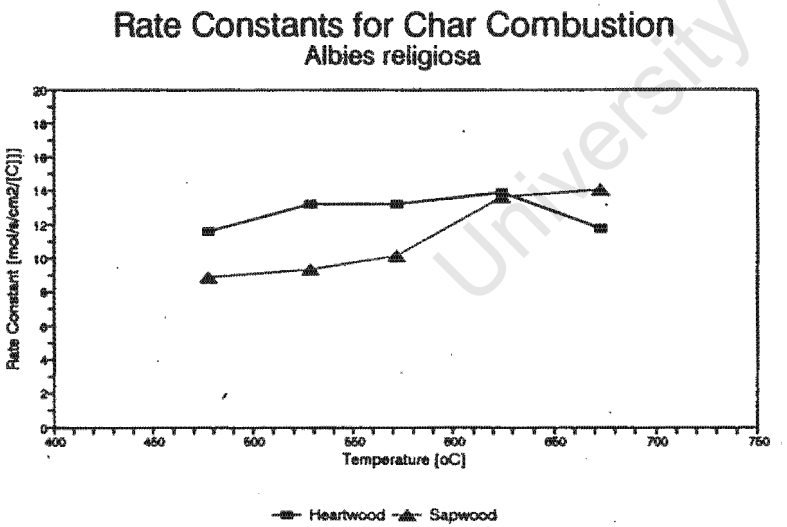

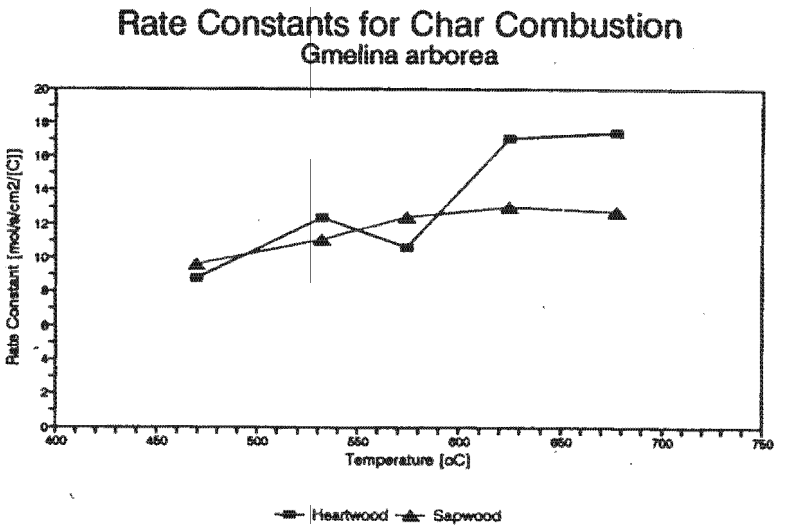

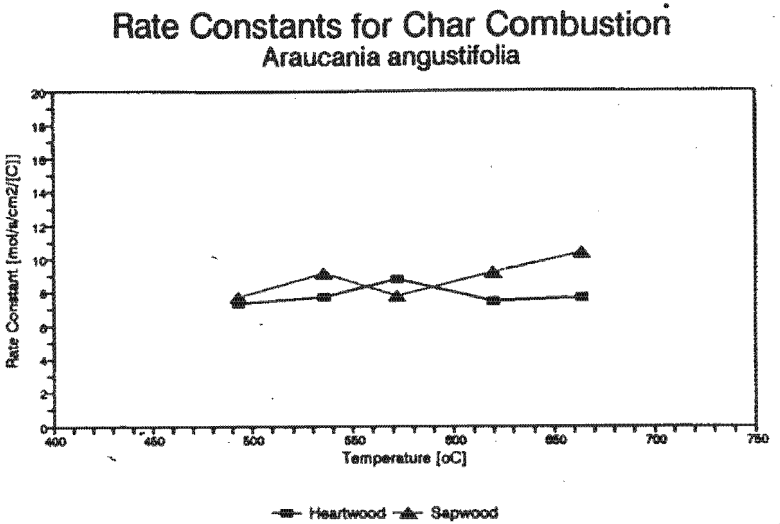

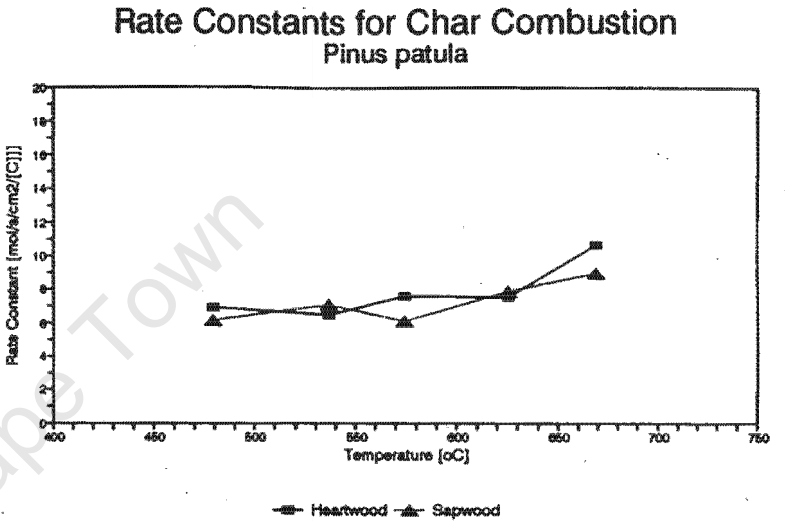

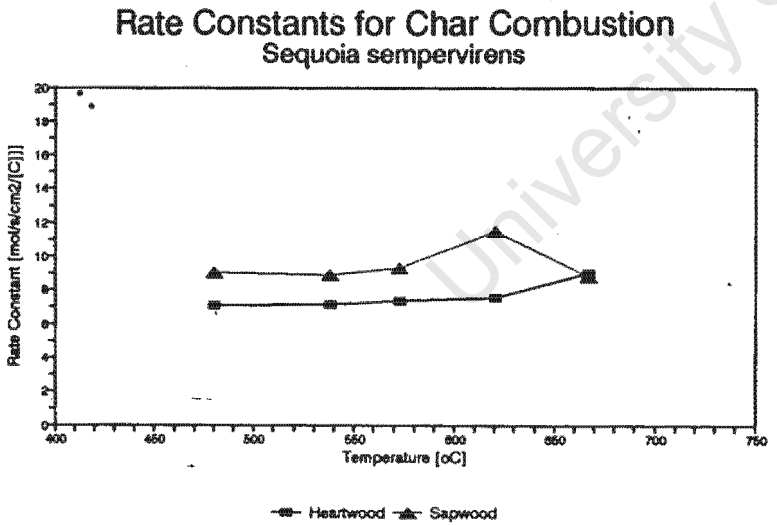

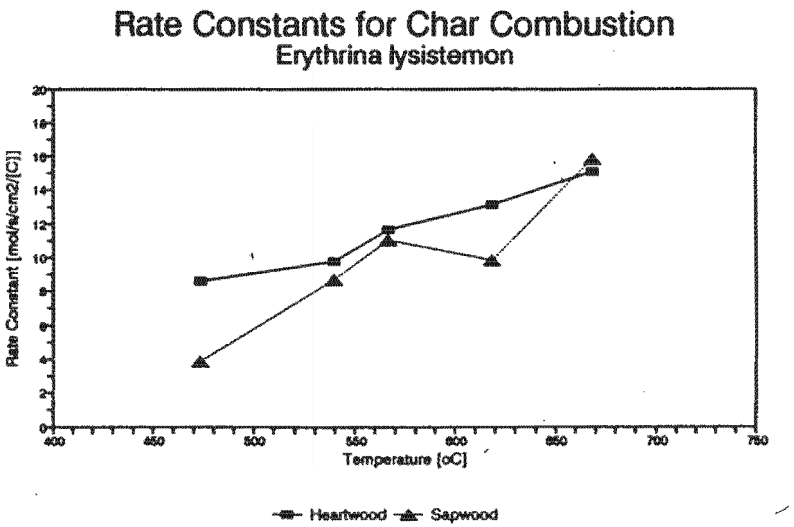

Mass Loss Rates for Char Combustion
Olea europea subsp. africana

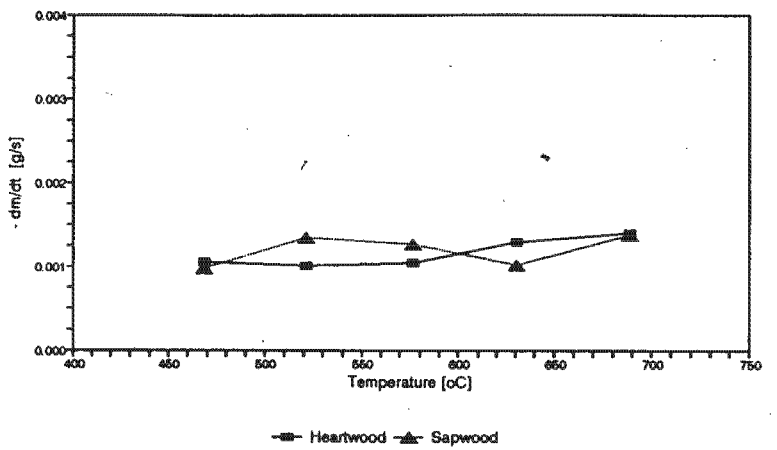

Mass Loss Rates for Char Combustion
Ptaeroxylon obliquum

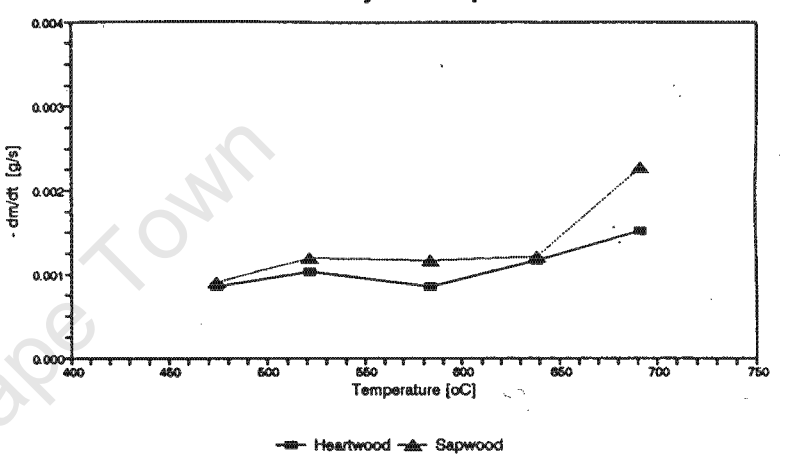

Mass Loss Rates for Char Combustion
Maytenus acuminata

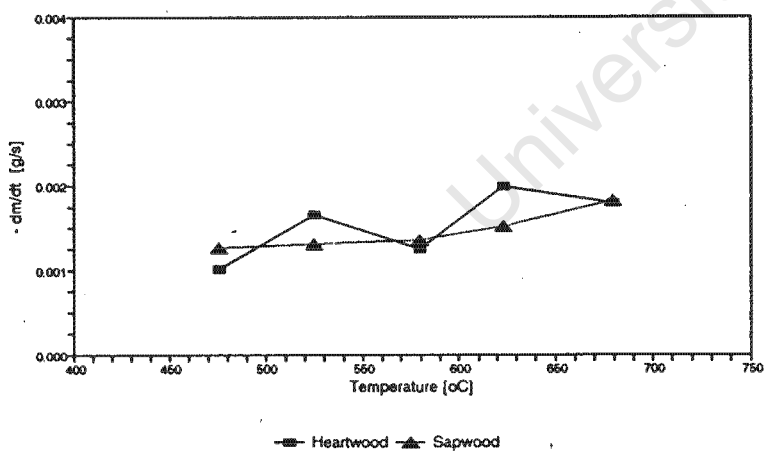

Mass Loss Rates for Char Combustion
Eucalyptus maidenii

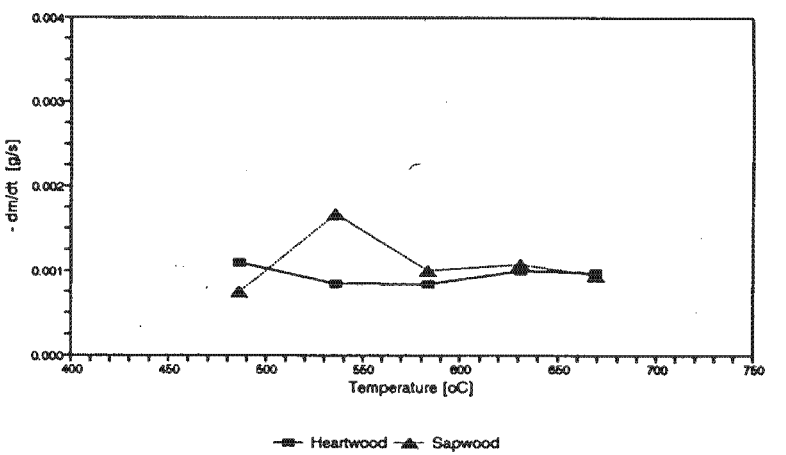

Mass Loss Rates for Char Combustion
Terminalia sericea

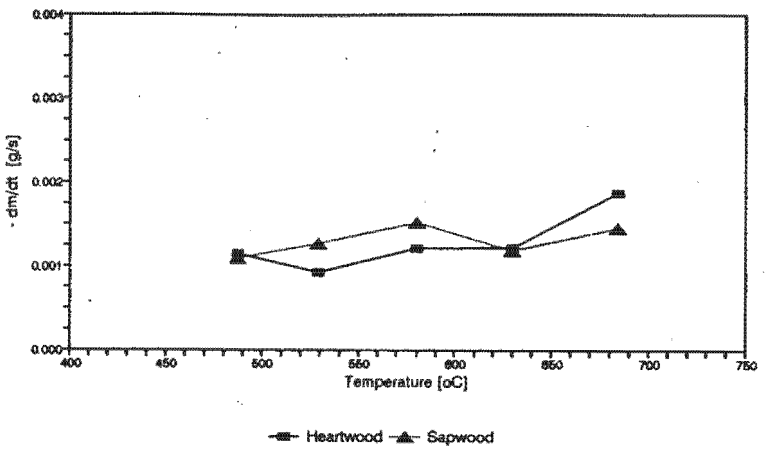

Mass Loss Rates for Char Combustion
Eucalyptus maculata

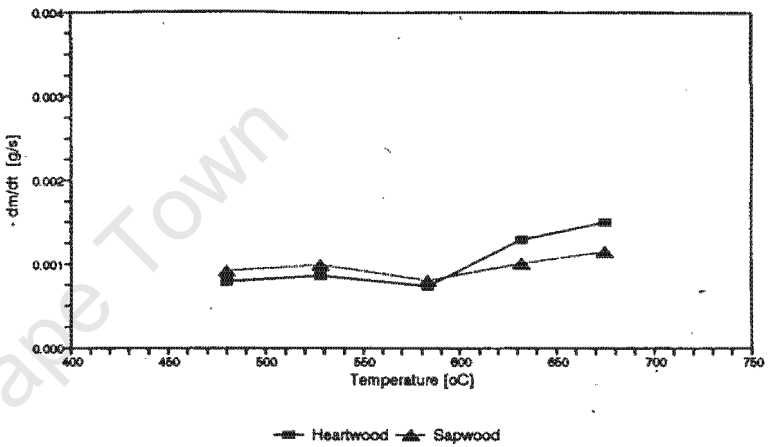

Mass Loss Rates for Char Combustion
Eucalyptus delegatensis

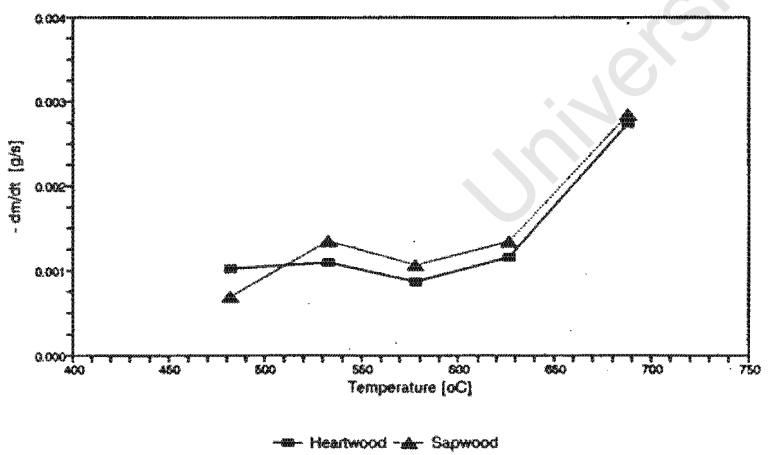

Mass Loss Rates for Char Combustion
Acacia sieberana